The Role of Epoxygenated Arachidonic Acid-Derived Metabolites in Neuronal Transmission

---

Dissertation

zur

Erlangung der naturwissenschaftlichen Doktorwürde

(Dr. sc. nat.)

vorgelegt der

Mathematisch-naturwissenschaftlichen Fakultät

der

Universität Zürich

von

Nandkishor Kisanrao Mule

aus

Indien

Promotionskommission

Prof. Dr. Michael Arand (Vorsitz und Leitung der Dissertation)

Prof. Dr. Hanns Ulrich Zeilhofer

Prof. Dr. Wolf-Hagen Schunck

Zürich, 2018

Table of Contents

Summary

Cell membranes are highly enriched in arachidonic acid (AA), which serves as a source for the activity-dependent generation of eicosanoids including the cytochrome P450-derived epoxyeicosatrienoic acids (EETs). EETs are hydrolyzed to supposedly less active dihydroxyeicosatrienoic acids (DHETs) by microsomal and soluble epoxide hydrolase (mEH and sEH). Research efforts spanning over decades implicated EETs and to a marginal extent DHETs in various physiological processes. However, little is known about their potential role in synaptic physiology.

This dissertation addressed the question if and how EETs and DHETs modulate neuronal excitability and synaptic transmission using the patch-clamp technique. We showed that in particular 11,12-EET and -DHET are capable of modulating neuronal excitability and synaptic transmission in hippocampal pyramidal cells (PCs) with 11,12-EET decreasing and -DHET increasing hippocampal excitability as a net effect. Our results suggested that EETs and DHETs likely mediate their effects via a combination of pre- and postsynaptic effectors. We found that 11,12-EET activates a postsynaptic G-protein coupled inwardly rectifying K^+ (GIRK) channel in CA1 PCs, leading to hyperpolarization and thus decreased excitability of the respective neuron. Additionally, 11,12-EET reduced the release of glutamate onto CA1 PCs via one or several presynaptic mechanism(s). Interestingly, 11,12-DHET counteracted the 11,12-EET effects and increased excitatory transmission, reflected by an increase in field excitatory postsynaptic potentials (fEPSPs) recorded at the Schaffer collateral-CA1 synapse.

Voltage-gated K^+ channels appeared to be the most promising molecular targets mediating EET and DHET effects. In hippocampal PCs, K_v1.1 and 1.2 channels are expressed presynaptically and regulate the release of glutamate, whereas K_v4.2 channels are expressed postsynaptically and regulate dendritic excitability. We expressed these three channels in heterologous cells and tested the effect of 11,12-EET and -DHET. The effect of 11,12-DHET was evaluated at a single depolarizing test potential of +10 mV and +40 mV for K_v1.2 and K_v4.2, respectively. 11,12-DHET significantly blocked K_v1.2 by 11.92±3% at the single test potential of +10 mV, whereas K_v4.2 was significantly blocked by 24.5±5.6% at a test potential of +40 mV. By contrast, 11,12-

EET increased $K_v1.2$ currents by 4.9±1.5% at a single depolarizing test potential of +10 mV. Moreover, we tested the inhibitory effect of 11,12-DHET on $K_v1.2$ and $K_v4.2$ using a multiple current (I)-voltage (V) step protocol. In this paradigm, 11,12-DHET blocked $K_v1.2$ by 29.7±9% at +40 mV and $K_v4.2$ channels by 36.8±5.3% at +10 mV. These EET and DHET-mediated activation and inhibition of K_v channels, respectively, are consistent with decreased and increased excitatory synaptic transmission at the CA3-CA1 synapse in brain slices.

Since mEH and sEH determine the EET:DHET ratio due to their ability to hydrolyze EETs, they might act as 'physiological switch' between inhibition and excitation. We tested this notion using three strains of transgenic mice, which either lacked mEH or sEH or expressed a hyperactive mEH variant (mEH E404D). The basal synaptic activity measured as input-output curves was significantly reduced in slices from mEH KO and sEH KO compared to WT mice. By contrast, slices from mEH E404D mice with higher EH activity and thus higher turnover to DHETs showed higher basal synaptic transmission relative to WT at the hippocampal CA3-CA1 synapse. Thus, EHs most likely play an important role in setting the level of excitability in the CNS.

The second project of this dissertation focused on the involvement of CYP-epoxygenase-derived fatty acids (FA) epoxides in morphine-mediated antinociception. Using the tail flick paradigm, we found that sEH KO mice exhibited significantly higher morphine-mediated antinociception at a subcutaneously applied dosage of 1 mg/kg compared to WT mice. This might be due to an accumulation of FA epoxides such as EETs, although other levels of FA epoxides such as those of epoxydocosapentaenoic acids (EpDPEs) or epoxyeicosatetraenoic acid (EpETEs) are also known to be enhanced in sEH KO relative to WT brain. We tested 14,15-EET as a potential modulator of mu-opioid receptor (MOR) signaling in HEK-293T cells, as morphine exerts its effects primarily through the MOR. However, 14,15-EET neither by itself nor when co-administered with the selective MOR agonist DAMGO showed any effect. This led to the conclusion, that either another FA epoxide (EpDPEs, EpETEs) modulates MORs or HEK-293T cells lack a crucial molecular component for enhancing EET-mediated MOR signaling.

Taken together, our findings implicate EETs and DHETs as endogenous neuroactive lipid mediators, which regulate neuronal excitability and synaptic transmission possibly via activating or inactivating K^+ channels, namely GIRK, $K_v1.2$, and $K_v4.2$ channels in hippocampal PCs.

Furthermore, the results of this dissertation offer mechanistic explanations for attenuated epileptic symptoms observed in sEH KO relative to WT mice described in earlier studies.

Zusammenfassung

Zellmembranen enthalten grosse Mengen an Arachidonsäure, die als Ausgangsstoff für die Synthese von Eikosanoiden dient. Ein Beispiel für solche Eikosanoide sind die sogenannten EETs (abgeleitet vom englischen Wort *epoxyeicosatrienoic acids*), die in einer durch Cytochrom P450-katalysierten Reaktion entstehen. In einem zweiten Schritt können EETs von der mikrosomalen oder löslichen Epoxidhydrolase zu sogenannten DHETs (abgeleitet vom englischen Wort *dihydroxyeicosatrienoic acids*) hydrolysiert werden, wobei DHETs generell als weniger biologisch aktiv als EETs gelten. EETs, und zu einem geringen Ausmass auch DHETs, sind in eine Vielzahl von physiologischen Prozessen involviert – allerdings ist wenig über ihre Rolle in synaptischer Transmission bekannt.

In dieser Arbeit wurde der Frage nachgegangen, ob, und wenn ja auf welche Weise, EETs und DHETs neuronale Erregung und synaptische Transmission modulieren. Wir konnten zeigen, dass insbesondere 11,12-EET und -DHET diese beiden Prozesse in hippokampalen Pyramidenzellen beeinflussen. Dabei dämpft 11,12-EET die Netzwerk-Aktivität, während 11,12-DHET diese erhöht. Diese Effekte werden mechanistisch über prä- und postsynaptisch lokalisierte Zielkanäle vermittelt. So aktiviert 11,12-EET einen postsynaptischen G-Protein gekoppelten einwärts rektifizierenden K^+ (GIRK) Kanal in CA1 Pyramidenzellen, was zur Hyperpolarisation der Zelle und dadurch zu reduzierter Erregung führt. Zudem verringert 11,12-EET die Freisetzung von Glutamat an der CA3-CA1 Synapse über verschiedene präsynaptische Mechanismen. 11,12-DHET wirkt den 11,12-EET-vermittelten Effekten interessanterweise entgegen und erhöht die exzitatorische Transmission, wie die Potenzierung von fEPSPs (*field excitatory postsynaptic potentials*) unter DHETs an der CA3-CA1 Synapse gezeigt hat.

Spannungs-gesteuerte K^+ Kanäle erschienen als wahrscheinlichste Zielkanäle für EETs und DHETs. $K_v1.1$ und 1.2 Kanäle finden sich auf der Präsynapse von Pyramidenzellen und regulieren die Freisetzung von Glutamat. $K_v4.2$ Kanäle sind hingegen in Dendriten exprimiert und beeinflussen die dendritische Erregungsleitung. Diese drei Kanal-Typen wurden in CHO- und HEK-Zellen exprimiert und der Effekt von 11,12-EET und –DHET auf diese untersucht. Die Wirkung von 11,12-DHET auf $K_v1.2$ und $K_v4.2$ wurde bei Einzelspannungen von +10 mV bzw. +40 mV gemessen. 11,12-DHET blockierte den $K_v1.2$ Kanal zu 11.92±3% bei einer

Testspannung von +10 mV und K_v4.2 zu 24.5±5.6% bei +40 mV. Im Gegensatz dazu erhöhte 11,12-EET K_v1.2-vermittelte Ströme um 4.9±1.5% bei einer Spannung von +10 mV. Zudem wurde der Effekt von 11,12-DHET auf K_v1.2 und K_v4.2 noch in einer Strom (I)-Spannungs (V)-Kurve untersucht, in der die Spannung in +10 mV-Inkrementen kontinuierlich bis +80 mV erhöht wurde. Hier blockierte 11,12-DHET K_v1.2-Kanäle zu 29.7±9% bei einer Spannung von +40 mV und K_v4.2-Kanäle zu 36.8±5.3% bei einer Spannung von +10 mV. Diese EET-vermittelte Aktivierung bzw. DHET-vermittelte Inhibition von K_v -Kanälen stimmt mit der von uns in hippokampalen Hirnschnitten beobachteten Netto-Wirkung der Fettsäuren überein, nachdem EETs dämpfend und DHETs potenzierend auf die exzitatorische Netzwerk-Aktivität wirken.

mEH und sEH beeinflussen nachhaltig das Verhältnis von EETs zu DHETs, da sie die Hydrolyse von ersterem zu letzterem katalysieren. Aufgrund der gegensätzlichen Wirkung von EETs und DHETs könnten Epoxidhydrolasen als eine Art Schalter zwischen Inhibition und Exzitation in Netzwerken fungieren. Wir testeten diese Hypothese, indem wir die basale Transmission in Hirnschnitten von gentechnisch veränderten Mäusen massen; diesen Mäusen fehlten entweder das sEH oder mEH Protein oder sie exprimierten eine mEH-Variante mit deutlich erhöhter Aktivität (mEH E404D) anstelle der WT mEH. Die basale synaptische Aktivität wurde in Form von Input-Output-Kurven ermittelt und war in Schnitten von mEH KO und sEH KO Mäusen deutlich reduziert im Vergleich zu WT Kontrollschnitten. Hingegen zeigten Schnitte von mEH E404D Mäusen erhöhte Aktivität im Vergleich zu WT Kontrollen. Das Fehlen von Epoxidhydrolasen, das zu einer Erhöhung der freien EET- und Reduktion der freien DHET-Konzentration relativ zu WT Kontrollen führt, geht mit gedämpfter exzitatorischer Transmission einher; erhöhte EH Aktivität, die zu erniedrigten EET- und erhöhten DHET- Konzentrationen führen sollte, geht mit erhöhter Transmission einher. Epoxidhydrolasen spielen folglich eine wichtige Rolle, wenn es darum geht, den Grad an Exzitabilität im ZNS zu bestimmen.

Im zweiten Projekt dieser Arbeit wurde die Rolle von CYP-Epoxygenase-generierten Fettsäure-Epoxiden in der Morphin-vermittelten Antinozizeption untersucht. sEH KO Mäuse sprachen deutlich länger und verstärkt auf subkutan appliziertes Morphin (Dosis: 1 mg/kg) an als WT Kontrollmäuse. Aufgrund des Fehlens der sEH reichern sich freie Fettsäure-Epoxide in sEH KO Mäusen in grösseren Mengen an als in WT Mäusen. Zu diesen Fettsäure-Epoxiden zählen EETs,

aber auch EpDPEs (*epoxydocosapentaenoic acids*) oder EpETEs (*epoxyeicosatetraenoic acid*). Diese Fettsäure-Epoxide könnten über eine Modulation des mu-Opioid-Rezeptors (MOR), über den Morphin hauptsächlich seine Wirkung entfaltet, die erhöhte Antinozizeption in sEH KO Mäusen verursachen. Wir untersuchten daher die Wirkung von 14,15-EET an in HEK-Zellen exprimierten MORs. Allerdings zeigte 14,15-EET weder allein appliziert, noch in Kombination mit dem selektiven MOR-Agonisten DAMGO irgendeine Wirkung. Folglich modulieren entweder andere Fettsäure-Epoxide wie EpDPEs oder EpETEs die Aktivität von MORs in sEH KO Mäusen oder HEK-Zellen fehlt eine essentielle molekulare Komponente, die für die erhöhte MOR Aktivität wesentlich ist.

Zusammengenommen zeigen unsere Resultate, dass EETs und DHETs als endogene Lipid-Signalmoleküle in der neuronalen Transmission wirken. Wahrscheinlich regulieren sie neuronale Erregung und synaptische Transmission, indem sie K^+ Kanäle aktivieren bzw. inaktivieren. In hippokampalen Pyramidenzellen dürften dies in erster Linie GIRK-Kanäle, $K_v1.2$- und $K_v4.2$-Kanäle sein. Zudem bieten die Resultate dieser Arbeit eine mechanistische Erklärung für die reduzierte Suszeptibilität von sEH KO Mäusen gegenüber Epilepsie-generierenden Pharmaka im Vergleich zu WT Kontrollmäusen.

Chapter 1

General Introduction

1.1. The hippocampal formation in mouse brain

The hippocampal formation (HF) is a well-characterized structure in terms of histology, connectivity, and electrophysiology, which makes it a suitable experimental system to study synaptic physiology. Therefore, mouse hippocampal slices were used as an experimental system in this dissertation to study the effect of lipid mediators on synaptic physiology. The following subsections will give a brief overview of mouse HF in terms of cytoarchitectonic organization, connectivity-information flow, and electrophysiological properties of the constituting neurons.

1.1.1. Neurotransmission in the hippocampus

Neurons in the hippocampus can be grouped into two categories based on their functionality, namely excitatory pyramidal cells (PCs) and the inhibitory interneurons (INs). PCs are excitatory and employ glutamate as the primary neurotransmitter, whereas INs are inhibitory and employ γ-aminobutyric acid (GABA) as the primary neurotransmitter (Taupin, 2007). Glutamate released at excitatory synapses can act on three ionotropic glutamate receptors, N-methyl-D-aspartate receptor (NMDAR), α-amino-3-hydroxy-5-methylisoxazole-4-propionic acid receptor (AMPAR) and kainate receptors (KAR) (Traynelis *et al.*, 2010). Ionotropic AMPARs, NMDARs, and KARs are expressed postsynaptically. At resting membrane potential, NMDARs are non-conducting due to the block produced by extracellular Mg^{2+}. Typically, activation of AMPARs leads to the inward flux of Na^{+} which results in depolarization of the postsynaptic membrane. This initial AMPARs-mediated depolarization removes the Mg^{2+} block of NMDARs which further allows an influx of Na^{+} as well as Ca^{2+} ions into the postsynaptic neuron. The AMPAR-, NMDAR- and KAR-mediated inward conductances of cations give rise to excitatory postsynaptic currents/potentials (EPSC/Ps). The inhibitory neurotransmitter GABA activates postsynaptic ionotropic $GABA_A$Rs, which conduct chloride currents. They give rise to inhibitory postsynaptic currents/potentials (IPSCs/Ps). Inhibitory INs can innervate PCs dendritically or perisomatically. INs, via dendritic and perisomatic inhibition, regulate input and output of PCs. Dendritic inhibition controls the efficacy of excitatory inputs, while perisomatic inhibition, particularly at the axon hillock, controls the generation of action potentials (Miles *et al.*, 1996).

1.1.2. Dentate gyrus granule cells and the mossy fiber synapse

Dentate gyrus granule cells (DGGCs) are tightly packed in the granule cell layer and have a typical cone-shaped tree of apical dendrites. The main afferents of DGGCs originate in the

EC layer II and synapse on the apical dendrites of DGGCs to form the perforant pathway (Amaral *et al.*, 2007). DGGCs send their main output to CA3 PCs through distinctive unmyelinated axonal projections called mossy fibers (Mfs). Mfs synapse on dendrites of CA3 PCs in a narrow zone termed *stratum lucidum*. Mf synapses are excitatory in nature and are unique in many aspects; most importantly, there are three different types of presynaptic terminals of DGGC axons: 1. Large mossy fiber boutons (MfBs); 2. Small filopodial extensions of MfBs and 3. *en passant* terminals *(Fig. 1.1*). These terminals are functionally specialized. Large MfBs selectively contact and excite CA3 PCs while filopodial extensions and *en passant* terminals contact and activate inhibitory INs (Danzer *et al.*, 2008). Mf synapses exhibit short-term plasticity in form of a large paired-pulse facilitation (PPF) with ratio>3 in most cases. Additionally, marked frequency facilitation is observed at Mf synapses. An increase in the frequency of stimulation from 0.5 Hz to 1 Hz results in several folds of potentiation in synaptic strength. The frequency facilitation observed at the Mf synapse is attributed to the low initial release probability of glutamate, which is presumably maintained via presynaptic A1 receptors (Nicoll *et al.*, 2005).

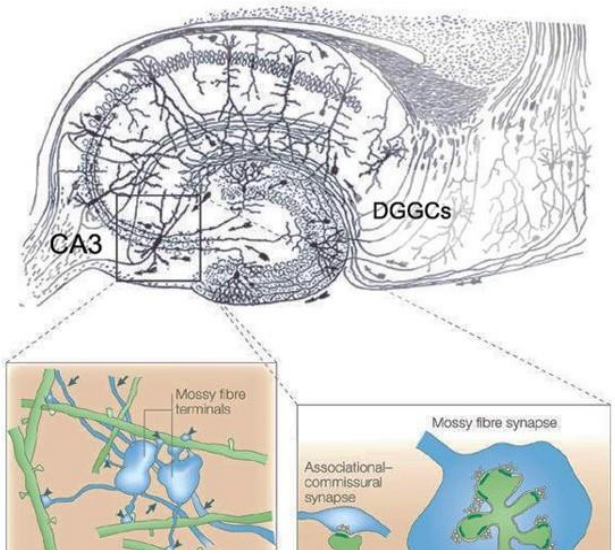

Fig.1.1. The Mf synapse, adapted from (Nicoll et al., 2005)

1.1.3. Hippocampal PCs and the Schaffer collateral-CA1 synapse

CA3 and CA1 PCs have pyramidal shaped somas, which are tightly packed in the pyramidal cell layer. Both CA3 and CA1 PCs give rise to basal and apical dendritic trees studded with dendritic spines on which they receive inputs. CA3 PCs have an additional specialized class of spines called 'thorny excrescences' on which they receive input from the Mf pathway. CA3 PCs send axonal fibers to CA1 PCs to form Schaffer collaterals (SCs), which synapse on basal and apical dendrites *(Fig 1.2).*

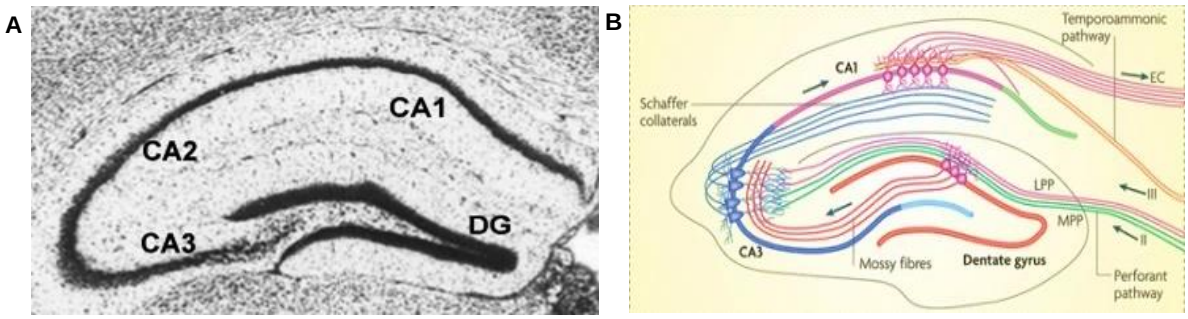

Fig.1.2. **(A)** Hippocampal CA fields and **(B)** Schematic showing hippocampal connectivity between CA fields, adapted from (Deng *et al*., 2010)

In addition, CA1 PCs receive input from different parts of the entorhinal cortex (EC) depending on the location of the PC on the transverse axis. CA1 PCs also project extensively to the adjoining subiculum (Andersen, 2007).

1.1.4. Field recordings in the hippocampus

Field excitatory postsynaptic potential recordings (fEPSPs) are extracellular recordings from populations of neurons as opposed to the conventional intracellular recording from single neurons. The hippocampus is amenable to extracellular field recordings due to the following reasons:

Since dendrites and axons of PCs and DGGCs are arranged in a parallel manner, activation of neighboring synapses adds up their effect linearly, giving rise to a cumulative change in the extracellular potential. Synaptic currents flow into the dendrites of the activated region and generate a so-called 'current sink', while they exit at the somas generating a so-called 'current source'. For example, stimulation of SCs generates negative fEPSPs in *stratum radiatum* (a current sink), while the polarity reverses as the recording electrode moves closer to the soma (current source) with respect to the ground electrode (Andersen, 2007). The sub-threshold stimulation of afferents, below the threshold to fire action potentials (AP) in target neurons, gives rise to the summation of pure synaptic events, field excitatory postsynaptic potentials (fEPSPs). The fEPSP signal contains two parts, the smaller downward deflection called fiber volley, which is followed by the larger downward deflection, the actual field. The fiber volley reflects the pre- and the field the postsynaptic component, respectively *(Fig. 1.3A-B)*. Further increase in stimulation intensity eventually stimulates the target neurons to fire APs and gives rise to a synchronous discharge called 'population spike' *(Fig. 1.3C)*. (Andersen, 2007; Buzsáki *et al.*, 2012).

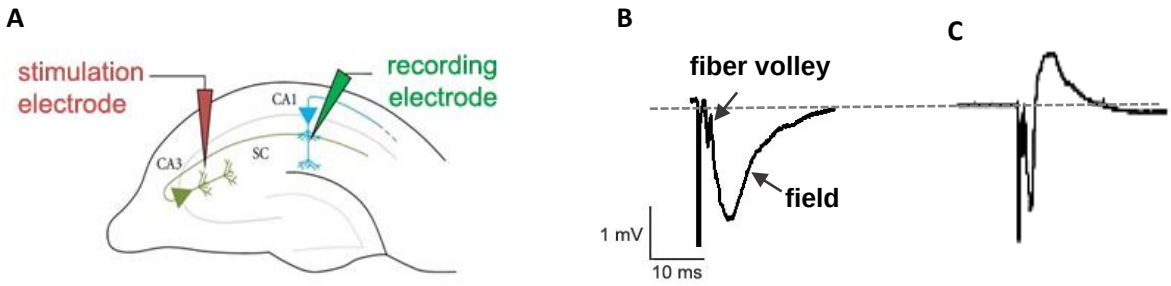

Fig. 1.3 (A) Schematic showing the site of stimulation and recording for fEPSP. Representative examples of a fEPSP and a population spike are shown in **(B)** and **(C)**, respectively.

1.1.5. Modulators of synaptic transmission

1.1.5.1. G-protein-coupled receptors (GPCRs)

GPCRs or metabotropic receptors are the largest and most diverse class of membrane proteins and characteristically consist of seven hydrophobic transmembrane domains. GPCRs are coupled to receptor-specific heterotrimeric G-proteins: α-, β- and γ-subunits. GPCRs, on ligand binding, activate associated G-proteins, which through intracellular secondary messengers produce cellular effects (Borroto-Escuela *et al.*, 2017). Associated G_{α} proteins such as $G_{\alpha q}$, $G_{\alpha s}$ can stimulate downstream signaling, $G_{i/o}$ inhibit downstream signaling.

A. Cannabinoid receptors

Endocannabinoids are arachidonic acid (AA)-derived endogenous metabolites and act as key modulators of synaptic functions. Endocannabinoids are synthesized *in situ* in an activity-dependent manner from AA, which is released from the neuronal membrane. N-arachidonoyl ethanolamine (anandamide) and 2-arachidonoyl glycerol (2-AG) are the two best-investigated endocannabinoids. Endocannabinoids are synthesized in the postsynaptic neuron and act on cannabinoid 1 (CB1) receptors, expressed on the presynaptic neuron, thus acting in a retrograde manner. Activation of presynaptic CB1 receptors suppresses the neurotransmitter release at glutamatergic as well as GABAergic synapses. CB1 receptors are coupled to the $G_{\alpha i/o}$ protein, from which the βγ subunit dissociates and presumably blocks voltage-gated calcium channels (VGCChs) (Castillo *et al.*, 2012). Endocannabinoid-mediated suppression of GABA release via retrograde signaling was termed depolarization-induced suppression of inhibition (DSI), while endocannabinoid-mediated suppression of glutamate release termed as depolarization-induced suppression of excitation (DSE) (Diana *et al.*, 2004). After eliciting pharmacological actions, endocannabinoids are promptly degraded by fatty acid amide

hydrolase (FAAH) and monoacylglycerol lipase (MAGL). FAAH and MAGL hydrolyze anandamide and 2-AG, respectively (Jhaveri *et al.*, 2007).

B. Opioid receptors

Mu- (MORs) and delta-opioid receptors (DORs) are GPCRs and the major opioid receptors activated by a family of pituitary-derived endogenous neuropeptides called endorphins. In the hippocampus, MORs and DORs are predominantly expressed on GABAergic interneurons projecting on the perisomatic and dendritic area of CA1 PCs, respectively (Erbs *et al.*, 2015; Svoboda *et al.*, 1999). On a cellular level, MORs are expressed in both axon terminals and in the somatodendritic compartment of interneurons (Drake *et al.*, 1999). MORs are coupled to $G_{i/o}$ proteins and generate site-dependent effects. Activation of axonal MORs suppresses the release of GABA from GABAergic terminals via Gβγ-mediated inhibition of VGCChs; activation of somatodendritic MORs activates G-protein coupled inwardly rectifying K^+ (GIRK) channels presumably via interaction with Gβγ protein, which results in hyperpolarization of PCs (Al-Hasani *et al.*, 2011; Svoboda *et al.*, 1999). MOR-mediated suppression of GABA release results in the prolongation of excitatory activity in the hippocampus through disinhibition of PCs (McQuiston *et al.*, 2003; Zieglgansberger *et al.*, 1979).

In addition to endorphins, exogenous opioids such as morphine and DAMGO activate opioid receptors with differential affinity and efficacy. Compared to morphine, DAMGO acts as a full and selective agonist on MORs (Onogi *et al.*, 1995). Prolonged and repeated exposure to agonists can result in progressively decreased efficacy of MOR activation, leading to a phenomenon known as 'tolerance'. The underlying molecular mechanisms of tolerance remain uncertain, but there is accumulating evidence linking it to MOR desensitization phosphorylation, arrestin association, endocytosis and recycling (Dang *et al.*, 2012). Prolonged morphine exposure results more rapidly in the development of tolerance compared to that of DAMGO (Williams *et al.*, 2013).

1.1.5.2. Voltage-gated potassium channels (VGPChs)

VGPChs have emerged as important regulators of synaptic transmission. Structurally, VGPChs are constituted of homo- or heterotetramer of pore-forming α-subunit isoforms. The stoichiometry of these α-subunits fine-tune the conductance and kinetic properties of the resulting channel (Coleman *et al.*, 1999; Wang *et al.*, 1993). Moreover, accessory subunits such as $K_v\beta$ can co-assemble with heteromultimeric channels to influence the gating

properties, axonal/somatodendritic targeting and surface expression of the associated VGPChs (Pongs *et al.*, 2010; Rhodes *et al.*, 1997). Based on their sub-cellular localization VGPChs exert different effects: When localized to the somatodendritic compartment they might alter the integration of synaptic inputs. By contrast, VGPChs present in axon terminals may modulate the shape of incoming APs and thus impact the release of neurotransmitter (Trimmer, 2015).

Recent studies have shown that CA1 and CA3 dendrites express VGPChs including those from the K_v4 subfamily (Spruston, 2008). The expression density of K_v4 shows a linear increase with the distance from cell soma of the hippocampal CA1 PCs (Hoffman *et al.*, 1997). These K_v4 channels conduct rapidly inactivating transient A-type (I_A) potassium currents, which modulate negatively the backpropagation of APs, the firing frequency, and integration of synaptic inputs in the hippocampal PCs (Fransén *et al.*, 2010; Hoffman *et al.*, 1997). Moreover, blocking of I_A current increases temporal summation of the postsynaptic potential and thus the intrinsic neuronal excitability in rat CA1 PCs (Rathour *et al.*, 2016).

VGPChs from the K_v1 subfamily are predominantly expressed in axonal initial segments and presynaptic terminals. They regulate spike frequency/duration and neurotransmitter release from axon terminals (Trimmer, 2015). $K_v1.1$, 1.2 and 1.4 are the most common isoforms expressed in hippocampal PCs. In terms of stoichiometry, $K_v1.1$ almost always heteromerizes either with $K_v1.2$ or in some instances with $K_v1.4$ and gives rise to the so-called D-type currents (I_D) (Ovsepian *et al.*, 2016; Wang *et al.*, 1993). Axonal K_v1 channels are important regulators of axonal AP generation and conduction along the axon proper to presynaptic terminals (Kole *et al.*, 2012). Blocking of axonal K_v1 channels with a local puff of the K_v1-specific blocker Dendrotoxin (DTx), with a laser or via mechanical axotomy significantly increases excitability recorded in the soma of CA3 PCs (Rama *et al.*, 2017). Moreover, $K_v1.1/1.4$ channels, which are expressed in the presynaptic terminals of Mfs, regulate the release of glutamate by controlling Ca^{2+} influx into MfBs (Geiger *et al.*, 2000). Additionally, the loss of function mutations in the human *KCNA1* gene is linked to the hyperexcitability disorder epilepsy, further pointing towards a crucial role for K_v1 channels in the regulation of neuronal excitability (Ovsepian *et al.*, 2016).

There are a few other K_v channels such as K_v3 channels and calcium-activated BK (BK_{Ca}) channels, which are expressed in presynaptic axon terminals. However, their potential contribution to glutamate release has not been determined or found to be non-significant at basal transmission level (Hu *et al.*, 2001; Trimmer, 2015).

1.2. Polyunsaturated fatty acids and their function in the CNS

Polyunsaturated fatty acids (PUFAs) are fatty acids (FAs) that contain more than one double bond in their backbone. Based on the position of the double bond from the methyl end, they are subdivided into omega-3 and omega-6 FAs. Omega-3 FAs include α-linolenic acid (ALA), eicosapentaenoic acid (EPA) and docosahexaenoic acid (DHA), while omega-6 FAs include linoleic acid (LA) and arachidonic acid (AA). In mammals, AA cannot be biosynthesized *de novo* from acetyl-CoA; it is biosynthesized from its precursor LA. LA is an essential FA and needs to be supplemented through diet. Consumed PUFAs are absorbed from the gastrointestinal tract and packaged into hepatic lipoproteins and transported to the brain via cardiovascular circulation, however, the precise mechanism of transport across the blood-brain barrier (BBB) remains controversial (Mitchell *et al.*, 2011). In brain, AA and DHA are the most important and biologically relevant FAs (Bazinet *et al.*, 2014). AA is typically esterified to the *sn-2* position of glycerophospholipids of the plasma membrane and the endoplasmic reticulum (ER). It is released by cytoplasmic phospholipase A_2 ($cPLA_2$), an intracellular calcium-dependent enzyme that selectively hydrolyzes the *sn-2* ester bond (Farooqui *et al.*, 2004; Farooqui *et al.*, 1997). Activation of $cPLA_2$ is coupled to a number of stimuli, including depolarization-induced increase in intracellular calcium, activation of serotoninergic, dopaminergic and cholinergic receptors or pathological processes such as ischemia, inflammation, and excitotoxicity (Bazinet *et al.*, 2014). Activity-dependent $cPLA_2$-mediated release of AA is a major source of free AA in neurons. Free AA can participate directly in signaling or serve as a precursor for the synthesis of a plethora of bioactive molecules (Bazinet *et al.*, 2014).

The reported plasma concentration of free AA is in the lower micromolar range (Abdelmagid *et al.*, 2015; Brash, 2001; Elinder *et al.*, 2017; Shinde *et al.*, 2012). However, these concentrations are not a useful indicator of local concentration at the potential site of action or in a given microenvironment. Pathological events such as ischemia, hypoxia, and experimentally-induced epilepsy dramatically increase plasma AA concentration by several folds (Bazan *et al.*, 1986; Bazán, 1970; Gardiner *et al.*, 1981; Siesjö *et al.*, 1989).

To make matters more complex, AA can be either re-esterified or metabolized further Specifically, AA can be oxidized by three distinct enzymatic systems, namely by cyclooxygenases (COX), lipoxygenases (LOX) and cytochrome P450 (CYPs) monooxygenase *(Fig. 1.4)* (Spector *et al.*, 2004). COX oxidizes AA to unstable cyclic endoperoxide intermediates, prostaglandins H_2 (PGH_2), which serve as precursors for various

other prostaglandins such as PGD_2, PGE_2, PGI_2 and thromboxanes (TxA_2). LOX metabolizes AA to hydroperoxyeicosatetraenoic acids (HpETEs) and hydroxyeicosatetraenoic acids (HETEs) and subsequently to lipoxins and leukotrienes (Samuelsson, 1987). COX and LOX derivatives have been studied extensively and are implicated in several pathophysiological processes (Funk, 2001; Harizi *et al.*, 2008). The CYP-epoxygenase pathway is the least explored, however, in recent years, numerous studies have added to a better understanding.

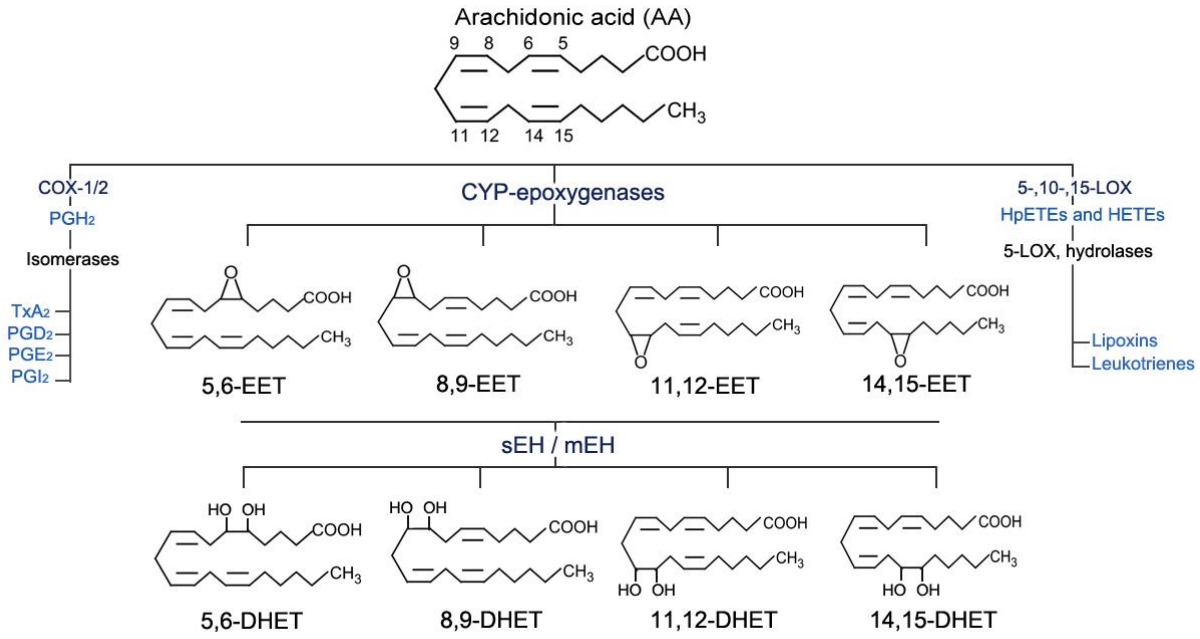

Fig. 1.4 COX, LOX and CYP-epoxygenases pathway of AA metabolism

1.2.1. Effects of AA in the CNS

Earlier studies suggested that AA or one of its metabolites may modulate synaptic transmission, particularly long-term potentiation (LTP). LTP is characterized by a persistent increase in synaptic strength following high-frequency stimulation and is considered instrumental for learning and memory (Lynch *et al.*, 1989; Williams *et al.*, 1989). PLA_2 activation is critical for the expression, but not for the maintenance of LTP in the CA1 region of the hippocampus (Massicotte *et al.*, 1990). Moreover, *in vivo* studies corroborated the involvement of AA or its metabolites on LTP and thus in learning and memory. In rats, pharmacological inhibition of PLA_2 in combination with the inhibition of nitric oxide synthase activity impaired spatial memory performance in the Morris water maze (Hölscher *et al.*, 1995). Similarly, specific inhibition of PLA_2 activity diminished memory retrieval after avoidance training in rats (Schaeffer *et al.*, 2007).

These effects of PLA_2 inhibition on LTP were further evaluated experimentally by employing exogenous AA. Application of AA enhanced LTP, generated by weak stimulation of the perforant path in anesthetized rats and in rat hippocampal slices; co-application of a LOX inhibitor did not antagonize the effect of AA (Williams *et al.*, 1989). Consistent with these findings, AA in presence of weak tetanic stimulation produced long-lasting potentiation in the CA1 region of the hippocampus. However in this case, the effect of AA was antagonized by a LOX inhibitor, suggesting the potential contribution of LOX metabolites (Drapeau *et al.*, 1990). Moreover, some reports implicated COX metabolites in the regulation of synaptic transmission and LTP (Sang *et al.*, 2005; Sang *et al.*, 2007).

The notion of AA acting as a 'retrograde messenger' was proposed and explored by several earlier studies (Lynch *et al.*, 1991; Lynch *et al.*, 1993; Williams *et al.*, 1989) and countered by others (Fitzsimonds *et al.*, 1998; O'dell *et al.*, 1991). However, more recently convincing evidence for AA acting as retrograde messenger was presented: In a study by Carta and colleagues, AA released from postsynaptic CA3 PCs blocked presynaptic K_v channels on Mf boutons. This resulted in robust facilitation of excitatory neurotransmission at the Mf-CA3 synapse in mouse hippocampus (Carta *et al.*, 2014).

1.2.2. Molecular targets of AA

AA effects in the CNS are attributed to the potential modulation of classical voltage-gated ion channels such as voltage-gated sodium channels (VGSChs), VGCChs and VGPChs in combination with other ion channels including the transient receptor potential (TRP), store-operated calcium entry (SOCE) channels and two-pore domain K^+ (K_2P) channels (Boland *et al.*, 2008; Kim, 2003; Meves, 2008; Schmitt *et al.*, 1995). AA and most other PUFAs decrease the availability of VGSChs, resulting in an increased threshold for AP firing in cells such as cardiac myocytes (Kang *et al.*, 1995). Moreover, AA inhibits L-type, T-type, and N-type calcium channels in excitable cells (Boland *et al.*, 2008; Schmitt *et al.*, 1995).

In particular, VGPChs such as $K_v4.x$ and $K_v1.x$ are modulated by AA. AA and its non-metabolizable analog 5,8,11,14-eicosatetraynoic acid (ETYA) inhibit the amplitude of peak I_A currents in oocytes (Villarroel *et al.*, 1996) and native neurons (Meves, 2008). AA and ETYA inhibit I_A currents and enhance the amplitude of back-propagating APs in CA1 PCs (Colbert *et al.*, 1999). AA not only blocks the peak I_A, but also significantly increases the I_A inactivation in neurons (Boland *et al.*, 2008). However, this effect of AA on kinetics was absent in heterologously expressed K_v channels. Evidently, co-expression of accessory K_v channel interacting proteins (KChIPs) is required for the modulatory effect of AA on I_A

kinetics (Holmqvist *et al.*, 2001). Moreover, 10 µM of AA applied extracellularly exert a similar effect as 1 pM of AA applied intracellularly; the former blocks I_A by 54.3±7% (Holmqvist *et al.*, 2001), the latter by 56.5±8%, respectively (Bittner *et al.*, 1999). Thus, the LTP-potentiating effect of AA can be at least partly attributed to its ability to inhibit I_A currents (mediated by K_v4 channels) in hippocampal PCs (Ramakers *et al.*, 2002).

Presynaptically, AA most probably blocks $K_v1.x$ channels, which are known to regulate glutamate release (Trimmer, 2015). Inhibition of presynaptic K_v channels in MfBs by AA broadens presynaptic APs and enhances glutamate release to facilitate synaptic transmission (Geiger *et al.*, 2000; Carta *et al.*, 2014). Moreover, AA inhibits $K_v1.4$ channels heterologously expressed in HEK-293T cells (Angelova *et al.*, 2009). Finally, AA is capable of endowing non-inactivating K_v1 channels with an uncharacteristic voltage-dependent inactivation and as such converts I_D currents into inactivating transient I_A currents (Oliver *et al.*, 2004).

The exact molecular mechanism underlying AA-mediated modulation of VGPChs is not well understood to date. AA-mediated effects on A-type VGPChs are not occluded by the classical pore blocker tetraethylammonium (TEA) chloride, suggesting the involvement of alternate mechanism(s) or sites (Oliver *et al.*, 2004). Moreover, AA-mediated inhibition of I_A was abolished in the presence of an antioxidant, suggesting the involvement of oxidative pathways (Angelova *et al.*, 2006). Alternatively, the esterification of AA into the lipid membrane and the resulting alteration of membrane fluidity might influence the activity of channels (Boland *et al.*, 2008). Potential binding sites for PUFAs (termed PUFA 1-5) have been proposed to be located on VGPChs; specific lipoelectric interaction with these sites might possibly underlie the AA effects on these channels (Elinder *et al.*, 2017).

1.2.2.1. The cytochrome P450 monooxygenase-derived eicosanoids

CYPs are a superfamily of heme-containing enzymes, which catalyze the addition of oxygen to the aliphatic position of diverse chemical entities and are thus also referred to as monooxygenases. NADPH-CYP-reductase (CPR) and cytochrome-b5 together with NADH-b5-reductase are indispensable for CYP-mediated monooxygenation reactions. CYPs are traditionally known for their role in xenobiotic metabolism of structurally diverse compounds ranging from environmental carcinogens/toxins to xenobiotic small molecule drugs such as isoniazid, fluoxetine or complex antibiotics such as rifampicin. They are most abundantly expressed in liver, the major site of xenobiotic metabolism, but also in extrahepatic tissue such as brain. Importantly, CYPs are also capable of oxidizing endogenous compounds such as FAs (Persson *et al.*, 2014).

CYP isozymes capable of epoxygenating membrane-derived AA are collectively termed CYP-epoxygenases. CYP-epoxygenases oxidate AA by inserting an oxygen atom at one of the four double bonds of AA, which results in the generation of four distinct regioisomers: 5,6-, 8,9-, 11,12- and 14,15-EET. Several CYP isoforms are capable of epoxygenation of AA, including CYP-1A, CYP-2B, CYP-2C, CYP-2D, CYP-2J, CYP-4F (Kaspera *et al.*, 2009) and the human orphan isoform CYP-4x1 (Stark *et al.*, 2008). However, members from the CYP-2C and -2J family are most noted for their epoxygenase activity (Iliff *et al.*, 2010).

CYP-isozymes exhibit specific preferences for generating regioisomer(s) and/or stereoisomer(s) of EET(s). This results in CYP-isozyme-specific mixtures of EET regio/stereoisomers (Rifkind *et al.*, 1995). For example, purified CYP-2C8 from human liver generates 11,12- and 14,15-EET in a 1:1.25 ratio. By contrast, human CYP-2C9 produces 8,9-, 11,12- and 14,15-EET in a ratio of 2.3:1.0:0.5. Generally, 11,12- and 14,15-EET seem to be the main EET regioisomers in most mammalian tissues, as 11,12- and 14,15-EET account for 67–80% of total EETs synthesized by the major CYP-epoxygenases CYP-2C8, CYP-2C9, and CYP-2J2 (Spector *et al.*, 2015). The stereoselectivity of these enzymes also varies in an isoform-specific manner with CYP-2C8 producing the *(S, R)*- and *(R, S)*-11,12-EET stereoisomers in a 20:80 ratio, while CYP-2C9 produces them in a 70:30 ratio (Daikh *et al.*, 1994).

1.2.3. CYP-epoxygenases in the CNS

CYP-epoxygenated AA-metabolites were first reported in anterior pituitary cells of rat brain (Snyder *et al.*, 1983). Following studies reported the biosynthesis of EETs by vascular endothelium (Amruthesh *et al.*, 1992; Medhora *et al.*, 2001) and astrocytes (Alkayed *et al.*, 1996) and suggested an important role for EETs in cerebrovascular function (Iliff *et al.*, 2010). The following CYP-epoxygenase isoforms have been identified in the mouse brain at transcript and/or protein level: CYP-2C, CYP-2J and CYP-4x1 (Al-Anizy *et al.*, 2006; Iliff *et al.*, 2010). CYP-2C immunoreactivity (IR) was detected in rat hippocampal PCs (Riedl *et al.*, 2000) and CYP-2J transcripts were found in the mouse hippocampus [*Allen brain atlas*, (Lein *et al.*, 2007)]. Moreover, microsomal preparations derived from mouse hippocampus are capable of synthesizing EETs *in vitro* (Marowsky *et al.*, 2009). The majority of CYPs are localized in the ER with only a few CYPs located in mitochondria (Bhagwat *et al.*, 1995; Iscan *et al.*, 1990; Omura, 2006).

1.2.4. Modulation of CYP-epoxygenase activity

Many chemicals known to modulate hepatic CYP expression/activity also modulate CYPs expressed in the brain. For example, phenobarbital induces the expression of CYP-2B in rat liver as well as in brain (Schilter *et al.*, 2000). Moreover, the aromatic hydrocarbon receptor (AHR) activator, 2,3,7,8-tetrachlorodibenzo-p-dioxin (TCDD) induces CYP-1A transcription and in turn increases epoxygenase products of AA *in vivo* (Diani-Moore *et al.*, 2014). CYP induction can also be organ-specific, as chronic nicotine treatment induces the drug metabolizing CYP-2D isoform in monkey brain, but not in liver (Mann *et al.*, 2008). Doxorubicin treatment leads to upregulation of CYP-epoxygenases and a concomitant increase in EETs production in rat kidney while an increase in CYP-mediated ω-hydroxylation products (20-HETE) was observed in rat liver (Zordoky *et al.*, 2011).

Genetic polymorphisms also influence CYP activity and potentially EETs biosynthesis. Genetic polymorphisms of CYP-epoxygenases are associated with the risk of cardiovascular diseases. The *CYP-2J2* polymorphism rs890293, which leads to the reduced expression of *CYP-2J2* mRNA, is associated with an increased risk of coronary artery diseases (Spiecker *et al.*, 2004) and premature myocardial infarction (Liu *et al.*, 2007). Moreover, allelic variants of *CYP-2C9* with reduced activity is associated with higher risk of myocardial infarction (Visser *et al.*, 2007). The *CYP-2J2* rs890293 polymorphism has been associated with an increased risk of late-onset Alzheimer's disease in Chinese population (Yan *et al.*, 2015).

1.2.5. The biological fate of EETs

The majority of biosynthesized EETs are re-esterified into membrane glycerophospholipids. The functional implication of EETs incorporation is not completely clear, but membrane lipids may act as a temporary storage for EETs until they can be released on demand (Spector *et al.*, 2004). Other pathways of EETs metabolism include binding to fatty acid binding proteins (FABPs) (Widstrom *et al.*, 2001), beta-oxidation, chain elongation and glutathione conjugation (Spector *et al.*, 2004). However, enzymatic hydrolysis of EETs by epoxide hydrolases represents the major pathway of EETs metabolism.

1.2.6. Soluble and microsomal epoxide hydrolase

Epoxide hydrolases (EHs) comprise a family of enzymes that catalyze the hydration of electrophilic epoxides by adding a water molecule to form the corresponding vicinal diols. (Arand *et al.*, 2005). The first EH to be characterized was mammalian microsomal EH (mEH, encoded by EPHX1) (Oesch, 1973), followed by soluble EH (sEH, encoded by EPHX2)

(Hammock *et al.*, 1976). Recently, two new members, EH3 and EH4 were added to the EH family (Decker *et al.*, 2012). Both mEH and sEH are involved in the detoxification of potentially carcinogenic epoxides with differential efficacy and substrate specificity (Decker *et al.*, 2012). Furthermore, sEH has received a lot of attention for its role in metabolizing bioactive endogenous epoxy FAs such as EETs to their corresponding diols (El-Sherbeni *et al.*, 2014). mEH was considered mainly as detoxifying enzyme until recent evidence showed that mEH is also involved in turnover of endogenous FA epoxides and might play important physiological roles (Marowsky *et al.*, 2017). Although sEH and mEH catalyze the same reaction, they differ in tissue expression, subcellular localization, substrate preferences and/or functions.

mEH is an ER-resident enzyme anchored to the membrane by a single N-terminal anchor. It hydrolyzes a very broad range of structurally diverse epoxides, ranging from drug epoxide intermediates such as carbamazepine-10,11-epoxide to procarcinogenic epoxides such as styrene-7,8-oxide and epoxides derived from polycyclic aromatic hydrocarbons like naphthalene and anthracene. *Cis*-substituted lipophilic epoxides are excellent substrates for mEH, while *trans*-substituted epoxides such as *trans*-stilbene oxide are poorly metabolized by mEH (Decker *et al.*, 2009).

sEH is primarily localized in the cytosol except in a few cell types (e.g. proximal renal tubule cells), where it is found in the cytosol and peroxisomes (Marowsky *et al.*, 2010). Unlike mEH, sEH inactivates both *cis*- and *trans*-substituted epoxides, provided the side chains are not excessively bulky as in *trans*-diphenyl-propene oxide and *trans*-stilbene oxide (Arand *et al.*, 2005; Decker *et al.*, 2009). Moreover, sEH is a bifunctional enzyme with its C-terminal domain exhibiting EH activity and its N-terminal domain exhibiting phosphatase activity (Cronin *et al.*, 2003).

1.2.7. sEH and mEH expression in the CNS

In human brain, mEH immunoreactivity (IR) is found in neurons and some astrocytes in the substantia nigra, raphé nuclei, pons, locus coeruleus, vestibular nuclei, motor nuclei and in the thalamus (Farin *et al.*, 1993). sEH IR is detected in neurons, with particularly strong IR found in cerebral cortex, in oligodendrocytes and smooth muscle cells surrounding arterioles in human brain (Sura *et al.*, 2008). Conflicting data have been presented for the mouse brain. Zhang and colleagues detected sEH in cell bodies of striatal and cortical neurons and in cerebral blood vessels (Zhang *et al.*, 2007). However, our group found sEH protein to be mainly located in astrocytes throughout the whole mouse brain and in neurons of the central

amygdala. In contrast, mEH was found to be strongly expressed in several neuronal subtypes, including hippocampal PCs with the strongest expression observed in CA3 PCs, mossy cells, and DGGCs. Furthermore, mEH IR was detected in striatal neurons and in neurons of the central amygdala. Non-neuronal expression of mEH was detected in cells of the choroid plexus, endothelial cells and smooth muscle cells (Marowsky *et al.*, 2009).

1.2.8. Modulation of sEH and mEH activity

Several inducers and repressors have been reported for both sEH and mEH. Expression of hepatic mEH is induced by phenobarbital, methylcholanthrene, polychlorinated biphenyls, *trans*-stilbene oxide, peroxisome proliferators and heavy metals (Newman *et al.*, 2005). Suppression of hepatic mEH activity has been reported in alloxan or streptozotocin-induced diabetes model in rats (Thomas *et al.*, 1989). Moreover, glucocorticoid treatment markedly down-regulates the mEH gene; this effect has been directly attributed to the interactions with the 50-flanking sequence of the *Ephx1* gene (Bell *et al.*, 1990).

Similarly, sEH expression is modulated by several compounds. Clofibrate, an activator of peroxisome proliferator-activated receptor-α (PPARα), induces sEH activity in rodent liver (Hammock *et al.*, 1983). Moreover, the potent endogenous vasoconstrictor Angiotensin-II upregulates sEH expression in rat vascular endothelial cells *in vitro* and *in vivo* (Ai *et al.*, 2007). Interestingly, sEH expression shows sexual dimorphism in an organ-specific manner: Expression of sEH in rat kidneys is 283% higher in males than in females, while a difference of only 55% was observed in rat liver (Pinot *et al.*, 1995). However, no indication for sexual dimorphism has been observed in mouse brain. (Marowsky *et al.*, 2009).

Human mEH and sEH genes are also subjected to genetic polymorphism. Several alleles have been identified with moderate effects on the enzyme half-life (Hosagrahara *et al.*, 2004; Przybyla-Zawislak *et al.*, 2003; Sandberg *et al.*, 2000). mEH polymorphisms are often linked with an increased susceptibility to develop different types of cancers. For instance, the single nucleotide polymorphism (SNP) (rs1051740, T337>C in exon 3 leading to 113Tyr->His), leading to an increased mEH activity, has been associated with an elevated risk to develop exposure-related lung carcinoma (Václavíková *et al.*, 2015). Apart from cancer, this polymorphism has been linked to the increased risk of pre-eclampsia (Zusterzeel *et al.*, 2001) and perinatal mortality (Raijmakers *et al.*, 2004). By contrast, slower mEH variants were correlated with increased susceptibility to emphysema (Smith *et al.*, 1997). sEH polymorphisms have been linked to vascular diseases among others. The R287Q SNP with lower sEH activity was linked to the reduced risk of coronary heart disease and K55R, a SNP

with decreased phosphatase activity, was linked to the reduced risk of ischemic stroke (Harris *et al.*, 2013).

1.2.9. The role of sEH and mEH in the hydrolysis of EETs

sEH hydrolyzes FA epoxides such as EETs and epoxy-octadecenoic acids (EpOMEs) to their supposedly less active diols, dihydroxyeicosatrienoic acid (DHETs) and dihydroxy-12Z-octadecenoic acid (DiHOMEs), respectively. Although mEH is predominantly considered as a detoxifying enzyme, a very old study reported endogenous substrates for mEH such as steroid estroxide and androstene oxide (Vogel *et al*., 1982). More recently, mEH was found to also metabolize FA epoxides such as EETs and EpOMEs. Indeed, recent evidence points toward a substantial contribution of mEH to the metabolism of FA epoxides (Marowsky *et al.*, 2009; Marowsky *et al.*, 2017). Although mEH and sEH both metabolize FA-derived epoxides, they differ substantially in their activity and preference.

Based on the catalytic efficiency (k_{cat}/K_m), mouse mEH prefers 11,12-EET >8,9-EET =14,15-EET >>5,6-EET, while mouse sEH prefers 14,15-EET =11,12-EET >8,9-EET >5,6-EET (*Table 1.1*). (Marowsky *et al.*, 2009). The catalytic efficiency of sEH is orders of magnitude higher than the one of mEH for all EET regioisomers. sEH is a faster enzyme at saturating substrate concentration as indicated by a higher V_{max} (maximum velocity). For instance, sEH hydrolyzes 20,000 nmol/mg/min of its favored substrate, 14,15-EET. By contrast, mEH only hydrolyzes 130 nmol/mg/min of its preferred substrate, 11,12-EET. Owing to its higher activity, sEH presumably metabolizes the bulk of EETs under saturating conditions. Nevertheless, mEH has a higher apparent affinity for EETs under non-saturating conditions as indicated by a lower K_m (K_m: the substrate concentration at which the reaction rate is half of its maximum value) compared to sEH (Marowsky *et al.*, 2009). In acutely dissociated mouse hippocampal cells, mEH contributed considerably to the turnover of 11,12-EET (25%) and 8,9-EET (20%), but far less to the turnover of 14,15-EET (5%) (Marowsky *et al.*, 2009). In addition to sEH and mEH, the newly identified EH3 also exhibits appreciable EET-metabolizing capability. However, its contribution to EET metabolism in mouse brain has yet to be determined (Decker *et al.*, 2012).

Table 1.1 Kinetic parameters of EETs turnover by recombinant mouse EHs [adapted from (Marowsky *et al.*, 2009)]. K_m1 and 2 in table refer to the first and second association of a substrate molecule to the homodimeric sEH, respectively.

	Recombinant mouse mEH			**Recombinant mouse sEH**		
substrates	**V_{max} [nmol/mg/ min]**	**K_m [µM]**	**$k_{cat.}/K_m$ [$M^{-1}\times s^{-1}$]**	**V_{max} [nmol/mg/ min]**	**K_m1*(K_m2) [µM]**	**$k_{cat.}/K_m$* [$M^{-1}\times s^{-1}$]**
5,6-EET	5	1	5×10^3	300	6 (12)	5×10^4
8,9-EET	100	1	1×10^5	2400	2 (11)	5×10^5
11,12-EET	130	0.5	2×10^5	11,000	0.6 (6)	5×10^6
14,15-EET	25	0.25	1×10^5	20,000	2 (20)	5×10^6

Pharmacological inhibition of sEH has been proven to be an efficient strategy to enhance EET levels and in turn decrease the production of DHETs. This altered EET:DHET ratio translates into several beneficial therapeutic effects (Imig *et al.*, 2009). Therefore, sEH emerged as a therapeutic target and a diverse class of chemical entities including amides, ureas, thioamides, thioureas, carbamates, and acyl hydrazones were developed as sEH inhibitors (sEHis) (Shen, 2010). sEHis are widely employed to study the role of EETs *in vivo* in experimental animals; they are also explored as potential clinical therapeutics for several vascular disorders (Ingraham *et al.*, 2011; Imig *et al.*, 2009).

1.3. The role of EETs in the CNS

1.3.1. EETs and the vascular system

EETs are best known for their vasodilatory potential and their role in neurovascular coupling. Neurovascular coupling refers to the increase in local blood flow in response to increased neuronal activity (functional hyperemia). It involves neurons, glia, and vascular cells (Imig *et al.*, 2011). Astrocytes as well as endothelial cells are probably capable of generating EETs (Alkayed *et al.*, 1996; Medhora *et al.*, 2001). Astrocyte-derived EETs dilate blood vessels via activating BK_{Ca} channels in vascular smooth muscles (Imig *et al.*, 2011). Owing to its endothelial origin and potent vasodilatory effects, EETs have been identified as endothelium-derived hyperpolarizing/relaxing factors (EDH/RF) in some vascular beds (Campbell *et al.*, 1996; Fisslthaler *et al.*, 1999). Also, EETs have been shown to be angiogenic in cerebral vasculature (Zhang *et al.*, 2002).

EETs are neuroprotective probably due to their pronounced vasodilatory, angiogenic and anti-inflammatory effects (Yang *et al.*, 2016). The neuroprotective potential of EETs could also be beneficial in cerebrovascular pathologies such as stroke. Indeed, sEH inhibition has been shown to be protective against ischemic brain damage *in vivo* presumably by a mechanism linked to enhanced cerebral blood flow (Zhang *et al.*, 2007). Moreover, genetic polymorphisms in CYP-epoxygenases and/or sEH, resulting in increased EET-generation or prolongation of EET activity, are associated with the reduced risk of cerebral ischemia (Iliff *et al.*, 2010). Pharmacological inhibition of sEH by means of sEHis and resultant stabilization of neuroprotective EETs have been explored as a therapeutic target for stroke (Iliff *et al.*, 2009; Liu *et al.*, 2016b; Zhang *et al.*, 2007).

1.3.2. EETs in morphine-mediated antinociception

Transgenic mice with an inability to generate FA epoxides such as EETs due to a neuron-specific ablation of CYP-reductase exhibit highly attenuated morphine-mediated antinociception (Conroy *et al*., 2010). These transgenic mice also exhibit a compromised stress-induced antinociception, which involves activation of the endogenous opioid signaling (Hough *et al*. 2014). Moreover, microinjection of CC12, a CYP-epoxygenase inhibitor, in the rostral ventromedial medulla of WT mice inhibits morphine-mediated antinociception (Conroy *et al*., 2013). All these findings collectively point towards the potential involvement of CYP-epoxygenases-derived FA epoxides(s) in opioid singling. Moreover, a recent study corroborated the involvement of CYP-epoxygenase by employing a cluster knock out strategy wherein the genetic ablation of CYP-2C (known for epoxygenase activity), but not CYP-2D and CYP-3A, reduced subcutaneously administered morphine-mediated antinociception by 41% (Hough *et al*., 2015).

CYP-derived FA epoxides also include docosahexaenoic acid-derived epoxydocosapentaenoic acids (EpDPEs), eicosapentaenoic acid-derived epoxyeicosatetraenoic acid (EpETEs) and linoleic acid derived epoxyoctadecenoic acid (EpOMEs). Amongst these FA epoxides, EETs are one of the best studied mediators and have been suggested to exhibit antinociceptive effects in rat neuropathic and inflammatory pain models (Wagner *et al*., 2013). Moreover, direct evidence implicating EETs in opioid-mediated antinociception comes from a study demonstrating strong antinociception after microinjection of 14,15-EET into the periaqueductal gray (PAG)-a brain region involved in the descending pathway of opioid antinociception, presumably by activating endogenous

endorphin release (Terashvili *et al.*, 2008). These studies point towards the potential involvement EETs in opioid-mediated anti-nociception.

1.3.3. EETs in neuronal excitability and synaptic transmission

Genetic ablation/pharmacological inhibition of sEH and potential metabolic stabilization of EETs have been linked to beneficial effects in several animal models of epilepsy. sEH inhibition or administration of a regioisomeric mixture of EETs delay the onset of seizures induced by a GABA antagonist in mice (Inceoglu *et al.*, 2013). Moreover, sEHis in combination with diazepam prevent progression of tetramethylenedisulfotetramine (TETS)-induced tonic seizures and lethality in mice. This antiepileptic effect of sEHis is attributed to the ability of EETs to tackle neuro-inflammation associated with epileptogenesis (Vito *et al.*, 2014). On similar lines, sEH inhibition is beneficial in two distinct models of temporal lobe epilepsy (pilocarpine-induced and amygdala kindling) (Hung *et al.*, 2015). Epilepsy is a disorder of hyperexcitability and the reported antiepileptic potential of EETs, in addition to the proposed mechanisms, might be due to the potential of EET-mediated modulation of neuronal excitability. The only study investigating the direct effects of EETs on basal synaptic neurotransmission in slices from pre-frontal cortex reports that application of the sEHi 12-(3-adamantan-1-yl-ureido) dodecanoic acid (AUDA) or exogenous 14,15-EET enhances excitatory synaptic neurotransmission, reflected by increase in fEPSP slopes (Wu *et al.*, 2015).

1.3.4. Molecular targets of EETs

EETs, acting in autocrine and paracrine manner, exhibit a plethora of bioactivities. However, the exact molecular targets for these diverse effects remain largely unknown.

1.3.4.1. Potassium channels

The BK_{Ca} channel is the best-characterized effector for EET-mediated vasodilation so far. Application of exogenous EETs increased the open probability of BK_{Ca} channels in coronary, renal, cerebral vascular smooth muscle cells (Campbell *et al.*, 2007; Earley *et al.*, 2005; Zou *et al.*, 1996). EETs might not directly activate BK_{Ca} channels, since they lack any effect on heterologously expressed BK_{Ca} channels in inside-out patch recordings from HEK-293T cells. However, the effect could be restored by the inclusion of equivalent GTP in the external compartment, suggesting the requirement of GTP for EET-mediated action (Fukao *et al.*, 2001). This notion is further strengthened by the observation that inhibition of G-proteins by GDPβS and anti-$G_{s\alpha}$ antibody block the effect of 11,12-EET on BK_{Ca} channels (Li *et al.*,

1997; Li *et al.*, 1999). However, the molecular identification and characterization of putative BK_{Ca}-coupled EETs receptor(s) remain unknown to date. EETs also activate K_{ATP} channels, likely via activation of protein kinase A (Lu *et al.*, 2006).

1.3.4.2. TRP channels

EETs modulate TRPV4 channels, calcium conducting member from the TRPV family, which are gated by physical stimuli and synthetic ligands alike (White *et al.*, 2016). Indeed, so far the TRPV4 channel is the only ion channel known to be activated directly by EETs. Both, 5,6- and 8,9-EET, but not 11,12- and 14,15 EET, activate TRPV4 at submicromolar concentrations (Watanabe *et al.*, 2003). Moreover, TRPV4 forms a novel complex with ryanodine receptors and BK_{Ca} channels that elicits smooth muscle hyperpolarization and dilation in response to the application of 11,12-EET (Earley *et al.*, 2005). 5,6-EET is released on neuronal activation and modulates nociceptor sensitivity via regulation of TRPA1 channels *in vitro* (Sisignano *et al*., 2012). Overexpression of CYP-2C9 or application of exogenous 11,12-EET increases the translocation of TRPC6 channel to the membrane in endothelial cells (Fleming *et al.*, 2007). Moreover, 11,12-EET activates a TRPV4–TRPC1–K_{Ca}1.1 complex to induce smooth muscle relaxation in human internal mammary arteries (Ma *et al.*, 2015).

1.3.4.3. Putative EETs-GPCR

Multiple *in vitro* binding studies have suggested the presence of a specific, high-affinity membrane binding site (K_d in the nM range) for 14,15-EET in guinea pig mononuclear cells (Wong *et al.*, 1992; Wong *et al.*, 2000) and monocytes (U-937) (Wong *et al.*, 1997). Moreover, membrane binding sites for synthetic radiolabeled EET agonist and antagonist have been demonstrated in U-937 cells (Chen *et al.*, 2009; Yang *et al.*, 2008). EETs may also act as GPCR blockers, as 14,15-EET acts as a competitive, selective antagonist on the thromboxane prostaglandin (TP) receptors in isolated vascular and respiratory smooth muscle cells (Behm *et al.*, 2009). Recently, Liu and colleagues screened 105 GPCRs for high-affinity binding and described activation of multiple GPCRs by 14,15-EET. The top five hits were from prostaglandin receptor subtypes (PTGER2, PTGER4, PTGFR, PTGDR, PTGER3 IV), but none of them had a high affinity for 14,15-EET (Liu *et al.*, 2016a).

Taken together, these studies strongly point towards a so far unidentified putative EET-GPCR as a molecular target for EETs. A few studies suggested the potential modulation of intracellular effectors such as FABPs (Widstrom *et al.*, 2001) and nuclear receptors such as PPAR-γ by EETs (Liu *et al.*, 2005; Samokhvalov *et al.*, 2014).

1.4. DHETs and their biological activity

DHETs are considered inactive catabolic products of bioactive EETs. However, a few studies have suggested that DHETs are bioactive in some non-neuronal systems. 8,9-, 11,12- and 14,15-DHET produce vasodilation in isolated canine coronary arterioles via activation of charybdotoxin-sensitive Ca^{2+} activated potassium channels (I_{KCa}) (Oltman *et al.*, 1998). 11,12-DHET activates BK_{Ca} channels, which hyperpolarize rat coronary vascular smooth muscles and consequently lead to vasodilation (Lu *et al.*, 2001). BK_{Ca}-mediated vasodilation is also reported with 14,15-DHET in bovine coronary arteries (Campbell *et al.*, 2002) and with 8,9-, 11,12- and 14,15-DHET in isolated human coronary arterioles (Larsen *et al.*, 2006). 14,15-DHET is also known as a potent activator of PPAR-α in COS-7 cells (Fang *et al.*, 2006). Moreover, 11,12-DHET modulates the progenitor cell proliferation in mice, likely via stimulating Wnt signaling (Frömel *et al.*, 2012) and is essential for orchestrating monocyte chemotaxis and thus inflammatory response in mice (Kundu *et al.*, 2013).

1.5. Aims of the dissertation

The main aims of this dissertation were as follows:

1. To investigate the potential role of AA-derived eicosanoids such as epoxyeicosatrienoic acids (EETs) and dihydroxyeicosatrienoic acids (DHETs) in neuronal transmission, using the patch-clamp technique in mouse brain slices.

2. To explore the potential role of sEH and mEH, the two major enzymes responsible for EETs metabolism to DHETs, in synaptic physiology using a combination of electrophysiological tools and transgenic mice (expressing ablated or hyperactive EHs).

3. To identify and characterize putative molecular targets underlying the effects exerted by EETs and DHETs.

1.6. Bibliography

Abdelmagid SA, Clarke SE, Nielsen DE, Badawi A, El-Sohemy A, Mutch DM, *et al.* (2015). Comprehensive profiling of plasma fatty acid concentrations in young healthy Canadian adults. *PloS one* **10**(2)**:** e0116195.

Ai D, Fu Y, Guo D, Tanaka H, Wang N, Tang C, *et al.* (2007). Angiotensin II up-regulates soluble epoxide hydrolase in vascular endothelium *in vitro* and *in vivo*. *Proceedings of the National Academy of Sciences* **104**(21)**:** 9018-9023.

Al-Hasani R, Bruchas MR (2011). Molecular mechanisms of opioid receptor-dependent signaling and behavior. *The Journal of the American Society of Anesthesiologists* **115**(6)**:** 1363-1381.

Al-Anizy M, Horley NJ, Kuo CW, Gillett LC, Laughton CA, Kendall D, *et al.* (2006). Cytochrome P450 Cyp4x1 is a major P450 protein in mouse brain. *The FEBS journal* **273**(5)**:** 936-947.

Alkayed NJ, Narayanan J, Gebremedhin D, Medhora M, Roman RJ, Harder DR (1996). Molecular characterization of an arachidonic acid epoxygenase in rat brain astrocytes. *Stroke* **27**(5)**:** 971-979.

Amaral DG, Scharfman HE, Lavenex P (2007). The dentate gyrus: fundamental neuroanatomical organization (dentate gyrus for dummies). *Progress in brain research* **163:** 3-790.

Amruthesh SC, Falck J, Ellis EF (1992). Brain synthesis and cerebrovascular action of epoxygenase metabolites of arachidonic acid. *Journal of neurochemistry* **58**(2)**:** 503-510.

Andersen P (2007). *The hippocampus book*. edn. Oxford university press.

Angelova P, Müller W (2006). Oxidative modulation of the transient potassium current IA by intracellular arachidonic acid in rat CA1 pyramidal neurons. *European Journal of Neuroscience* **23**(9)**:** 2375-2384.

Angelova PR, Müller WS (2009). Arachidonic acid potently inhibits both postsynaptic-type K_v4. 2 and presynaptic-type K_v1. 4 IA potassium channels. *European Journal of Neuroscience* **29**(10)**:** 1943-1950.

Arand M, Cronin A, Adamska M, Oesch F (2005). Epoxide hydrolases: Structure, function, mechanism, and assay. In: *Methods in Enzymology* Vol. 400, pp 569-588.

Bazan N, Birkle D, Tang W, Reddy TS (1986). The accumulation of free arachidonic acid, diacylglycerols, prostaglandins, and lipoxygenase reaction products in the brain during experimental epilepsy. *Advances in neurology* **44:** 879-902.

Bazán NG (1970). Effects of ischemia and electroconvulsive shock on free fatty acid pool in the brain. *Biochimica et Biophysica Acta (BBA)-Lipids and Lipid Metabolism* **218**(1)**:** 1-10.

Bazinet RP, Layé S (2014). Polyunsaturated fatty acids and their metabolites in brain function and disease. *Nature Reviews Neuroscience*.

Behm DJ, Ogbonna A, Wu C, Burns-Kurtis CL, Douglas SA (2009). Epoxyeicosatrienoic acids function as selective, endogenous antagonists of native thromboxane receptors: identification of a novel mechanism of vasodilation. *Journal of Pharmacology and Experimental Therapeutics* **328**(1)**:** 231-239.

Bell PA, Falany CN, McQuiddy P, Kasper CB (1990). Glucocorticoid repression and basal regulation of the epoxide hydrolase promoter. *Archives of biochemistry and biophysics* **279**(2)**:** 363-369.

Bhagwat S, Leelavathi B, Shankar S, Boyd M, Ravindranath V (1995). Cytochrome P450 and associated monooxygenase activities in the rat and human spinal cord: Induction, immunological characterization and immunocytochemical localization. *Neuroscience* **68**(2)**:** 593-601.

Bittner K, Müller W (1999). Oxidative Downmodulation of the Transient K-Current IA by Intracellular Arachidonic Acid in Rat Hippocampal Neurons. *Journal of Neurophysiology* **82**(1)**:** 508-511.

Boland LM, Drzewiecki MM (2008). Polyunsaturated fatty acid modulation of voltage-gated ion channels. *Cell biochemistry and biophysics* **52**(2)**:** 59-84.

Borroto-Escuela DO, Carlsson J, Ambrogini P, Narváez M, Wydra K, Tarakanov AO, *et al.* (2017). Understanding the role of GPCR heteroreceptor complexes in modulating the brain networks in health and disease. *Frontiers in cellular neuroscience* **11**.

Brash AR (2001). Arachidonic acid as a bioactive molecule. *The Journal of clinical investigation* **107**(11)**:** 1339-1345.

Buzsáki G, Anastassiou CA, Koch C (2012). The origin of extracellular fields and currents-EEG, ECoG, LFP and spikes. *Nature Reviews Neuroscience* **13**(6)**:** 407-420.

Campbell WB, Deeter C, Gauthier KM, Ingraham RH, Falck JR, Li P-L (2002). 14, 15-Dihydroxyeicosatrienoic acid relaxes bovine coronary arteries by activation of K Ca channels. *American Journal of Physiology-Heart and Circulatory Physiology* **282**(5)**:** H1656-H1664.

Campbell WB, Falck JR (2007). Arachidonic acid metabolites as endothelium-derived hyperpolarizing factors. *Hypertension* **49**(3)**:** 590-596.

Campbell WB, Gebremedhin D, Pratt PF, Harder DR (1996). Identification of epoxyeicosatrienoic acids as endothelium-derived hyperpolarizing factors. *Circulation Research* **78**(3)**:** 415-423.

Carta M, Lanore F, Rebola N, Szabo Z, Da Silva SV, Lourenço J, *et al.* (2014). Membrane lipids tune synaptic transmission by direct modulation of presynaptic potassium channels. *Neuron* **81**(4)**:** 787-799.

Castillo PE, Younts TJ, Chávez AE, Hashimotodani Y (2012). Endocannabinoid signaling and synaptic function. *Neuron* **76**(1)**:** 70-81.

Chen Y, Falck JR, Tuniki VR, Campbell WB (2009). 20-125Iodo-14, 15-epoxyeicosa-5 (Z)-enoic acid: a high-affinity radioligand used to characterize the epoxyeicosatrienoic acid antagonist binding site. *Journal of Pharmacology and Experimental Therapeutics* **331**(3)**:** 1137-1145.

Colbert CM, Pan E (1999). Arachidonic acid reciprocally alters the availability of transient and sustained dendritic K^+ channels in hippocampal CA1 pyramidal neurons. *Journal of Neuroscience* **19**(19)**:** 8163-8171.

Coleman SK, Newcombe J, Pryke J, Dolly JO (1999). Subunit composition of K_v1 channels in human CNS. *Journal of neurochemistry* **73**(2)**:** 849-858.

Conroy JL, Fang C, Gu J, Zeitlin SO, Yang W, Yang J, *et al.* (2010). Opioids activate brain analgesic circuits through cytochrome P450/epoxygenase signaling. *Nature neuroscience* **13**(3)**:** 284-286.

Cronin A, Mowbray S, Dürk H, Homburg S, Fleming I, Fisslthaler B, *et al.* (2003). The N-terminal domain of mammalian soluble epoxide hydrolase is a phosphatase. *Proceedings of the National Academy of Sciences* **100**(4)**:** 1552-1557.

Daikh BE, Lasker JM, Raucy JL, Koop DR (1994). Regio-and stereoselective epoxidation of arachidonic acid by human cytochromes P450 2C8 and 2C9. *Journal of Pharmacology and Experimental Therapeutics* **271**(3)**:** 1427-1433.

Dang VC, Christie MJ (2012). Mechanisms of rapid opioid receptor desensitization, resensitization and tolerance in brain neurons. British journal of pharmacology 165(6): 1704-1716.

Danzer SC, Kotloski RJ, Walter C, Hughes M, McNamara JO (2008). Altered morphology of hippocampal dentate granule cell presynaptic and postsynaptic terminals following conditional deletion of TrkB. *Hippocampus* **18**(7)**:** 668-678.

Decker M, Adamska M, Cronin A, Di Giallonardo F, Burgener J, Marowsky A, *et al.* (2012). EH3 (ABHD9): the first member of a new epoxide hydrolase family with high activity for fatty acid epoxides. *Journal of lipid research* **53**(10)**:** 2038-2045.

Decker M, Arand M, Cronin A (2009). Mammalian epoxide hydrolases in xenobiotic metabolism and signalling. *Archives of Toxicology* **83**(4)**:** 297-318.

Deng W, Aimone JB, Gage FH (2010). New neurons and new memories: how does adult hippocampal neurogenesis affect learning and memory? *Nature Reviews Neuroscience* **11**(5)**:** 339-350.

Diana MA, Marty A (2004). Endocannabinoid-mediated short-term synaptic plasticity: Depolarization-induced suppression of inhibition (DSI) and depolarization-induced suppression of excitation (DSE). *British journal of pharmacology* **142**(1)**:** 9-19.

Diani-Moore S, Ma Y, Gross SS, Rifkind AB (2014). Increases in Levels of Epoxyeicosatrienoic and Dihydroxyeicosatrienoic Acids (EETs and DHETs) in Liver and Heart *in Vivo* by 2, 3, 7, 8-Tetrachlorodibenzo-p-Dioxin (TCDD) and in Hepatic EET: DHET Ratios by Cotreatment with TCDD and the Soluble Epoxide Hydrolase Inhibitor AUDA. *Drug Metabolism and Disposition* **42**(2)**:** 294-300.

Drake CT, Milner TA (1999). Mu opioid receptors are in somatodendritic and axonal compartments of GABAergic neurons in rat hippocampal formation. *Brain research* **849**(1)**:** 203-215.

Drapeau C, Pellerin L, Wolfe LS, Avoli M (1990). Long-term changes of synaptic transmission induced by arachidonic acid in the CA1 subfield of the rat hippocampus. *Neuroscience letters* **115**(2)**:** 286-292.

Earley S, Heppner TJ, Nelson MT, Brayden JE (2005). TRPV4 forms a novel Ca^{2+} signaling complex with ryanodine receptors and BK_{Ca} channels. *Circulation Research* **97**(12)**:** 1270-1279.

El-Sherbeni AA, El-Kadi AO (2014). The role of epoxide hydrolases in health and disease. *Archives of Toxicology* **88**(11)**:** 2013-2032.

Elinder F, Liin SI (2017). Actions and mechanisms of polyunsaturated fatty acids on voltage-gated ion channels. *Frontiers in physiology* **8**.

Erbs E, Faget L, Scherrer G, Matifas A, Filliol D, Vonesch J-L, *et al.* (2015). A mu–delta opioid receptor brain atlas reveals neuronal co-occurrence in subcortical networks. *Brain Structure and Function* **220**(2)**:** 677-702.

Fang X, Hu S, Xu B, Snyder GD, Harmon S, Yao J, *et al.* (2006). 14, 15-Dihydroxyeicosatrienoic acid activates peroxisome proliferator-activated receptor-α. *American Journal of Physiology-Heart and Circulatory Physiology* **290**(1)**:** H55-H63.

Farin FM, Omiecinski CJ (1993). Regiospecific expression of cytochrome P-450s and microsomal epoxide hydrolase in human brain tissue. *Journal of Toxicology and Environmental Health, Part A Current Issues* **40**(2-3)**:** 317-335.

Farooqui AA, Horrocks LA (2004). Brain phospholipases A_2-a perspective on the history. *Prostaglandins, leukotrienes and essential fatty acids* **71**(3)**:** 161-169.

Farooqui AA, Yang HC, Rosenberger TA, Horrocks LA (1997). Phospholipase A_2 and its role in brain tissue. *Journal of neurochemistry* **69**(3)**:** 889-901.

Fisslthaler B, Popp R, Kiss L, Potente M, Harder DR, Fleming I, *et al.* (1999). Cytochrome P450 2C is an EDHF synthase in coronary arteries. *Nature* **401**(6752)**:** 493-497.

Fitzsimonds RM, Poo M-m (1998). Retrograde signaling in the development and modification of synapses. *Physiological reviews* **78**(1)**:** 143-170.

Fleming I, Rueben A, Popp R, Fisslthaler B, Schrodt S, Sander A, *et al.* (2007). Epoxyeicosatrienoic acids regulate Trp channel–dependent Ca^{2+} signaling and hyperpolarization in endothelial cells. *Arteriosclerosis, thrombosis, and vascular biology* **27**(12)**:** 2612-2618.

Fransén E, Tigerholm J (2010). Role of A-type potassium currents in excitability, network synchronicity and epilepsy. *Hippocampus* **20**(7)**:** 877.

Frömel T, Jungblut B, Hu J, Trouvain C, Barbosa-Sicard E, Popp R, *et al.* (2012). Soluble epoxide hydrolase regulates hematopoietic progenitor cell function via generation of fatty acid diols. *Proceedings of the National Academy of Sciences* **109**(25)**:** 9995-10000.

Fukao M, Mason HS, Kenyon JL, Horowitz B, Keef KD (2001). Regulation of BK_{Ca} channels expressed in human embryonic kidney 293 cells by epoxyeicosatrienoic acid. *Molecular Pharmacology* **59**(1)**:** 16-23.

Funk CD (2001). Prostaglandins and leukotrienes: advances in eicosanoid biology. *Science* **294**(5548)**:** 1871-1875.

Gardiner M, Nilsson B, Rehncrona S, Siesjö BK (1981). Free fatty acids in the rat brain in moderate and severe hypoxia. *Journal of neurochemistry* **36**(4)**:** 1500-1505.

Geiger JR, Jonas P (2000). Dynamic control of presynaptic Ca^{2+} inflow by fast-inactivating K^+ channels in hippocampal mossy fiber boutons. *Neuron* **28**(3)**:** 927-939.

H Ingraham R, D Gless R, Y Lo H (2011). Soluble epoxide hydrolase inhibitors and their potential for treatment of multiple pathologic conditions. *Current medicinal chemistry* **18**(4)**:** 587-603.

Hammock BD, Gill SS, Stamoudis V, Gilbert LI (1976). Soluble mammalian epoxide hydratase: action on juvenile hormone and other terpenoid epoxides. *Comparative Biochemistry and Physiology Part B: Comparative Biochemistry* **53**(2)**:** 263-265.

Hammock BD, Ota K (1983). Differential induction of cytosolic eposide hydrolase, microsomal epoxide hydrolase, and glutathione S-transferase activities. *Toxicology and applied pharmacology* **71**(2)**:** 254-265.

Harizi H, Corcuff J-B, Gualde N (2008). Arachidonic-acid-derived eicosanoids: roles in biology and immunopathology. *Trends in molecular medicine* **14**(10)**:** 461-469.

Harris TR, Hammock BD (2013). Soluble epoxide hydrolase: gene structure, expression and deletion. *Gene* **526**(2)**:** 61-74.

Hoffman DA, Magee JC, Colbert CM, Johnston D (1997). K^+ channel regulation of signal propagation in dendrites of hippocampal pyramidal neurons. *Nature* **387**(6636)**:** 869-875.

Holmqvist MH, Cao J, Knoppers MH, Jurman ME, Distefano PS, Rhodes KJ, *et al.* (2001). Kinetic modulation of K_V4-mediated A-current by arachidonic acid is dependent on potassium channel interacting proteins. *Journal of Neuroscience* **21**(12)**:** 4154-4161.

Hölscher C, Canevari L, Richter-Levin G (1995). Inhibitors of PLA_2 and NO synthase cooperate in producing amnesia of a spatial task. *Neuroreport* **6**(5)**:** 730-732.

Hosagrahara VP, Rettie AE, Hassett C, Omiecinski CJ (2004). Functional analysis of human microsomal epoxide hydrolase genetic variants. *Chemico-biological interactions* **150**(2)**:** 149-159.

Hu H, Shao L-R, Chavoshy S, Gu N, Trieb M, Behrens R, *et al.* (2001). Presynaptic Ca^{2+}-activated K^+ channels in glutamatergic hippocampal terminals and their role in spike repolarization and regulation of transmitter release. *Journal of Neuroscience* **21**(24)**:** 9585-9597.

Hung Y-W, Hung S-W, Wu Y-C, Wong L-K, Lai M-T, Shih Y-H, *et al.* (2015). Soluble epoxide hydrolase activity regulates inflammatory responses and seizure generation in two mouse models of temporal lobe epilepsy. *Brain, behavior, and immunity* **43:** 118-129.

Iliff JJ, Alkayed NJ (2009). Soluble epoxide hydrolase inhibition: targeting multiple mechanisms of ischemic brain injury with a single agent.

Iliff JJ, Jia J, Nelson J, Goyagi T, Klaus J, Alkayed NJ (2010). Epoxyeicosanoid signaling in CNS function and disease. *Prostaglandins & other lipid mediators* **91**(3)**:** 68-84.

Imig JD, Hammock BD (2009). Soluble epoxide hydrolase as a therapeutic target for cardiovascular diseases. *Nature Reviews Drug Discovery* **8**(10)**:** 794-805.

Imig JD, Simpkins AN, Renic M, Harder DR (2011). Cytochrome P450 eicosanoids and cerebral vascular function. *Expert reviews in molecular medicine* **13:** e7.

Inceoglu B, Zolkowska D, Yoo HJ, Wagner KM, Yang J, Hackett E, *et al.* (2013). Epoxy fatty acids and inhibition of the soluble epoxide hydrolase selectively modulate GABA mediated neurotransmission to delay onset of seizures. *PloS one* **8**(12)**:** e80922.

Iscan M, Reuhl K, Weiss B, Maines M (1990). Regional and subcellular distribution of cytochrome P-450-dependent drug metabolism in monkey brain: the olfactory bulb and the mitochondrial fraction have high levels of activity. *Biochemical and biophysical research communications* **169**(3)**:** 858-863.

Jhaveri M, Richardson D, Chapman V (2007). Endocannabinoid metabolism and uptake: novel targets for neuropathic and inflammatory pain. British journal of pharmacology 152(5): 624-632.

Kang JX, Xiao Y-F, Leaf A (1995). Free, long-chain, polyunsaturated fatty acids reduce membrane electrical excitability in neonatal rat cardiac myocytes. *Proceedings of the National Academy of Sciences* **92**(9)**:** 3997-4001.

Kaspera R, Totah RA (2009). Epoxyeicosatrienoic acids: formation, metabolism and potential role in tissue physiology and pathophysiology. *Expert opinion on drug metabolism & toxicology* **5**(7)**:** 757-771.

Kim D (2003). Fatty acid-sensitive two-pore domain K^+ channels. *Trends in pharmacological sciences* **24**(12)**:** 648-654.

Klausberger T, Somogyi P (2008). Neuronal diversity and temporal dynamics: the unity of hippocampal circuit operations. *Science* **321**(5885)**:** 53-57.

Kole MH, Stuart GJ (2012). Signal processing in the axon initial segment. *Neuron* **73**(2)**:** 235-247.

Kundu S, Roome T, Bhattacharjee A, Carnevale KA, Yakubenko VP, Zhang R, *et al.* (2013). Metabolic products of soluble epoxide hydrolase are essential for monocyte chemotaxis to MCP-1 *in vitro* and *in vivo*. *Journal of lipid research* **54**(2)**:** 436-447.

Larsen BT, Miura H, Hatoum OA, Campbell WB, Hammock BD, Zeldin DC, *et al.* (2006). Epoxyeicosatrienoic and dihydroxyeicosatrienoic acids dilate human coronary arterioles via BK_{Ca} channels: implications for soluble epoxide hydrolase inhibition. *American Journal of Physiology-Heart and Circulatory Physiology* **290**(2)**:** H491-H499.

Lein ES, Hawrylycz MJ, Ao N, Ayres M, Bensinger A, Bernard A, *et al.* (2007). Genome-wide atlas of gene expression in the adult mouse brain. *Nature* **445**(7124)**:** 168-176.

Li P-L, Campbell WB (1997). Epoxyeicosatrienoic acids activate K^+ channels in coronary smooth muscle through a guanine nucleotide binding protein. *Circulation Research* **80**(6)**:** 877-884.

Li P-L, Chen C-L, Bortell R, Campbell WB (1999). 11, 12-Epoxyeicosatrienoic acid stimulates endogenous mono-ADP-ribosylation in bovine coronary arterial smooth muscle. *Circulation Research* **85**(4)**:** 349-356.

Liu P-Y, Li Y-H, Chao T-H, Wu H-L, Lin L-J, Tsai L-M, *et al.* (2007). Synergistic effect of cytochrome P450 epoxygenase CYP2J2* 7 polymorphism with smoking on the onset of premature myocardial infarction. *Atherosclerosis* **195**(1)**:** 199-206.

Liu X, Qian Z-y, Xie F, Fan W, Nelson JW, Xiao X, *et al.* (2016a). Functional screening for G protein-coupled receptor targets of 14, 15-epoxyeicosatrienoic acid. *Prostaglandins & other lipid mediators*.

Liu Y, Wan Y, Fang Y, Yao E, Xu S, Ning Q, *et al.* (2016b). Epoxyeicosanoid signaling provides multi-target protective effects on neurovascular unit in rats after focal ischemia. *Journal of Molecular Neuroscience* **58**(2)**:** 254-265.

Liu Y, Zhang Y, Schmelzer K, Lee T-S, Fang X, Zhu Y, *et al.* (2005). The antiinflammatory effect of laminar flow: the role of PPARγ, epoxyeicosatrienoic acids, and soluble epoxide hydrolase. *Proceedings of the National Academy of Sciences of the United States of America* **102**(46)**:** 16747-16752.

Lu T, Katakam PV, VanRollins M, Weintraub NL, Spector AA, Lee HC (2001). Dihydroxyeicosatrienoic acids are potent activators of Ca^{2+}-activated K^+ channels in isolated rat coronary arterial myocytes. *The Journal of physiology* **534**(3)**:** 651-667.

Lu T, Ye D, Wang X, Seubert JM, Graves JP, Bradbury JA, *et al.* (2006). Cardiac and vascular K_{ATP} channels in rats are activated by endogenous epoxyeicosatrienoic acids through different mechanisms. *The Journal of physiology* **575**(2)**:** 627-644.

Lynch M, Clements M, Voss K, Bramham C, Bliss T (1991). Is arachidonic acid a retrograde messenger in long-term potentiation? : Portland Press Limited.

Lynch M, Errington M, Bliss T (1989). Nordihydroguaiaretic acid blocks the synaptic component of long-term potentiation and the associated increases in release of glutamate and arachidonate: an in vivo study in the dentate gyrus of the rat. *Neuroscience* **30**(3)**:** 693-701.

Lynch M, Voss K, Clements M, Bliss T (1993). The Role of Arachidonic Acid as a Retrograde Messenger in Long-Term Potentiation. *Phospholipids and Signal Transmission*, edn: Springer:135-149.

Ma Y, Zhang P, Li J, Lu J, Ge J, Zhao Z, *et al.* (2015). Epoxyeicosatrienoic acids act through TRPV4–TRPC1–K_{Ca}1.1 complex to induce smooth muscle membrane hyperpolarization and relaxation in human internal mammary arteries. *Biochimica et Biophysica Acta (BBA)-Molecular Basis of Disease* **1852**(3)**:** 552-559.

Mann A, Miksys S, Lee A, Mash DC, Tyndale RF (2008). Induction of the drug metabolizing enzyme CYP2D in monkey brain by chronic nicotine treatment. *Neuropharmacology* **55**(7)**:** 1147-1155.

Marowsky A, Burgener J, Falck J, Fritschy J-M, Arand M (2009). Distribution of soluble and microsomal epoxide hydrolase in the mouse brain and its contribution to cerebral epoxyeicosatrienoic acid metabolism. *Neuroscience* **163**(2)**:** 646-661.

Marowsky A, Cronin A, Frère F, Adamska M, Arand M (eds) (2010). *4.15-Mammalian Epoxide Hydrolases*. Elsevier Ltd.

Marowsky A, Meyer I, Erismann-Ebner K, Pellegrini G, Mule N, Arand M (2017). Beyond detoxification: a role for mouse mEH in the hepatic metabolism of endogenous lipids. *Archives of Toxicology***:** 1-15.

Massicotte G, Oliver MW, Lynch G, Baudry M (1990). Effect of bromophenacyl bromide, a phospholipase A_2 inhibitor, on the induction and maintenance of LTP in hippocampal slices. *Brain research* **537**(1)**:** 49-53.

McQuiston AR, Saggau P (2003). Mu-opioid receptors facilitate the propagation of excitatory activity in rat hippocampal area CA1 by disinhibition of all anatomical layers. *Journal of Neurophysiology* **90**(3)**:** 1936-1948.

Medhora M, Narayanan J, Harder D (2001). Dual regulation of the cerebral microvasculature by epoxyeicosatrienoic acids. *Trends in cardiovascular medicine* **11**(1)**:** 38-42.

Meves H (2008). Arachidonic acid and ion channels: an update. *British journal of pharmacology* **155**(1)**:** 4-16.

Miles R, Tóth K, Gulyás AI, Hájos N, Freund TF (1996). Differences between somatic and dendritic inhibition in the hippocampus. Neuron **16**(4): 815-823.

Mitchell RW, Hatch GM (2011). Fatty acid transport into the brain: of fatty acid fables and lipid tails. *Prostaglandins, Leukotrienes and Essential Fatty Acids (PLEFA)* **85**(5)**:** 293-302.

Newman JW, Morisseau C, Hammock BD (2005). Epoxide hydrolases: their roles and interactions with lipid metabolism. *Progress in lipid research* **44**(1)**:** 1-51.

Nicoll RA, Schmitz D (2005). Synaptic plasticity at hippocampal mossy fibre synapses. *Nature Reviews Neuroscience* **6**(11)**:** 863-876.

O'dell TJ, Hawkins RD, Kandel ER, Arancio O (1991). Tests of the roles of two diffusible substances in long-term potentiation: evidence for nitric oxide as a possible early retrograde messenger. *Proceedings of the National Academy of Sciences* **88**(24)**:** 11285-11289.

Oesch F (1973). Mammalian epoxide hydrases: inducible enzymes catalysing the inactivation of carcinogenic and cytotoxic metabolites derived from aromatic and olefinic compounds. *Xenobiotica* **3**(5)**:** 305-340.

Oliver D, Lien C-C, Soom M, Baukrowitz T, Jonas P, Fakler B (2004). Functional conversion between A-type and delayed rectifier K^+ channels by membrane lipids. *Science* **304**(5668)**:** 265-270.

Oltman CL, Weintraub NL, VanRollins M, Dellsperger KC (1998). Epoxyeicosatrienoic acids and dihydroxyeicosatrienoic acids are potent vasodilators in the canine coronary microcirculation. *Circulation research* **83**(9)**:** 932-939.

Omura T (2006). Mitochondrial P450s. *Chemico-biological interactions* **163**(1)**:** 86-93.

Onogi T, Minami M, Katao Y, Nakagawa T, Aoki Y, Toya T, et al. (1995). DAMGO, a μ-opioid receptor selective agonist, distinguishes between μ-and δ-opioid receptors around their first extracellular loops. FEBS letters 357(1): 93-97.

Ovsepian SV, LeBerre M, Steuber V, O'leary VB, Leibold C, Dolly JO (2016). Distinctive role of K V 1.1 subunit in the biology and functions of low threshold K^+ channels with implications for neurological disease. *Pharmacology & Therapeutics* **159:** 93-101.

Persson A, Ingelman-Sundberg M (2014). Pharmacogenomics of Cytochrome P450 Dependent Metabolism of Endogenous Compounds: Implications for Behavior, Psychopathology and Treatment. *Journal of Pharmacogenomics & Pharmacoproteomics* **2014**.

Pinot F, Grant DF, Spearow JL, Parker AG, Hammock BD (1995). Differential regulation of soluble epoxide hydrolase by clofibrate and sexual hormones in the liver and kidneys of mice. *Biochemical pharmacology* **50**(4)**:** 501-508.

Pongs O, Schwarz JR (2010). Ancillary subunits associated with voltage-dependent K^+ channels. *Physiological reviews* **90**(2)**:** 755-796.

Przybyla-Zawislak BD, Srivastava PK, Vázquez-Matías J, Mohrenweiser HW, Maxwell JE, Hammock BD, *et al.* (2003). Polymorphisms in human soluble epoxide hydrolase. *Molecular Pharmacology* **64**(2)**:** 482-490.

Raijmakers M, Galan-Roosen D, Tanja E, Schilders GW, Merkus JM, Steegers EA, *et al.* (2004). The Tyr113His polymorphism in exon 3 of the microsomal epoxide hydrolase gene is a risk factor for perinatal mortality. *Acta obstetricia et gynecologica Scandinavica* **83**(11)**:** 1056-1060.

Rama S, Zbili M, Fékété A, Tapia M, Benitez MJ, Boumedine N, *et al.* (2017). The role of axonal K_v1 channels in CA3 pyramidal cell excitability. *Scientific Reports* **7**.

Ramakers GM, Storm JF (2002). A postsynaptic transient K^+ current modulated by arachidonic acid regulates synaptic integration and threshold for LTP induction in hippocampal pyramidal cells. *Proceedings of the National Academy of Sciences* **99**(15)**:** 10144-10149.

Rathour RK, Malik R, Narayanan R (2016). Transient potassium channels augment degeneracy in hippocampal active dendritic spectral tuning. *Scientific Reports* **6**.

Rhodes KJ, Strassle BW, Monaghan MM, Bekele-Arcuri Z, Matos MF, Trimmer JS (1997). Association and colocalization of the $K_v\beta1$ and $K_v\beta2$ β-subunits with K_v1 α-subunits in mammalian brain K^+ channel complexes. *Journal of Neuroscience* **17**(21)**:** 8246-8258.

Riedl AG, Watts PM, Douek DC, Edwards RJ, Boobis AR, Rose S, *et al.* (2000). Expression and distribution of CYP2C enzymes in rat basal ganglia. *Synapse* **38**(4)**:** 392-402.

Rifkind AB, Lee C, Chang TK, Waxman DJ (1995). Arachidonic acid metabolism by human cytochrome P450s 2C8, 2C9, 2E1, and 1A2: regioselective oxygenation and evidence for a role for CYP2C enzymes in arachidonic acid epoxygenation in human liver microsomes. *Archives of biochemistry and biophysics* **320**(2)**:** 380-389.

Samokhvalov V, Vriend J, Jamieson KL, Akhnokh M, Manne R, Falck JR, *et al.* (2014). PPARγ signaling is required for mediating EETs protective effects in neonatal cardiomyocytes exposed to LPS. *Frontiers in pharmacology* **5:** 242.

Samuelsson B (1987). An elucidation of the arachidonic acid cascade. *Drugs* **33**(1)**:** 2-9.

Sandberg M, Hassett C, Adman ET, Meijer J, Omiecinski CJ (2000). Identification and functional characterization of human soluble epoxide hydrolase genetic polymorphisms. *Journal of Biological Chemistry* **275**(37)**:** 28873-28881.

Sang N, Zhang J, Chen C (2007). COX-2 oxidative metabolite of endocannabinoid 2-AG enhances excitatory glutamatergic synaptic transmission and induces neurotoxicity. *Journal of neurochemistry* **102**(6)**:** 1966-1977.

Sang N, Zhang J, Marcheselli V, Bazan NG, Chen C (2005). Postsynaptically synthesized prostaglandin E2 (PGE2) modulates hippocampal synaptic transmission via a presynaptic PGE2 EP2 receptor. *Journal of Neuroscience* **25**(43)**:** 9858-9870.

Schaeffer E, Gattaz W (2007). Requirement of hippocampal phospholipase A2 activity for long-term memory retrieval in rats. *Journal of Neural Transmission* **114**(3)**:** 379-385.

Schilter B, Andersen MR, Acharya C, Omiecinski CJ (2000). Activation of cytochrome P450 gene expression in the rat brain by phenobarbital-like inducers. *Journal of Pharmacology and Experimental Therapeutics* **294**(3)**:** 916-922.

Schmitt H, Meves H (1995). Modulation of neuronal calcium channels by arachidonic acid and related substances. *Journal of Membrane Biology* **145**(3)**:** 233-244.

Shen HC (2010). Soluble epoxide hydrolase inhibitors: a patent review. *Expert opinion on therapeutic patents* **20**(7)**:** 941-956.

Shinde DD, Kim K-B, Oh K-S, Abdalla N, Liu K-H, Bae SK, *et al.* (2012). LC–MS/MS for the simultaneous analysis of arachidonic acid and 32 related metabolites in human plasma: basal plasma concentrations and aspirin-induced changes of eicosanoids. *Journal of Chromatography B* **911:** 113-121.

Siesjö BK, AGARDH CD, Bengtsson F, SMITH ML (1989). Arachidonic acid metabolism in seizures. *Annals of the New York Academy of Sciences* **559**(1)**:** 323-339.

Sisignano M, Park C-K, Angioni C, Zhang DD, von Hehn C, Cobos EJ, *et al.* (2012). 5, 6-EET is released upon neuronal activity and induces mechanical pain hypersensitivity via TRPA1 on central afferent terminals. *Journal of Neuroscience* **32**(18)**:** 6364-6372.

Smith CA, Harrison DJ (1997). Association between polymorphism in gene for microsomal epoxide hydrolase and susceptibility to emphysema. *The Lancet* **350**(9078)**:** 630-633.

Snyder GD, Capdevila J, Chacos N, Manna S, Falck J (1983). Action of luteinizing hormone-releasing hormone: involvement of novel arachidonic acid metabolites. *Proceedings of the National Academy of Sciences* **80**(11)**:** 3504-3507.

Spector AA, Fang X, Snyder GD, Weintraub NL (2004). Epoxyeicosatrienoic acids (EETs): metabolism and biochemical function. *Progress in lipid research* **43**(1)**:** 55-90.

Spector AA, Kim H-Y (2015). Cytochrome P 450 epoxygenase pathway of polyunsaturated fatty acid metabolism. *Biochimica et Biophysica Acta (BBA)-Molecular and Cell Biology of Lipids* **1851**(4)**:** 356-365.

Spiecker M, Darius H, Hankeln T, Soufi M, Sattler AM, Schaefer JR, *et al.* (2004). Risk of coronary artery disease associated with polymorphism of the cytochrome P450 epoxygenase CYP2J2. *Circulation* **110**(15)**:** 2132-2136.

Spruston N (2008). Pyramidal neurons: dendritic structure and synaptic integration. *Nature Reviews Neuroscience* **9**(3)**:** 206-221.

Stark K, Dostalek M, Guengerich F (2008). Expression and purification of orphan cytochrome P450 4X1 and oxidation of anandamide. *FEBS journal* **275**(14)**:** 3706-3717.

Sura P, Sura R, EnayetAllah AE, Grant DF (2008). Distribution and expression of soluble epoxide hydrolase in human brain. *Journal of Histochemistry & Cytochemistry* **56**(6)**:** 551-559.

Svoboda KR, Adams CE, Lupica CR (1999). Opioid receptor subtype expression defines morphologically distinct classes of hippocampal interneurons. *Journal of Neuroscience* **19**(1)**:** 85-95.

Taupin P (2007). *The hippocampus: neurotransmission and plasticity in the nervous system*. edn. Nova Publishers.

Terashvili M, Tseng LF, Wu H, Narayanan J, Hart LM, Falck JR, *et al.* (2008). Antinociception produced by 14, 15-epoxyeicosatrienoic acid is mediated by the activation of β-endorphin and Met-enkephalin in the rat ventrolateral periaqueductal gray. *Journal of Pharmacology and Experimental Therapeutics* **326**(2)**:** 614-622.

Thomas H, Schladt L, Knehr M, Oesch F (1989). Effect of diabetes and starvation on the activity of rat liver epoxide hydrolases, glutathione S-transferases and peroxisomal β-oxidation. *Biochemical pharmacology* **38**(23)**:** 4291-4297.

Traynelis SF, Wollmuth LP, McBain CJ, Menniti FS, Vance KM, Ogden KK, *et al.* (2010). Glutamate receptor ion channels: structure, regulation, and function. *Pharmacological reviews* **62**(3)**:** 405-496.

Trimmer JS (2015). Subcellular localization of K^+ channels in mammalian brain neurons: remarkable precision in the midst of extraordinary complexity. *Neuron* **85**(2)**:** 238-256.

Václavíková R, Hughes DJ, Souček P (2015). Microsomal epoxide hydrolase 1 *(EPHX1)*: Gene, structure, function, and role in human disease. *Gene* **571**(1)**:** 1-8.

Villarroel A, Schwarz TL (1996). Inhibition of the K_v4 (Shal) family of transient K^+ currents by arachidonic acid. *Journal of Neuroscience* **16**(3)**:** 1016-1025.

Visser LE, van Schaik RH, Danser AHJ, Hofman A, Witteman JC, van Duijn CM, *et al.* (2007). The risk of myocardial infarction in patients with reduced activity of cytochrome P450 2C9. *Pharmacogenetics and genomics* **17**(7)**:** 473-479.

Vito ST, Austin AT, Banks CN, Inceoglu B, Bruun DA, Zolkowska D, *et al.* (2014). Post-exposure administration of diazepam combined with soluble epoxide hydrolase inhibition stops seizures and modulates neuroinflammation in a murine model of acute TETS intoxication. *Toxicology and applied pharmacology* **281**(2)**:** 185-194.

Vogel B, Bentley P, Oesch F (1982). Endogenous role of microsomal epoxide hydrolase. Ontogenesis, induction inhibition, tissue distribution, immunological behaviour and purification of microsomal epoxide hydrolase with 16α, 17α-epoxyandrostene-3-one as substrate. Eur J Biochem 126: 425-431.

Wang H, Kunkel DD, Martin TM, Schwartzkroin PA, Tempel BL (1993). Heteromultimeric K^+ channels in terminal and juxtaparanodal regions of neurons. *Nature* **365**(6441)**:** 75.

Watanabe H, Vriens J, Prenen J, Droogmans G, Voets T, Nilius B (2003). Anandamide and arachidonic acid use epoxyeicosatrienoic acids to activate TRPV4 channels. *Nature* **424**(6947)**:** 434-438.

White JP, Cibelli M, Urban L, Nilius B, McGeown JG, Nagy I (2016). TRPV4: molecular conductor of a diverse orchestra. *Physiological reviews* **96**(3)**:** 911-973.

Widstrom RL, Norris AW, Spector AA (2001). Binding of cytochrome P450 monooxygenase and lipoxygenase pathway products by heart fatty acid-binding protein. *Biochemistry* **40**(4)**:** 1070-1076.

Williams JH, Errington ML, Lynch MA, Bliss TVP (1989). Arachidonic acid induces a long-term activity-dependent enhancement of synaptic transmission in the hippocampus. *Nature* **341**(6244)**:** 739-742.

Williams JT, Ingram SL, Henderson G, Chavkin C, von Zastrow M, Schulz S, *et al.* (2013). Regulation of μ-opioid receptors: Desensitization, phosphorylation, internalization, and tolerance. *Pharmacological reviews* **65**(1)**:** 223-254.

Wong P, Lin K, Yan Y, Ahern D, Iles J, Shen S, *et al.* (1992). 14 (R), 15 (S)-epoxyeicosatrienoic acid (14 (R), 15 (S)-EET) receptor in guinea pig mononuclear cell membranes. *Journal of lipid mediators* **6**(1-3)**:** 199-208.

Wong PY-K, Lai P-S, Falck J (2000). Mechanism and signal transduction of 14 (R), 15 (S)-epoxyeicosatrienoic acid (14, 15-EET) binding in guinea pig monocytes. *Prostaglandins & other lipid mediators* **62**(4)**:** 321-333.

Wong PY, Lai P-S, Shen S-Y, Belosludtsev YY, Falck J (1997). Post-receptor signal transduction and regulation of 14 (R), 15 (S)-epoxyeicosatrienoic acid (14, 15-EET) binding in U-937 cells. *Journal of lipid mediators and cell signalling* **16**(3)**:** 155-169.

Wu H-F, Yen H-J, Huang C-C, Lee Y-C, Wu S-Z, Lee T-S, *et al.* (2015). Soluble epoxide hydrolase inhibitor enhances synaptic neurotransmission and plasticity in mouse prefrontal cortex. *Journal of biomedical science* **22**(1)**:** 1.

Yan H, Kong Y, He B, Huang M, Li J, Zheng J, *et al.* (2015). CYP2J2 rs890293 polymorphism is associated with susceptibility to Alzheimer's disease in the Chinese Han population. *Neuroscience letters* **593:** 56-60.

Yang Q, He G-W, Underwood MJ, Yu C-M (2016). Cellular and molecular mechanisms of endothelial ischemia/reperfusion injury: perspectives and implications for postischemic myocardial protection. *American journal of translational research* **8**(2)**:** 765.

Yang W, Tuniki VR, Anjaiah S, Falck JR, Hillard CJ, Campbell WB (2008). Characterization of epoxyeicosatrienoic acid binding site in U937 membranes using a novel radiolabeled agonist, 20-125i-14, 15-epoxyeicosa-8 (Z)-enoic acid. *Journal of Pharmacology and Experimental Therapeutics* **324**(3)**:** 1019-1027.

Zhang C, Harder DR (2002). Cerebral capillary endothelial cell mitogenesis and morphogenesis induced by astrocytic epoxyeicosatrienoic acid. *Stroke* **33**(12)**:** 2957-2964.

Zhang W, Koerner IP, Noppens R, Grafe M, Tsai H-J, Morisseau C, *et al.* (2007). Soluble epoxide hydrolase: a novel therapeutic target in stroke. *Journal of Cerebral Blood Flow & Metabolism* **27**(12)**:** 1931-1940.

Zieglgansberger W, French ED, Siggins GR, Bloom FE (1979). Opioid peptides may excite hippocampal pyramidal neurons by inhibiting adjacent inhibitory interneurons. *Science* **205**(4404)**:** 415-417.

Zordoky BN, Anwar-Mohamed A, Aboutabl ME, El-Kadi AO (2011). Acute doxorubicin toxicity differentially alters cytochrome P450 expression and arachidonic acid metabolism in rat kidney and liver. *Drug Metabolism and Disposition* **39**(8)**:** 1440-1450.

Zou A, Fleming J, Falck J, Jacobs E, Gebremedhin D, Harder D, *et al.* (1996). Stereospecific effects of epoxyeicosatrienoic acids on renal vascular tone and $K^{(+)}$-channel activity. *American Journal of Physiology-Renal Physiology* **270**(5)**:** F822-F832.

Zusterzeel PL, Peters WH, Visser W, Hermsen KJ, Roelofs HM, Steegers EA (2001). A polymorphism in the gene for microsomal epoxide hydrolase is associated with pre-eclampsia. *Journal of medical genetics* **38**(4)**:** 234-237.

Chapter 2

11,12 -Epoxyeicosatrienoic acid (11,12 EET) reduces excitability and excitatory transmission in the hippocampus

Nandkishor K. Mule [a], Anette C. Orjuela Leon [a], John R. Falck [b], Michael Arand [a], Anne Marowsky [a, *]

[a] Institute of Pharmacology and Toxicology, University of Zurich, Winterthurerstr. 190, 8057 Zurich, Switzerland
[b] Department of Biochemistry, Southwestern Medical Center, Dallas, Tx, USA

c Corresponding author.
E-mail address: marowsky@pharma.uzh.ch (A. Marowsky).

Author's contributions: Nandkishor K. Mule designed and performed experiments and contributed towards data analysis, generation of figures and writing of the manuscript.

Contents lists available at ScienceDirect

Neuropharmacology

journal homepage: www.elsevier.com/locate/neuropharm

11,12 -Epoxyeicosatrienoic acid (11,12 EET) reduces excitability and excitatory transmission in the hippocampus

Nandkishor K. Mule [a], Anette C. Orjuela Leon [a], John R. Falck [b], Michael Arand [a], Anne Marowsky [a, *]

[c] Institute of Pharmacology and Toxicology, University of Zurich, Winterthurerstr. 190, 8057 Zurich, Switzerland

[d] Department of Biochemistry, Southwestern Medical Center, Dallas, Tx, USA

ARTICLE INFO

Article history:
Received 30 January 2017
Received in revised form
25 April 2017
Accepted 13 May 2017
Available online 17 May 2017

Keywords:
EETs
Soluble epoxide hydrolase
Neurotransmission
Hippocampus
GIRK channel
Epilepsy

ABSTRACT

Recent studies suggest a role for the arachidonic acid-derived epoxyeicosatrienoic acids (EETs) in attenuating epileptic seizures. However, their effect on neurotransmission has never been investigated in detail. Here, we studied how 11,12- and 14,15 EET affect excitability and excitatory neurotransmission in mouse hippocampus. 11,12 EET (2 μM), but not 14,15 EET (2 μM), induced the opening of a hyper-polarizing K^+ conductance in CA1 pyramidal cells. This action could be blocked by $BaCl_2$, the G protein blocker GDPβ-S and the GIRK1/4 blocker tertiapin Q and the channel was thus identified as a GIRK channel. The 11,12 EET-mediated opening of this channel significantly reduced excitability of CA1 pyramidal cells, which could not be blocked by the functional antagonist EEZE (10 μM). Furthermore, both 11,12 EET and 14,15 EET reduced glutamate release on CA1 pyramidal cells with 14,15 EET being the less potent regioisomer. In CA1 pyramidal cells, 11,12 EET reduced the amplitude of excitatory postsynaptic currents (EPSCs) by 20% and the slope of field excitatory postsynaptic potentials (fEPSPs) by 50%, presumably via a presynaptic mechanism. EEZE increased both EPSC amplitude and fEPSP slope by 40%, also via a presynaptic mechanism, but failed to block 11,12 EET-mediated reduction of EPSCs and fEPSPs. This strongly suggests the existence of distinct targets for 11,12 EET and EEZE in neurons. In summary, 11,12 EET substantially reduced excitation in CA1 pyramidal cells by inhibiting the release of glutamate and opening a GIRK channel. These findings might explain the therapeutic potential of EETs in reducing epileptiform activity.

© 2017 The Authors. Published by Elsevier Ltd. This is an open access article under the CC BY license (http://creativecommons.org/licenses/by/4.0/).

2.1. Introduction

Lipid signaling molecules in the central nervous system (CNS) are diverse, including prominent eicosanoids such as the arachidonic acid (AA) derivatives endocannabinoids and prostaglandins. Lesser known are the AA-derived epoxyeicosatrienoic acids (EETs), which are synthesized by cytochrome P450 (CYP) epoxygenases. Due to the four double bonds in AA, four EET regioisomers are formed: 5,6-, 8,9-, 11,12- and 14,15-EET, with each regioisomer consisting of a mixture of R/S and S/R enantiomers (Capdevila et al., 2000). Although often considered as a single entity, several studies suggest that EETs act in a regioisomer- and enantiomer-specific manner (Ding et al., 2014; Lu et al., 2002; Node et al., 2001; Wang et al., 2008; Zou et al., 1996).

Generally, the relative quantities of EET regioisomers vary with the CYP isoenzyme present in the respective tissue. Of the 160 CYP isoenzymes in the mouse, members of the CYP2C and CYP2J family are most commonly considered to exert the highest epoxygenase activity toward AA (Spector and Norris, 2007). However, it should be noted that several other CYP isoforms also act as epoxygenases and generate EETs such as rat CYP2D18 (Thompson et al., 2000) and mouse CYP4X1 (Al-Anizy et al., 2006). The CNS cell types expressing epoxygenases comprise endothelial cells, astrocytes and neurons (reviewed in (Iliff et al., 2010b)). Specifically, the epoxygenases CYP4X1 (Al-Anizy et al., 2006), CYP2C29, CYP2C38 (Luo et al., 1998), CYP2J9 (Qu et al., 2001), CYP2J8, CYP2J11, CYP2J13 (Graves et al., 2013) and CYP2J5 (Allen brain atlas (Lein et al., 2007), http://www.brainmap.org) were identified in mouse brain. EETs are released in a calcium- and activity-dependent manner from diverse CNS cells, including sensory neurons (Sisignano et al., 2012) and astrocytes (Alkayed et al., 1997). However, if they are exclusively

* Corresponding author.
E-mail address: marowsky@pharma.uzh.ch (A. Marowsky).

http://dx.doi.org/10.1016/j.neuropharm.2017.05.013

0028-3908/© 2017 The Authors. Published by Elsevier Ltd. This is an open access article under the CC BY license (http://creativecommons.org/licenses/by/4.0/).

synthesized on demand like most AA metabolites or released from endogenous EET pools, in which they are present as esters of glycerophospholipids (Capdevila et al., 2000), is still disputed.

Earlier studies established EETs as potent vasodilators with a central role in neurovascular coupling, the linking of neuronal activity via astrocytes to evoke cerebral arteriolar dilatory responses (Imig et al., 2011). Furthermore, EETs display angiogenic, anti-apoptotic and anti-inflammatory properties, which together with the vasodynamic effect probably underlie EET-mediated neuro-protection (Koerner et al., 2007; Li et al., 2012; Liu et al., 2016b). Further EET-mediated effects in the CNS include the release of neuropeptides (Iliff et al., 2010a) and powerful anti-nociception, which is observed after injection of 14,15 EET into the periaqueductal gray, the primary control center for descending pain modulation (Terashvili et al., 2008). The bioactivity of EETs is limited by their hydrolysis to, reportedly, less active diols (dihydroxyeicosatrienoic acids, DHETs), a reaction catalyzed predominantly by soluble epoxide hydrolase (sEH) in the mouse brain (Zhang et al., 2007). Consistent with this, inhibitors of sEH (sEHi) effectively increase EET levels *in vivo* and have garnered widespread attention for their potential therapeutic use in multiple disorders such as hypertension, stroke, dyslipidemia, pain, immunological and neurological diseases (Shen, 2010).

Still, the exact mechanisms by which EETs exert their various effects remain poorly defined. It is generally agreed that EETs may function as autocrine and paracrine effectors. Potential molecular targets include the K_{ATP} channel (Lu et al., 2002) and the calcium-activated BK channel (BK_{Ca}) (Campbell et al., 1996; Li and Campbell, 1997). More recently, EET-mediated modulation of TRP channels has received attention with several studies reporting effects of EETs on TRPV4 (Earley et al., 2005; Vriens et al., 2005; Watanabe et al., 2003), TRPC6 (Fleming et al., 2007), TRPA1 (Sisignano et al., 2012) and TRPV4-TRPC1 (Ma et al., 2015). However, EETs are less likely to bind to and activate an ion channel directly. They are rather thought to activate a G protein-coupled receptor (Carroll et al., 2006; Hayabuchi et al., 1998; Li and Campbell, 1997), which activates a signal transduction pathway that ultimately modulates ion channel functions.

Even though most of the channels modulated by EETs are widely expressed in the CNS, little is known about the effects of EETs on neuronal excitability and transmission. Three recent studies suggest a possible involvement of EETs in the attenuation of pharmacologically-induced epileptic seizures in mice: i) Seizures generated by inhibition of the GABAergic system, but not by inhibition of 4-AP sensitive K^+ channels, were attenuated by prior application of a sEHi (Inceoglu et al., 2013); ii) Diazepam in combination with a sEHi prevented progression of tetramethylenedisulfotetramine-induced tonic seizures and lethality in mice (Vito et al., 2014), and iii) sEHi treatment led to significant suppression of pilocarpine-induced seizures and an increase in the seizure-induction threshold of fully kindled mice compared to non-treated animals (Hung et al., 2015). However it should be noted that EETs are not the only sEH substrates in the brain; other substrates include epoxides from docosahexaenoic acid (DHA) and eicosapentaenoic acid (EPA), which exert at least partially similar effects to those observed with EETs (Morisseau et al., 2010). While these reports implied that EETs suppress rather than increase neuronal excitation, the only study examining EET-mediated effects on neurotransmission did not affirm this notion. Indeed, 14,15-EET and the sEHi AUDA were both shown to enhance excitatory synaptic transmission in mouse prefrontal cortex, presumably by promoting the insertion of glutamatergic receptors in the postsynaptic membrane (Wu et al., 2015).

In light of the recent evidence that EETs help to suppress epileptic seizures, we hypothesized that EETs are strong modulators of excitatory synaptic transmission and neuronal excitability in the hippocampus, a brain region central for memory and learning and often the starting point for temporal lobe epilepsy. Specifically, we wanted a) to identify potential pre- and/or postsynaptically located molecular targets, underlying the EET-mediated effect and b) to test, if the so-called functional EET antagonist 14,15-epoxyeicosa-5(Z)-enoic acid (EEZE) (Gauthier et al., 2002) is able to counteract EET-mediated actions on neuronal transmission and excitability.

In this study, we recorded from CA1 pyramidal cells (PCs) in mouse hippocampus, using the patch-clamp technique and field potential recordings, as well as the respective pharmacology to isolate excitatory events. Finally, to address the question how endogenous EETs affect epileptic seizures, the effect of the selective sEHi tAUCB was studied on epileptiform activity in the hippocampus.

2.2. Materials and methods

All experiments were performed in accordance with regulations of the University of Zurich and the veterinary department of the canton of Zurich, Switzerland, for animal handling and experimentation.

2.2.1. Immunohistochemistry

Distribution of CYP2J protein was visualized by immunoperoxidase staining of parasagittal sections from perfusion-fixed tissue of male 10 week-old C57Bl/6 mice. Mice were deeply anesthetized with Nembutal and perfused with 4% paraformaldehyde in 0.15 M phosphate buffer (pH 7.4). Brains were post-fixed for 3 h, cryoprotected with sucrose and sectioned with a microtome (40 μm). Sections were incubated overnight at 4 °C with the CYP2J antibody (rabbit, diluted 1:1000 (Qu et al., 2001) in Tris buffer, pH 7.4 containing 2% normal goat serum and 0.2% Triton-100. The next day, a biotinylated secondary antibody directed against rabbit (1:300 Jackson ImmunoResearch, West Grove, PA, USA) was applied for 30 min, followed by Vectastain elite kit processing (Vector Laboratories, Burlingame, CA, USA) and incubation with diaminobenzidine as chromogen. Sections were mounted onto gelatin-coated glass slides, air-dried, dehydrated, and cover-slipped with Eukitt. Images were digitized with a high-resolution camera and processed using the software Mosaic (ExploraNova, La Rochelle, France).

2.2.2. Hippocampal slice preparation

C57Bl/6J mice were obtained from Charles River laboratories (Freiburg, Germany). Transverse hippocampal slices (350-400 μm thick) of male, 3-4 week old mice were obtained using a vibrating blade microtome, HM 650 V (Thermo Scientific, UK). Briefly, a mouse was anaesthetized and euthanized by decapitation. The brain was extracted and immediately transferred into ice-cold artificial cerebrospinal fluid (ACSF) equilibrated with 95% O_2 and 5% CO_2 containing (in mM) NaCl (125), $CaCl_2$ (2.5), $MgCl_2$ (1), $NaHCO_3$ (26), KCl (2.5), NaH_2PO_4 (1.25) and glucose (10). Slices were immediately transferred to an incubating chamber with ACSF at 35 °C for 20 min and thereafter kept at room temperature.

2.2.3. Electrophysiology

Slices were mounted on poly-L-lysine-coated coverslips and transferred to the recording chamber, where they were continuously superfused with ACSF at a rate of 1.8 ml/min. All experiments were performed at 30-32 °C using an in-line heating system.

Hippocampal formation and CA1 PCs were visualized by using an upright microscope (BX51Wl, Olympus), equipped with a 20x water-immersion objective, infrared/differential interference contrast (DIC) optics and an infrared video imaging camera (VX55, Till Photonics).

Patch pipettes with tip resistances of 3-5 MΩ were pulled from borosilicate glass (GC150F-10, Harvard apparatus, UK) with a horizontal puller (Zeitz instrument, Germany). For most experiments, pipettes were filled with a K-gluconate based internal solution containing (in mM): K-gluconate (145), EGTA (1), HEPES (10), MgATP (5), NaGTP (0.5) and NaCl (5). The pH was adjusted to 7.3 with KOH; osmolarity was 295-305 mOsm. For one set of experiments a CsCl-based internal solution was used containing (in mM): CsCl (100), $MgCl_2$ (2), EGTA (0.1), MgATP (2), NaGTP (0.3) and HEPES (40). The pH was adjusted to 7.3 with CsOH; osmolarity was 290-300 mOsm. For the recordings of evoked excitatory post-synaptic currents (EPSCs), CA1 PCs were held at a holding potential of V_h = -70 mV and a glass capillary filled with ACSF was placed in stratum radiatum on Schaffer collaterals (SCs). Stimuli were given at 0.1 Hz. Bicuculline (25 μM) was present throughout the entire experiment to block inhibitory transmission. To assess the paired pulse ratio, paired stimuli with interstimulus intervals of 50 ms were given. For miniature EPSCs (mEPSCs) recordings, tetrodotoxin (TTX, 1 μM) and bicuculline (25 μM) were added to the bath solution. Ramp recordings were carried out in presence of TTX (1 μM) with CA1 PCs initially voltage clamped at V_h = -70 mV and then ramped from -120 mV to -50 mV in 0.6 s. Before the start of a ramp experiment, cells were held in current clamp mode and current pulses of -10 pA were injected to determine the resting membrane potential (RMP), capacitance, and the input resistance R_{input} of the cell. EET-induced currents were normalized to cell capacitance and expressed as pA/pF. To monitor series resistance R_S and R_{input} throughout voltage-clamp recordings, a hyperpolarizing pulse of -5 mV (50 ms) was given at constant intervals. Recordings, in which R_S changed more than 20% were discarded. To assess the spiking ability of CA1 PCs, cells were held in current clamp and a rectangular current (0.8 s) was injected every minute with the amplitude adapted to the individual cell such that a robust number of action potentials was evoked. EET- and EEZE-induced changes in RMP and the numbers of action potentials were analyzed. Field excitatory postsynaptic recordings (fEPSPs) were recorded in 400 μm thick hippocampal slices with an ACSF-filled glass pipette used as recording pipette. fEPSPs were evoked by stimulating SCs at 0.1 Hz, using a wide-tip ACSF-filled glass capillary. Stimulation intensity, ranging from 20 to 150 μA, was adapted for each recording to obtain a sub-maximal fEPSP signal with minimal non-synaptic contamination. For the recording of population spikes and bicuculline-induced epileptic discharges, the stimulating electrode was again placed on SCs, the recording electrode on stratum pyramidale.

Data were recorded with a Multiclamp 700B amplifier (Axon instruments), filtered at 3-10 kHz and digitized at 20 kHz (A/D hardware from National instruments). Data were acquired and analyzed with IGOR Pro software (Wave Metrics, Lake Oswego). Spontaneous events were analyzed off-line with the Mini Analysis Program (Synaptosoft). Prism 5 (GraphPad, USA) was used for statistical analysis and preparation of the graphs. Appropriate statistical tests were employed as indicated. Results of several experiments are presented as average values ± standard error of mean (SEM).

2.2.4. Pharmacology

All drugs were bath applied except GDPβS, which was dissolved in the internal solution. Stock solutions of tAUCB (trans-4-(4-[3-adamantan-1-yl-ureido]-cyclohexyloxy)-benzoic acid; 10 mM; kindly provided by C. Morisseau) and bicuculline (Tocris) were prepared in DMSO. Stocks for Guanosine-5'-O (2-thiodiphosphate)(GDPßS)sodium salt (10 mM; Biolog, Germany), $BaCl_2$ (1 M; Sigma-Aldrich, Germany) and tetrodotoxin citrate (1 mM; ANAWA, Switzerland) were prepared in purified water (Millipore Systems, USA). EEZE, (±) 11,12- and (±)14,15-EETs as well as 11,12-DHET were obtained from Cayman (Adipogen, Switzerland), dissolved in ethanol. They were dried under nitrogen gas and re-dissolved in ACSF (1-10 mM) before bath-application.

2.3. Results

2.3.1. CYP2J epoxygenase expression in mouse hippocampus

Detailed expression pattern for CYP epoxygenases in mouse hippocampus are rare. To our knowledge, the only cellular distribution pattern so far available is the one for the isoenzyme CYP2J5, which is however based on mRNA expression (Allen brain atlas (Lein et al., 2007)). We studied the expression pattern of CYP2J proteins (as an example for a family of epoxygenases) by immunohistochemistry in brain slices from C57Bl/6J mice, using a CYP2J pan antibody (Qu et al., 2001). In the hippocampus, strong CYP2J immunoreactivity (IR) was detected in cell bodies of CA1-CA3 PCs as well as in their apical and basal dendritic fields with particularly strong IR detected in apical dendrites of CA1 PC in the stratum radiatum (See Fig. 2.1a).

2.3.2. Effects of tAUCB, 11,12-EET and EEZE on CA1 synaptic transmission

To ensure that exogenously applied EETs were not immediately eliminated by sEH, the dominant epoxide hydrolase in mouse hippocampus (Marowsky et al., 2009), the potent and selective sEHi tAUCB (Hwang et al., 2007) was used. In a first experiment, we tested if tAUCB alone exerted any effects on synaptic transmission. Stimulating SCs, we recorded EPSCs in CA1 PCs; tAUCB (1 μM) was bath-applied. EPSC amplitude, kinetic parameters (rise time and decay constants) as well as the holding current I_{hold} were not affected by tAUCB (Fig. 2.1b, Suppl.Table 1). All subsequent experiments in which EETs were applied were therefore carried out in presence of 1 μM tAUCB.

Of the four EET regioisomers, we chose the ones synthesized in highest quantities in the hippocampus, 11,12 and 14,15 EET (Sanchez-Mejia et al., 2008). The focus was on the 11,12-regioisomer, additional experiments were conducted with 14,15 EET for comparison. First, we evaluated the effect of 11,12 EET on EPSCs in CA1 PCs, voltage-clamped at V_h = -70 mV. EPSCs were evoked by two consecutive stimuli with an interstimulus interval of 50 ms in presence of bicuculline (25 μM) to block inhibitory transmission. Bath-application of 11,12 EET (2 μM) led to a rapid and significant reduction of both EPSC amplitudes with the first amplitude reduced to 78 ± 5% (n = 5, paired Student's *t* test, p = 0.0256*) and the second to 86 ± 4% (p = 0.0481*, Fig. 2.1c, c_1, e). Comparison of the paired pulse ratio (PPR: Amp2/Amp1) under control conditions and in presence of EETs revealed an increase from 1.94 ± 0.13 to 2.15 ± 0.1 (paired Student's *t* test, p = 0.032*). Such a change in paired-pulse facilitation is usually an indication for a presynaptic site of action. We next tested if the antagonist EEZE is able to block the EET-induced reduction of EPSCs. Application of EEZE (10 μM) significantly potentiated both EPSC amplitudes (Fig. 2.1d, d_1) to 141 ± 10% (Amp1, n = 9, paired Student's *t* test, p = 0.0026**) and 119 ± 8, respectively (Amp2, p = 0.043*). The concomitant change in the PPR from 2.13 ± 0.11 to 1.77 ± 0.10 (Fig. 2.1f; p = 0.00078***) again pointed to a presynaptic site of

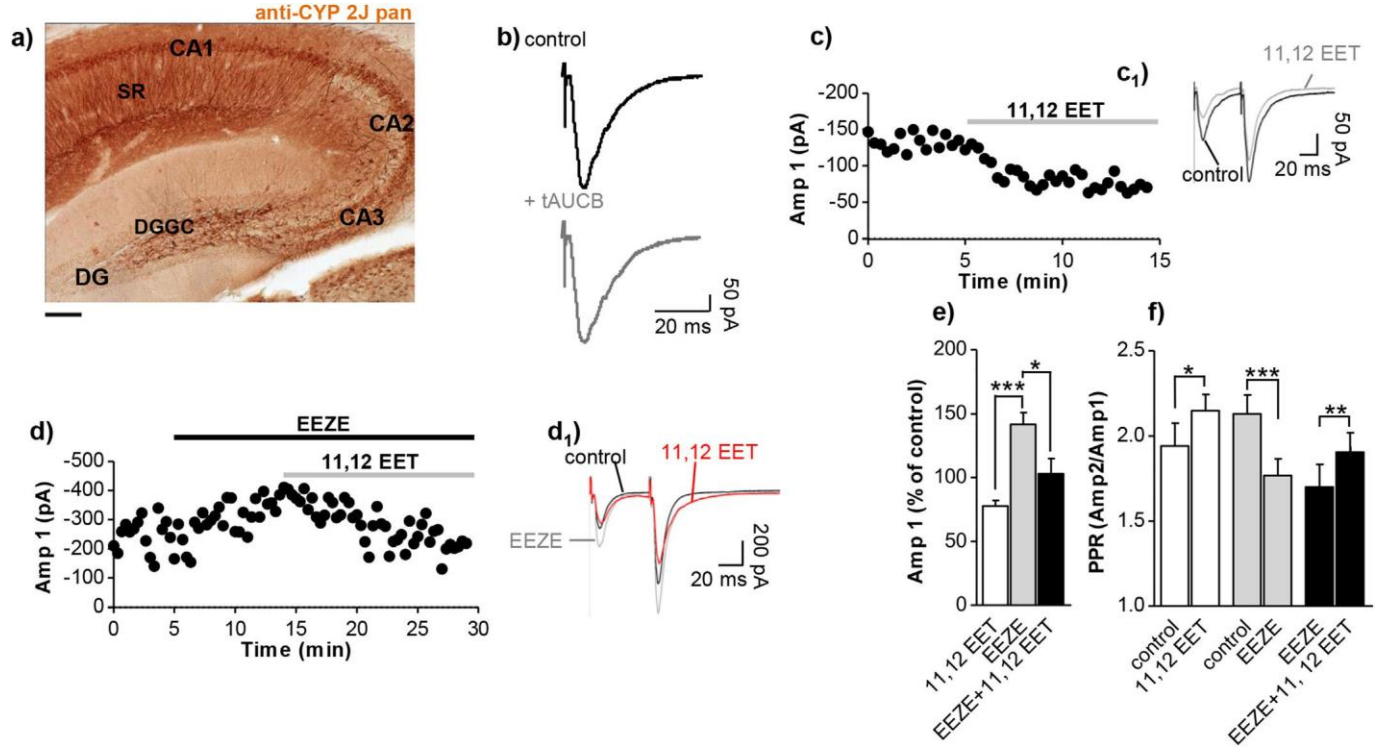

Fig. 2.1. 11,12 EET reduces, but EEZE potentiates EPSCs recorded in CA1 PCs.

a) CYP2J expression in mouse hippocampal formation illustrated by immunoperoxidase staining. Note the strong CYP2J IR in pyramidal cell bodies and particularly in CA1 dendrites, while dentate gyrus granule cells are spared. Scale bar: 250 μm; b) Representative traces of EPSCs before (upper graph) and after tAUCB (lower graph); summary of EPSC parameters are presented in Suppl. Table 1; c) Plot of EPSC peak amp 1 vs. time for a representative CA1 PC with the horizontal line indicating the time of bath-application of 2 μM 11,12 EET; c_1) Average of 10-20 traces from c) before and after application of 11,12 EET; d) Plot of EPSC peak amplitude vs. time for a representative CA1 PC exposed to the functional EET-antagonist EEZE (10 μM), followed by 11,12 EET (2 μM) as indicated by the horizontal lines; d_1) Average of 10-20 traces before and after application of EEZE and 11,12 EET; e) Summary of the effect of 11,12 EET (2 μM), EEZE (10 μM) and 11,12 EET (2 μM) +EEZE(10 μM) on EPSC amp; 1-way-ANOVA followed by Bonferroni, post-hoc analysis; for detailed data and statistics see Suppl. Table 2; f) Application of 11,12 EET, EEZE or 11,12 EET in presence of EEZE significantly changes the PPRs, suggesting presynaptic molecular targets for these compounds. $p < 0.05$*, $p < 0.01$**, $p < 0.001$***. Abbreviations: CA cornu ammonis; DG dentate gyrus; DGGC dentate gyrus granule cells; SR stratum radiatum.

action. Surprisingly, prior application of EEZE followed by 11,12 EET was unable to prevent EET-mediated reduction of EPSC amplitudes (Fig. 2.1d). Moreover, even in the presence of EEZE, EETs still seemed to exert their effect by a presynaptic mechanism as indicated by the change in the PPR (Fig. 2.1f). (Detailed data for evoked EPSC recordings are shown in Suppl. Table 2).

To examine in more detail the presynaptic actions of EETs and EEZE, we next recorded mEPSCs in CA1 PCs in presence of TTX (1 μM) to abolish action potentials. mEPSCs are due to random release of single presynaptic glutamate vesicles at different synaptic sites. While application of 11,12 EET affected neither mEPSC amplitude nor frequency (n = 5, Fig. 2.2a-a_2, c), EEZE led to a rapid increase in the occurrence of mEPSCs, shown in Fig. 2.2b, b_1 and d (n = 5). However, EEZE had no consistent effect on mEPSC amplitudes in CA1 PCs (Fig. 2.2b_2, d). (Detailed data for mEPSCs recordings are shown in Suppl. Table 3). A change in mEPSC frequency is usually attributed to effects on quantal transmitter release and as such the effect is undisputedly of presynaptic origin. Taken together, the results indicate that EEZE affects transmitter release in the absence of action potentials, whereas 11,12 EET has no effect under these conditions. This strongly suggests two different pre-synaptic molecular targets.

In addition to the effect on EPSC amplitude, we observed another striking effect in some of the evoked EPSC and mEPSC experiments: The holding current I_{hold} was substantially modulated by 11,12 EET (see Figs. 2.2a and 2.3a), in a manner compatible with an increase in outward current. Re-analysis of the EET-mediated effect on I_{hold} in mEPSC recordings revealed that on average I_{hold} increased robustly by +21 ± 4 pA (n = 6, Student's paired *t* test p = 0.00615**, Fig. 2.3c, Suppl. Table 3). This increase in I_{hold} was accompanied by a decrease in input resistance (Fig. 2.3d), indicative of channel opening and the activation of a conductance. To gain further insight into the nature of the conductance, we repeated these experiments with a CsCl-based internal solution, as Cs^+ is known to block K^+ -conducting ion channels. Under these conditions, relative to the control, ΔI_{hold} and R_{input} were unchanged upon application of EETs (Fig. 2.3c,e). This demonstrates that no further conductance was activated and suggests that 11,12 EET activates a postsynaptic K^+ current.

2.3.3. Characterization of the 11,12 EET-induced current

For a more detailed characterization of the EET-activated current, we investigated its current-voltage relationship. To this end, current-voltage curves were obtained (n = 5) in the presence of TTX (1 μM). The 11,12 EET-induced current reversed at -102 ± 6 mV (Fig. 2.4a). These experiments were carried out with an extracellular K^+ concentration of 2.5 mM and an internal K^+ concentration of 145 mM (using a K-gluconate internal solution), therefore according to the Nernst equation the calculated K^+ reversal potential was -106 mV at 32 °C. The reversal potential determined by us was compatible with a K^+ current. For comparison, the same experiment was conducted with 14,15 EET (2 μM, n = 4); however, 14,15 EET failed to open any conductance in CA1 PCs (Fig. 2.4b). To narrow down the spectrum of possible K^+ channel candidates, we bath-applied 500 μM $BaCl_2$, a classical inhibitor of G protein-coupled

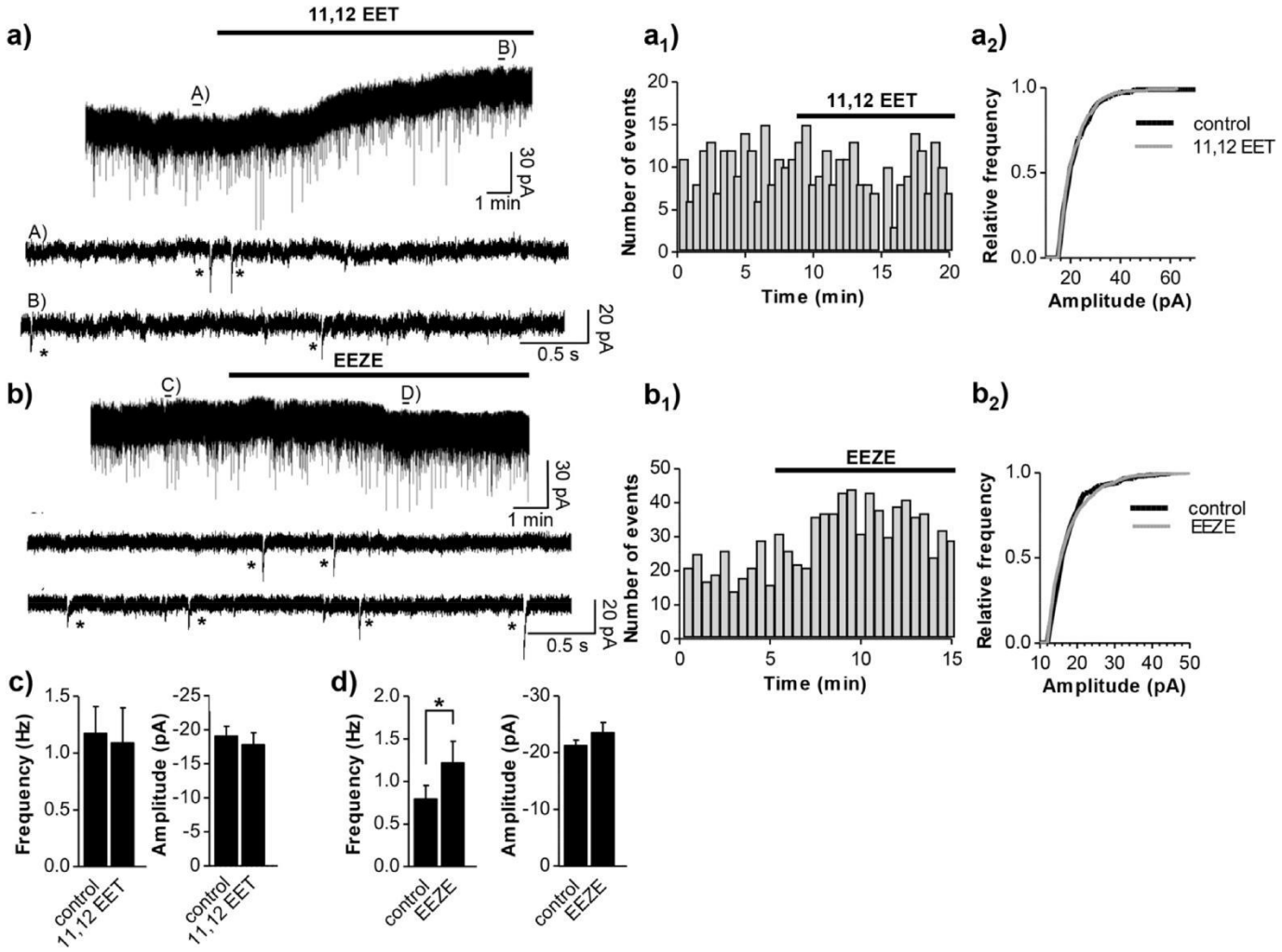

Fig. 2.2. EEZE modulates mEPSC frequency.

a) Representative trace of a mEPSC recording in a CA1 PC with application of 11,12 EET (2 μM) indicated by the horizontal line. Short horizontal lines marked with A) and B) denote stretches that are shown enlarged below to resolve the individual events, marked by asterisks; a_1) Frequency histogram for the mEPSC trace to the left; a_2) Cumulative probability plot depicting mEPSC amplitudes before and after addition of 11,12 EET for the mEPSC recording to the left. b) Representative trace of a mEPSC recording in a CA1 PC with application of EEZE (10 μM) indicated by the horizontal line. Horizontal lines marked with C) and D) denote short stretches shown enlarged below; b_1) Frequency histogram for the mEPSC trace to the left; b_2) Cumulative probability plot depicting mEPSC amplitudes before and after addition of EEZE for the mEPSC recording to the left; c) Summary of the 11,12 EET effect on mEPSC frequency and amplitude in CA1 PCs; d) Summary of the EEZE effect on mEPSC frequency and amplitude in CA1 PCs.

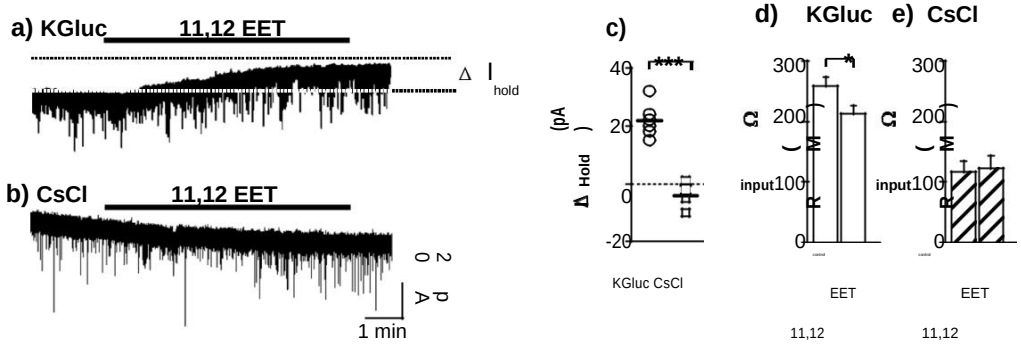

Fig. 2.3. 11,12 EET opens a postsynaptic Cs-sensitive conductance.

a) and b) representative traces of mEPSCs, V_h = -70 mV, recorded with a K-gluconate -based (a) and a CsCl-based (b) internal solution with 11,12 EET (2 μM) application indicated by horizontal lines. 11,12 EET potentiates the outward current only with the K-gluconate-based internal solution; c) and d) Summary of 11,12 EET-mediated changes in I_{hold} and R_{input}, recorded in CA1 PCs with the two different internal solution. $p < 0.05$*, $p < 0.001$***.

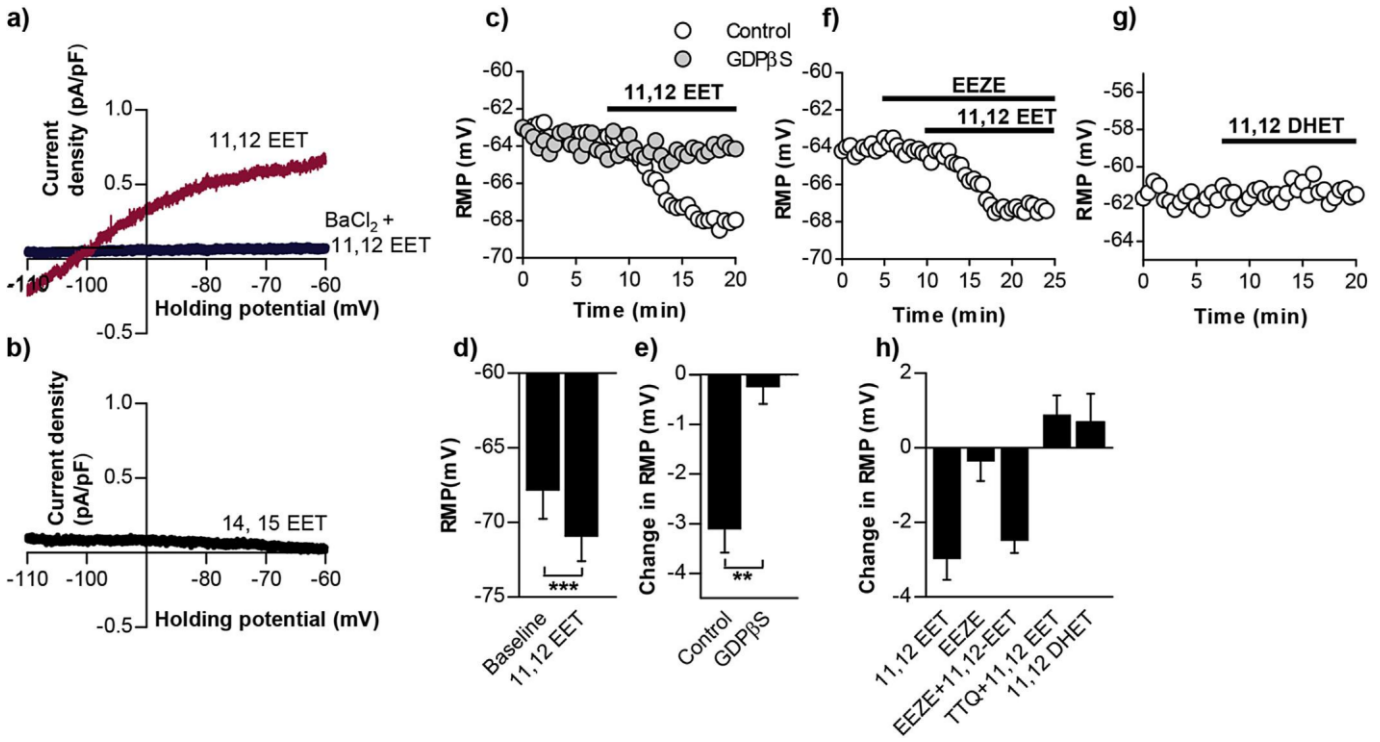

Fig.2.4. 11,12 EET activates a GIRK1/4 conductance in CA1 PCs.

a)Voltage-clamp recordings of CA1 PCs with a K-gluconate-based internal solution. Red trace: A voltage ramp from -120 to -50 mV was applied in control condition and after bath application of 11,12 EET (2 μM). Control traces were subtracted from EET traces; the red trace represents the average of n = 5 cells. Blue trace: The same voltage ramp was applied in presence of 500 μM $BaCl_2$ followed by 11,12 EET (2 μM). $BaCl_2$ traces were subtracted from $BaCl_2$ + 11,12 EET traces. The blue trace represents the average of n = 8 cells. b) The same as a) with 14,15 EET (2 μM). The trace represents the average of n = 4 cells. Due to the lack of effect of 14,15 EET, no experiments were carried out in presence of $BaCl_2$; c) Example of current-clamp recordings of CA1 PCs to monitor RMP. The control cell (white circles) was dialyzed with normal K-gluconate based internal solution, while the other (gray circles) was dialyzed with the same internal solution containing 1 mM GDPβS. 11,12 EET (2 μM) was applied as indicated by the horizontal line; d) Average effect of 11,12 EET (2 μM) on RMP of control cells with normal internal solution; e) Comparison of 11,12 EETs-induced RMP change between control cells and those dialyzed with 1 mM GDPβS; f) Application of EEZE (10 μM) prior to 11,12 EET (2 μM) did not prevent EET-induced hyperpolarization in CA1 PCs, example trace of a representative cell; g) Application of 11,12 DHET had no effect on RMP, example trace of a representative cell; h) Summary graph of RMP changes after application of 11,12 EET (2 μM) or EEZE (10 μM) or 11,12 DHET (5 μM) alone, and in slices pretreated with EEZE (10 μM) or the selective GIRK1/4 blocker tertiapin Q (TTQ, 1 mM) followed by 11,12 EET (2 μM). (For interpretation of the references to colour in this figure legend, the reader is referred to the web version of this article.)

inward rectifier potassium (GIRK) channels (Sodickson and Bean, 1996), prior to 11,12 EET application (n = 8; Fig. 2.4a). In the presence of $BaCl_2$, 11,12 EET was unable to open a conductance. Since activation of GIRK channels modifies substantially the RMP of a neuron to more negative values, we next recorded CA1 PCs in current-clamp mode and monitored RMP before and after application of 11,12 EET; kynurenic acid and bicuculline were present throughout the experiment to suppress any spontaneous synaptic transmission. 11,12 EET hyperpolarized CA1 PC from -67.8 ± 1.8 mV to -70.9 ± 1.6 mV (Fig. 2.4d; n = 9, paired Student's *t* test p = 0.000217***) with an average of ΔRMP of -3.1 ± 0.5 mV (Fig. 2.4h).

EETs may open a GIRK channel either directly or via a G protein. To distinguish between these two scenarios, the G protein blocker GDPβS (1 mM) was included in the internal solution; to ensure complete diffusion, cells were dialyzed 20 min before the start of the recording (n = 5). GDPβS completely abolished EET-mediated hyperpolarization (Fig. 2.4c,e), verifying the involvement of a G-protein and refuting the notion of direct activation of a GIRK conductance by EETs. Final evidence for the EET-mediated activation of a GIRK current was obtained by bath-application of the selective GIRK1/4 (Kir3.1/3.4) blocker tertiapin Q (TTQ, 1 μM) prior to application of EETs. Under these conditions, 11,12 EET was unable to open an additional hyperpolarizing membrane conductance, and cells tended to depolarize slightly instead (n = 5, Fig. 2.4h).

EEZE alone had no effect on RMP and was unable to block EET-induced hyperpolarization in CA1 PCs, when washed in prior to 11,12 EET (Fig. 2.4f, h). Furthermore, the diol, 11,12 DHET (5 μM) was unable to induce a significant change in the RMP of CA1 PCs (Fig. 2.4g and h). Taken together, these results show that 11,12 EET opens, via a G protein-coupled mechanism, a GIRK 1/4 conductance in CA1 PCs, which leads to the observed hyperpolarization in these cells.

To assess if, and to what degree, the EET-activated GIRK current affects excitability of CA1 PCs, we studied the spiking ability of these cells in presence of 11,12 EET and EEZE. CA1 PCs were held in current-clamp mode and injected with a current pulse (Fig. 2.5a) to elicit a short train of action potentials. The injected current was adapted to the individual cell, ranging from +70 to +150 pA. Bath-application of 11,12 EET led to a hyperpolarization similar to that seen before (-3.4 ± 0.5, n = 9, data not shown) and reduced significantly the number of spikes to 76±%3 (n = 9, paired Student's *t* test p = 0.00012***; Fig. 2.5b). In presence of EEZE, the number of spikes was unchanged (n = 7, paired Student's *t* test, p = 0.175, Fig. 2.5c and d), and subsequent application of 11,12 EET reduced the number of spikes in a similar manner to that observed with 11,12 EET alone (75.0 ± 6%, paired Student's *t* test, p = 0.00018***; Fig. 2.5c and d).

2.3.4. Net effects of EETs and EEZE on hippocampal fEPSPs

Next, we addressed if as a net effect in the hippocampus EETs and EEZE dampen or increase excitatory neurotransmission. To this

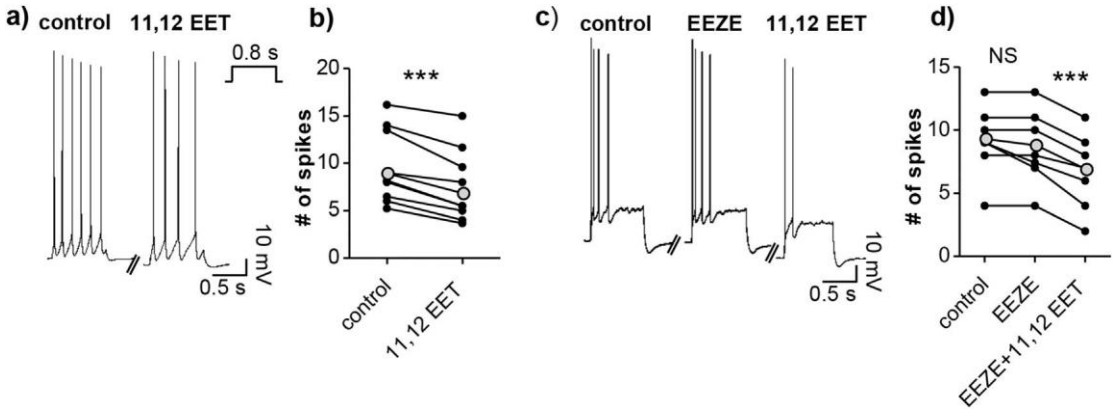

Fig. 2.5. 11,12 EET decreases excitability in CA1 PCs.

a) Representative current-clamp recording of a CA1 PC with response to somatic current injection (80 pA) before (left) and after the application of 11,12 EET (2 μM, right); b) Graph showing how the number of spikes in individual CA1 PCs (black circles) changes in presence of 11,12 EET (2 μM). The average of all cells is shown in gray circles; c) Representative current-clamp recording of a CA1 PC with response to somatic current injection (130 pA) before (left) and after the application of EEZE (10 μM, middle), followed by application of 11,12 EET (2 μM, right); d) Graph showing how the number of spikes in individual PCs (black circles) changes in presence of EEZE (10 μM) followed by 11,12 EET (2 μM). Average of all cells is shown in gray circles. $p < 0.001$***.

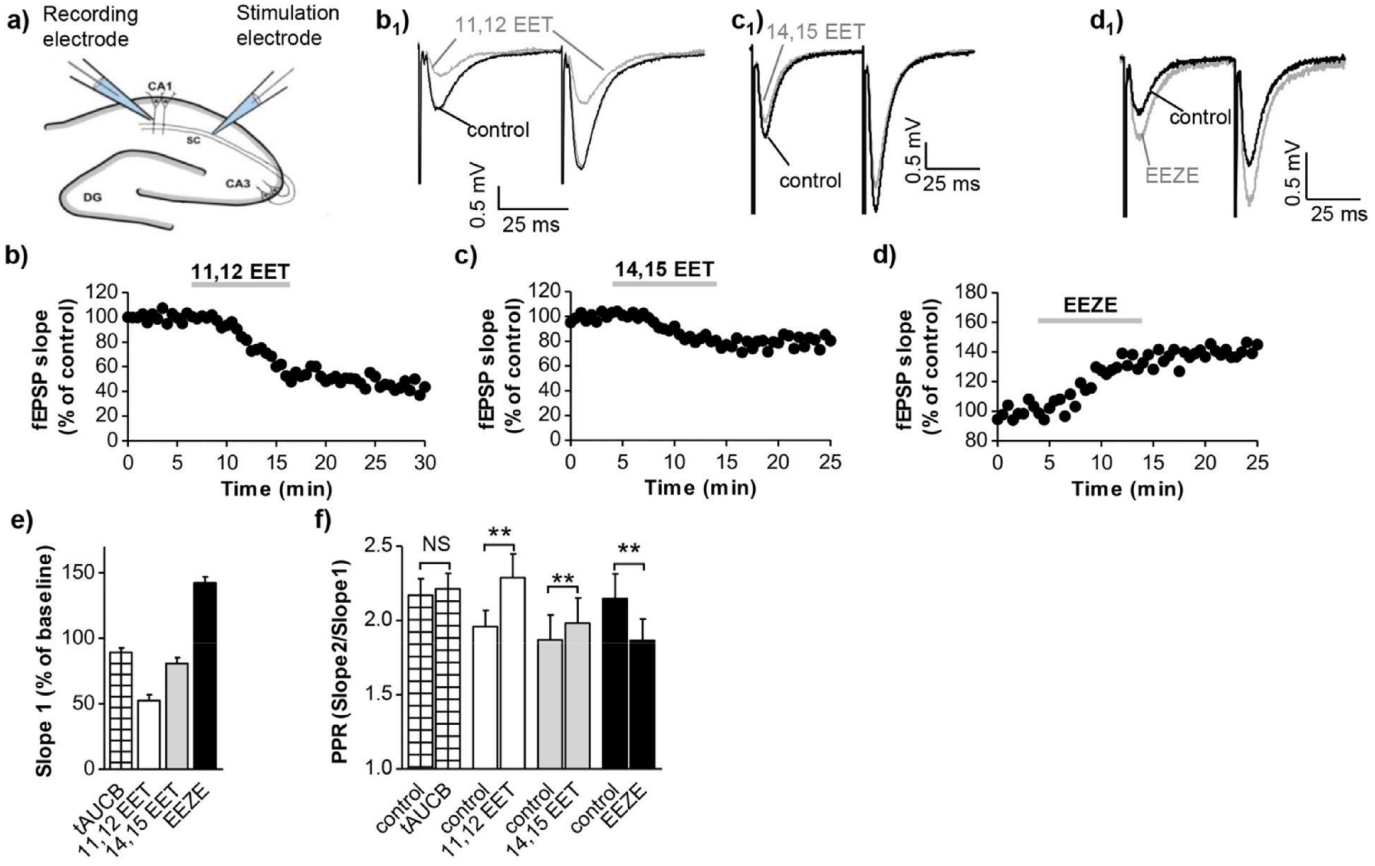

Fig.2.6. 11,12 EET and 14,15 EET decrease, EEZE potentiates hippocampal fEPSPs.

a) Schematic drawing of a hippocampal slice, showing the localization of recording and stimulation electrode; b) Representative fEPSP slope vs. time graph with the application of 11,12 EET (2 μM) indicated by the gray horizontal line; b_1) Average of 20-30 traces before and after application of 11,12 EET; c) and c_1) Same as b) and b_1) for 14,15 EET (2 μM); d) and d_1) Same as b) and b_1) for EEZE (10 μM); e) Summary graph showing the effects of the different compounds on fEPSP slope 1; 1-way ANOVA followed by Bonferroni post hoc analysis: all comparisons $p < 0.001$*** except for tAUCB vs 14,15 EET. For further statistics employing paired Student's *t* test see Table 2.1; f) Both EET regioisomers and EEZE change the respective PPRs significantly, pointing towards a presynaptic mechanism. DG dentate gyrus; SC Schaffer collaterals. $p < 0.01$**.

end stimulating and recording electrodes were both placed in stratum radiatum on SCs (see scheme, Fig. 2.6a) and fEPSPs, evoked by two consecutive stimuli with an interstimulus interval of 50 ms, were recorded with inhibitory transmission left intact. Although under these conditions inhibition is not recorded directly, it is known to substantially modulate and shape hippocampal fEPSPs (Chapman et al., 1998). Unexpectedly, application of tAUCB (1 μM) resulted in a small, but significant decrease of fEPSP slopes and amplitudes, presumably due to effects exerted by accumulation of endogenous EETs (Fig. 2.6e, Table 2.1). Subsequent application of 11,12

Table 2.1
Summary of effects on fEPSPs.

Substance	Slope 1	Slope 2	Amp1	Amp2	*n*	Compared to
tAUCB (1 μM)	89.2 ± 3.2*	90.8 ± 3.0*	91.4 ± 3.2*	92.2 ± 3.1*	8	untreated
11,12 EET (2 μM)	52.4 ± 4.5***	60.2 ± 4.0***	52.8 ± 4.6***	59.4 ± 5.2**	7	tAUCB
14,15 EET (2 μM)	80.8 ± 4.6*	85.5 ± 4.2*	84.5 ± 5.0*	86.1 ± 4.3*	7	tAUCB
EEZE (10 μM)	142.2 ± 4.6***	123.3 ± 3.0**	136.1 ± 9.1**	125.5 ± 5.3**	7	untreated

Values are given as mean percentage ±SEM. For each compound normalized comparisons were carried out as indicated in the furthest column to the right. Asterisks indicate the significant difference obtained from these comparisons. ($p < 0.05$*, $p < 0.01$**, $p < 0.001$***, paired Student's *t* test). *n* number of experiments performed.

EET led to a significant reduction of fEPSP slope1 to 52.4 ± 4.5% and slope2 to 60.2 ± 4.0%, respectively (Fig. 2.6b,b_1,e; for detailed data and fEPSP statistics, see Table 2.1). In comparison to 11,12 EET, 14,15 EET was less potent, only reducing fEPSP slope1 to 80.8 ± 4.6% of baseline values (see Fig. 2.6c, c_1, e). Both 11,12 EET and 14,15 EET significantly increased the PPR (Fig. 2.6f), further supporting the existence of a presynaptic target. By contrast, EEZE markedly potentiated fEPSP slope 1 and amplitude 1 to 140% and 136%, respectively (Fig. 2.6d, d_1, e). Since the potentiating effect was less pronounced for the second slope and amplitude, the PPR decreased under EEZE (Fig. 2.6f), again consistent with previous observations pointing towards a presynaptic site of action. Taken together, 11,12 and 14,15 EETs both reduce excitatory neurotransmission in the hippocampus with 11,12 EET being the more potent of the two. By contrast, EEZE increases excitatory transmission in the hippocampus, and is not capable of antagonizing the EET-mediated reduction.

2.3.5. tAUCB effect on epileptic discharges in the hippocampal formation

The tAUCB-mediated reduction of fEPSPs suggested that recordings from a population of neurons (rather than from a single neuron) might allow for the detection of effects exerted by endogenous EETs, released and accumulated in the brain slice. In a final experiment we, therefore, addressed the effect of tAUCB on epileptiform activity in brain slices. It is known that reduced GABAergic inhibition easily leads to large-scale synchronization and epileptic discharges in the hippocampal network. Thus, we applied bicuculline and, to get a better estimate of the synchronous action potential firing, recorded population spikes by placing the recording electrode on the stratum pyramidale. As expected, bicuculline (25 μM) led to a dramatic change in the waveform of single-pulse evoked population spikes (see Fig. 2.7a) and also substantially increased their amplitude and duration. To quantify the intensity of these epileptic-like bursts, we chose the so-called coastline bursting index CBI (Korn et al., 1987; Riekki et al., 2008). Essentially, beginning and end of the burst waveform were marked and the total duration was measured (see arrows in Fig. 2.7a). After 10 min, application of bicuculline resulted in a marked increase in CBI from 25.6 ± 1.5 to 62.0 ± 3.7 ms ($p = 0.00062$***, n = 5, paired Student's *t* test). By contrast, tAUCB (1 μM) reduced the CBI slightly, but significantly (Fig. 2.7b, d; $p = 0.0077$**, n = 6). When bicuculline was subsequently applied, it led to much less dramatic bursting (Fig. 2.7b,d) compared to bicuculline alone (Fig. 2.7e, unpaired Student's *t* test $p = 0.000136$***). This showed that tAUCB, most likely via stabilizing endogenous EETs, is capable of reducing epileptiform discharges in brain slices consistent with recent data obtained in systemic epilepsy models in rodents.

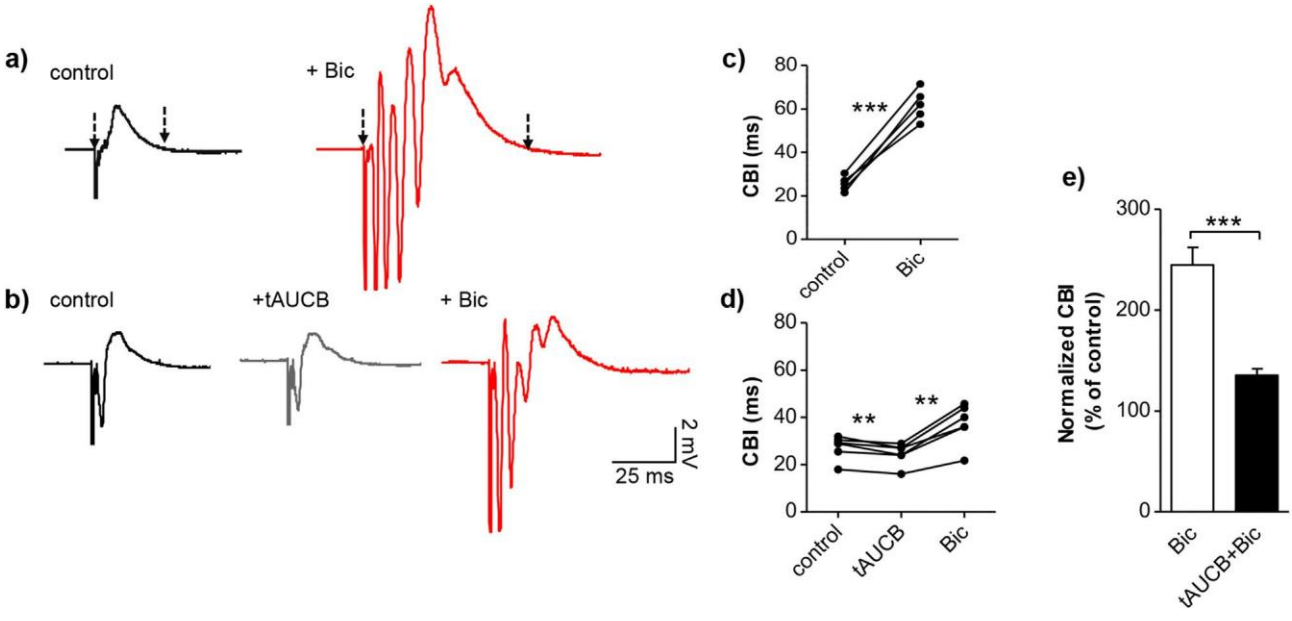

Fig. 2.7. tAUCB attenuates burst-like activity in the hippocampal formation.
a) Representative graphs of single-pulse evoked population spikes recorded from stratum pyramidale under control conditions (untreated slice; left) and 10 min after washing in of bicuculline (25 μM; right). Arrows indicate the total duration, used to calculate the respective CBI; b) Representative graphs of single-pulse evoked population spikes recorded under control conditions (untreated slice; left), after application of tAUCB (1 μM; middle), which was followed by application of bicuculline (25 μM; right). tAUCB and bicuculline graphs were taken each 10 min after start of bath-application of the respective compound; c) Summary graph for a), showing how CBI in individual experiments changes after application of bicuculline; d) Summary graph for b), showing how CBI changes under tAUCB and subsequently under bicuculline; e) Comparison of the normalized CBI observed under bicuculline on untreated slices and the CBI observed in slices pretreated with tAUCB. $p < 0.01$**; $p < 0.001$***.

2.4. Discussion

The present study has four major findings: First, 11,12 EET and to a lesser degree 14,15 EET inhibit EPSCs and fEPSPs in the hippocampus, thus reducing excitatory transmission. Second, 11,12 EET exerts its effect by acting on both pre- and postsynaptic targets in CA1 PCs, whereas the 14,15 EET-mediated effect seems limited to a presynaptic target. Third, postsynaptically, 11,12 EET opens a K^+ conductance via activation of a G protein, resulting in hyperpolarization and attenuated excitability of CA1 PCs. Finally, the functional antagonist EEZE seems to exclusively act via a presynaptic target, which with high probability differs from the one activated by 11,12 EET.

2.4.1. 11,12 EET-mediated hyperpolarization involves the opening of GIRK1/4 channels most likely via activation of $G_{\alpha i/o}$ proteins

We observed a 11,12 EET-specific opening of a hyperpolarizing current, which we identified as a K^+ current due to its reversal potential and the fact that it could be blocked by intracellular Cs^+. Since dialyzing the cell with the G protein blocker GDPβS prevented the EET-mediated opening of the K^+ current, a direct effect of EETs appeared unlikely and suggested that the activation of a G protein is a prerequisite. Both $BaCl_2$ and tertiapin Q blocked the 11,12 EET-mediated opening of the K^+ conductance and these findings together with the IV-curve (Fig. 2.4a) provide compelling evidence that 11,12 EET opens a GIRK channel in CA1 PCs. GIRKs usually require activation by the β/γ subunit of $G_{i/o}$ proteins, whereas G_s proteins only activate GIRK under nonphysiological conditions (e.g. following overexpression) (Dascal and Kahanovitch, 2015). However, studies focusing on intracellular pathways activated by EETs exclusively reported the involvement of G_s proteins. It needs to be noted, however, that all these studies used non-neuronal cells, e.g. endothelial cells (Ding et al., 2014; Node et al., 2001), preglomerular microvessels (Carroll et al., 2006), coronary arteries (Li and Campbell, 1997) and HEK cells (Fukao et al., 2001), implying that the cell type is of central importance as to which G protein is activated by EETs. Taken together, our discovery of the 11,12 EET-mediated opening of a GIRK channel, including the activation of $G_{i/o}$ proteins, constitutes a so far undescribed, new cellular pathway. This result may also shed new light on previous findings that EETs contribute to μ-opioid receptor-mediated anti-nociception (Conroy et al., 2010; Terashvili et al., 2008), a GPCR system commonly linked to $G_{i/o}$ proteins.

2.4.2. Potential postsynaptic targets for 11,12 EET in CA1 PCs

A large body of data, accumulated over the last three decades, suggests that EETs act through a specific binding site, most likely a cell surface receptor (Chen et al., 2009; Falck et al., 2003; Snyder et al., 2002). Because the majority of EET-mediated physiological responses occur with nanomolar concentrations, the existence of a high-affinity EET-receptor was proposed. We used low micro-molecular concentrations (2 μM) of 11,12 EET throughout our study, but it is difficult to relate that to the final concentration reaching to the recording spot in brain slice. Tissue preparations are notorious for their ability to take up and sequester lipophilic, detergent-like compounds like EETs, which was also evident in our recordings as EET-mediated effects were difficult to reverse via wash out (see Fig. 2.6b with the effect lingering for 20 min after EET application). Furthermore, in our hands 11,12 EET concentrations in the nanomolar range produced extremely inconsistent results, often failing to elicit any response, which we attributed to the highly lipophilic nature of the compound. As a result, it was not possible to establish a meaningful dose-response relation and we decided to use a fixed concentration that gave reproducible results.

Although an EET-specific GPCR still awaits identification, some well-characterized GPCRs have been identified to which EETs, and specifically 11,12 EET, reportedly bind; these include the cannabinoid receptors CB1 and CB2, the dopamine receptor D3 and the GPR40. However, it takes 11,12 EET concentrations in the 100 micromolar range to displace high-affinity radio ligands from CB1, CB2 and D3 receptors (Inceoglu et al., 2007). EC_{50} values for the human GPR 40 are in a comparatively lower range with 6-8 μM (Itoh et al., 2003). Still, the GPR 40 constitutes an unlikely candidate for two reasons: 1.) EETs and DHETs were shown to activate the GPR40 to a similar degree (Itoh et al., 2003), while in our study only 11,12 EET, but not the corresponding DHET, was capable to activate a GIRK channel (see Fig. 2.4g). Furthermore, the GPR 40 is reportedly coupled to $G_{q/11}$ (Briscoe et al., 2003) and thus highly unlikely to activate a GIRK channel, which is classically linked to $G_{i/o}$ proteins (Dascal and Kahanovitch, 2015). Recently, 105 GPCRs were screened for their ability to respond to 14,15 EET, but unfortunately not 11,12 EET. While several GPCRs responded to micromolecular concentrations of 14,15 EET (the top five all being prostaglandin receptors), none could be identified meeting the criteria for a high-affinity receptor (Liu et al., 2016a). Similar unsatisfactory results with a smaller number of GPCRs, none of them responsive to 14,15 EET, were reported earlier in a study by Behm and colleagues (Behm et al., 2009), in which 14,15 EET was ultimately identified as an antagonist of native thromboxane receptors. Given our results, in which 11,12 EET shows distinct actions on GIRKs, it seems desirable to repeat these screenings with 11,12 EET.

2.4.3. Presynaptic effects mediated by 11,12 EET and possible molecular targets

Both EET regioisomers and EEZE modulate the PPR of evoked EPSCs and fEPSPS, which is consistent with a presynaptic mechanism. Notably, EEZE can a) not block the 11,12 EET-mediated reduction of EPSCs and b) changes mEPSC frequency, which 11,12 EET does not. These observations suggest distinct molecular mechanisms and targets for EEZE and EET. Specifically, the inability of 11,12 EET to alter mEPSC frequency strongly implies that its potential target requires action potential-induced depolarization. Possible candidates include therefore voltage-dependent ion channels such as Ca^{2+} or K^+ channels. The BK_{Ca} channel is an attractive candidate, given both the extensive data on its interaction with EETs and the fact that it is located on presynaptic sites in the CNS. However, at the CA3-CA1 synapse, from which we recorded, BK_{Ca} channels are not recruited under basal condition, but only under extreme conditions as in epileptic states and ischemia (Hu et al., 2001; Runden-Pran et al., 2002). The cardiac L-type Ca^{2+} channel may be another possible target. Interestingly, it is inhibited by nanomolar concentrations of 11,12 EET (Chen et al., 1999), but activated by higher concentrations of EETs via the cAMP/PKA system (Xiao et al., 1998, 2004). However, data showing CNS-residing Ca^{2+} channels interacting with EETs are still lacking. Finally, members of the TRPV family might be activated by EETs in the hippocampus. Particularly the TRPV1 channel family seems an eligible target, as it depresses glutamatergic synaptic transmission upon activation by another AA derivative, 12-(S)-HPETE (Gibson et al., 2008). While this effect seems similar to the one we observed with EETs, TRPV1 channels are exclusively located at excitatory synapses on hippocampal interneurons, excluding them as possible EETs targets on CA3-CA1 synapses. 11,12 EET was also reported to activate a TRPV4-TRPC1-BK_{Ca} complex in smooth muscle cells (Ma et al., 2015), but it remains to be proven if such channel complexes are also existent in neurons. More work is needed to identify the proper presynaptic targets for 11,12 and

14,15 EETs as well as EEZE.

2.4.4. EEZE effects on hippocampal neurotransmission

It is difficult to clearly conclude from our experiments, if the presynaptic effect exerted by EEZE is attributable to the antagonization of EET- mediated action or if EEZE elicits an effect by itself. Importantly, at least in two types of experiments EEZE was applied alone (mEPSC recordings, Fig. 2.2b; fEPSP recordings, Fig. 2.6d) on slices, which were not pretreated with tAUCB (tAUCB application was limited to experiments in which EETs were washed in). Thus, levels of ambient EETs were not elevated, making it less plausible that EEZE action reflects the blockade of an augmented endogenous EET tone.

On the postsynaptic site, EEZE unarguably failed to elicit any antagonistic actions; in fact, it showed no postsynaptic activity at all, since it neither modulated mEPSC kinetics and amplitudes, nor did it affect I_{hold} or RMP. The inability of EEZE to antagonize EET activity in neurons is not entirely unexpected; EEZE has shown inconsistent effects before with the most remarkably being that it vasodilates murine mesenteric arteries to a similar extent as a stable EET analog (Harrington et al., 2004).

2.4.5. tAUCB and its effect on fEPSPs and epileptiform activity in brain slices

The sEHi tAUCB has been used in several recent studies to investigate the effect of endogenous EETs (e.g. Akhnokh et al., 2016; Imig et al., 2012). In our first experiments focusing on EPSCs in single cells, tAUCB alone did not show any effect; however, in field recording, tAUCB significantly reduced fEPSP slopes and amplitudes. An explanation might be that the tAUCB effect is too small to be successfully measured in a single neuron, but becomes apparent when recordings from a whole population of neurons with synchronized activity are carried out. In fact, in the current study a similar phenomenon could be observed with bicuculline, as the $GABA_A$ receptor antagonist allowed for the undisturbed isolation of evoked EPSCs in single pyramidal cells, but led to epileptiform activity in field recording. Interestingly, the tAUCB effect on fEPSPs in absence of any $GABA_A$ receptor antagonists (Fig. 2.6), thus with intact inhibition, was small, since it generated on average only a 10% reduction. Such a slight effect might be due to comparatively low spontaneous activity and weak extracellular stimulation in the slice, which elicits only low Ca^{2+} influx into astrocytes and/or neurons and results in the release of respectively low quantities of EETs. Nevertheless, these amounts of endogenous EETs appeared to be sufficient to dampen subsequent bicuculline-induced epileptic bursts recorded from the somata of CA1 PCs (Fig. 2.7). However, tAUCB results should be interpreted with caution, as DHA or EPA-derived epoxides may also accumulate in the presence of tAUCB and are likely capable to interfere with neuronal transmission.

In summary, this study demonstrates for the first time that EETs have complex and regioisomer-specific pre- and postsynaptic actions in the hippocampus, including the 11,12 EET-mediated opening of a GIRK channel. These findings not only reveal a so far unknown signaling pathway of EETs, but may also help to explain their therapeutic potential in reducing epileptiform activity.

Funding

This work was supported by the Swiss National Foundation (grant PDFMP_127330, M.A.).

Acknowledgements

We thank Urs Gerber and George Hausmann for their helpful comments and careful reading of the manuscript.

Appendix A. Supplementary data

Supplementary data related to this article can be found at http://dx.doi.org/10.1016/j.neuropharm.2017.05.013.

2.5. Bibliography

Akhnokh, M.K., Yang, F.H., Samokhvalov, V., Jamieson, K.L., Cho, W.J., Wagg, C., Takawale, A., Wang, X., Lopaschuk, G.D., Hammock, B.D., Kassiri, Z., Seubert, J.M., 2016. Inhibition of soluble epoxide hydrolase limits mitochondrial damage and preserves function following ischemic injury. Front. Pharmacol. 7, 133.

Al-Anizy, M., Horley, N.J., Kuo, C.W., Gillett, L.C., Laughton, C.A., Kendall, D., Barrett, D.A., Parker, T., Bell, D.R., 2006. Cytochrome P450 Cyp4x1 is a major P450 protein in mouse brain. FEBS J. 273, 936e947.

Alkayed, N.J., Birks, E.K., Narayanan, J., Petrie, K.A., Kohler-Cabot, A.E., Harder, D.R., 1997. Role of P-450 arachidonic acid epoxygenase in the response of cerebral blood flow to glutamate in rats. Stroke 28, 1066e1072.

Behm, D.J., Ogbonna, A., Wu, C., Burns-Kurtis, C.L., Douglas, S.A., 2009. Epoxyeicosatrienoic acids function as selective, endogenous antagonists of native thromboxane receptors: identification of a novel mechanism of vasodilation. J. Pharmacol. Exp. Ther. 328, 231e239.

Briscoe, C.P., Tadayyon, M., Andrews, J.L., Benson, W.G., Chambers, J.K., Eilert, M.M., Ellis, C., Elshourbagy, N.A., Goetz, A.S., Minnick, D.T., Murdock, P.R., Sauls Jr., H.R., Shabon, U., Spinage, L.D., Strum, J.C., Szekeres, P.G., Tan, K.B., Way, J.M., Ignar, D.M., Wilson, S., Muir, A.I., 2003. The orphan G protein-coupled receptor GPR40 is activated by medium and long chain fatty acids. J. Biol. Chem. 278, 11303e11311.

Campbell, W.B., Gebremedhin, D., Pratt, P.F., Harder, D.R., 1996. Identification of epoxyeicosatrienoic acids as endothelium-derived hyperpolarizing factors. Circ. Res. 78, 415e423.

Capdevila, J.H., Falck, J.R., Harris, R.C., 2000. Cytochrome P450 and arachidonic acid bioactivation. Molecular and functional properties of the arachidonate mono-oxygenase. J. Lipid Res. 41, 163e181.

Carroll, M.A., Doumad, A.B., Li, J., Cheng, M.K., Falck, J.R., McGiff, J.C., 2006. Adenosine2A receptor vasodilation of rat preglomerular microvessels is mediated by EETs that activate the cAMP/PKA pathway. Am. J. Physiol. Ren. Physiol. 291, F155eF161.

Chapman, C.A., Perez, Y., Lacaille, J.C., 1998. Effects of GABA(A) inhibition on the expression of long-term potentiation in CA1 pyramidal cells are dependent on tetanization parameters. Hippocampus 8, 289e298.

Chen, J., Capdevila, J.H., Zeldin, D.C., Rosenberg, R.L., 1999. Inhibition of cardiac L-type calcium channels by epoxyeicosatrienoic acids. Mol. Pharmacol. 55, 288e295.

Chen, Y., Falck, J.R., Tuniki, V.R., Campbell, W.B., 2009. 20-125Iodo-14,15-epoxyeicosa-5(Z)-enoic acid: a high-affinity radioligand used to characterize the epoxyeicosatrienoic acid antagonist binding site. J. Pharmacol. Exp. Ther. 331, 1137e1145.

Conroy, J.L., Fang, C., Gu, J., Zeitlin, S.O., Yang, W., Yang, J., VanAlstine, M.A., Nalwalk, J.W., Albrecht, P.J., Mazurkiewicz, J.E., Snyder-Keller, A., Shan, Z., Zhang, S.Z., Wentland, M.P., Behr, M., Knapp, B.I., Bidlack, J.M., Zuiderveld, O.P., Leurs, R., Ding, X., Hough, L.B., 2010. Opioids activate brain analgesic circuits through cytochrome P450/epoxygenase signaling. Nat. Neurosci. 13, 284e286.

Dascal, N., Kahanovitch, U., 2015. The roles of gbetagamma and galpha in gating and regulation of GIRK channels. Int. Rev. Neurobiol. 123, 27e85.

Ding, Y., Fromel, T., Popp, R., Falck, J.R., Schunck, W.H., Fleming, I., 2014. The biological actions of 11,12-epoxyeicosatrienoic acid in endothelial cells are specific to the R/S-enantiomer and require the G(s) protein. J. Pharmacol. Exp. Ther. 350, 14e21.

Earley, S., Heppner, T.J., Nelson, M.T., Brayden, J.E., 2005. TRPV4 forms a novel Ca^{2+} signaling complex with ryanodine receptors and BKCa channels. Circ. Res. 97, 1270e1279.

Falck, J.R., Reddy, L.M., Reddy, Y.K., Bondlela, M., Krishna, U.M., Ji, Y., Sun, J., Liao, J.K., 2003. 11,12-epoxyeicosatrienoic acid (11,12-EET): structural determinants for inhibition of TNF-alpha-induced VCAM-1 expression. Bioorg. Med. Chem. Lett. 13, 4011e4014.

Fleming, I., Rueben, A., Popp, R., Fisslthaler, B., Schrodt, S., Sander, A., Haendeler, J., Falck, J.R., Morisseau, C., Hammock, B.D., Busse, R., 2007. Epoxyeicosatrienoic acids regulate Trp channel dependent Ca^{2+} signaling and hyperpolarization in endothelial cells. Arterioscler. Thromb. Vasc. Biol. 27, 2612e2618.

Fukao, M., Mason, H.S., Kenyon, J.L., Horowitz, B., Keef, K.D., 2001. Regulation of BK(Ca) channels expressed in human embryonic kidney 293 cells by epoxyeicosatrienoic acid. Mol. Pharmacol. 59, 16e23.

Gauthier, K.M., Deeter, C., Krishna, U.M., Reddy, Y.K., Bondlela, M., Falck, J.R., Campbell, W.B., 2002. 14,15-Epoxyeicosa-5(Z)-enoic acid: a selective epoxyeicosatrienoic acid antagonist that inhibits endothelium-dependent hyperpolarization and relaxation in coronary arteries. Circ. Res. 90, 1028e1036. Gibson, H.E., Edwards, J.G., Page, R.S., Van Hook, M.J., Kauer, J.A., 2008. TRPV1 channels mediate long-term depression at synapses on hippocampal interneurons. Neuron 57, 746e759.

Graves, J.P., Edin, M.L., Bradbury, J.A., Gruzdev, A., Cheng, J., Lih, F.B., Masinde, T.A., Qu, W., Clayton, N.P., Morrison, J.P., Tomer, K.B., Zeldin, D.C., 2013. Characterization of four new mouse cytochrome P450 enzymes of the CYP2J subfamily. Drug Metab. Dispos. 41, 763e773.

Harrington, L.S., Falck, J.R., Mitchell, J.A., 2004. Not so EEZE: the 'EDHF' antagonist 14, 15 epoxyeicosa-5(Z)-enoic acid has vasodilator properties in mesenteric arteries. Eur. J. Pharmacol. 506, 165e168.

Hayabuchi, Y., Nakaya, Y., Matsuoka, S., Kuroda, Y., 1998. Endothelium-derived hyperpolarizing factor activates Ca^{2+}-activated Kþ channels in porcine coronary artery smooth muscle cells. J. Cardiovasc Pharmacol. 32, 642e649.

Hu, H., Shao, L.R., Chavoshy, S., Gu, N., Trieb, M., Behrens, R., Laake, P., Pongs, O., Knaus, H.G., Ottersen, O.P., Storm, J.F., 2001. Presynaptic Ca^{2+}-activated K^+ channels in glutamatergic hippocampal terminals and their role in spike repolarization and regulation of transmitter release. J. Neurosci. 21, 9585e9597.

Hung, Y.W., Hung, S.W., Wu, Y.C., Wong, L.K., Lai, M.T., Shih, Y.H., Lee, T.S., Lin, Y.Y., 2015. Soluble epoxide hydrolase activity regulates inflammatory responses and seizure generation in two mouse models of temporal lobe epilepsy. Brain Behav. Immun. 43, 118e129.

Hwang, S.H., Tsai, H.J., Liu, J.Y., Morisseau, C., Hammock, B.D., 2007. Orally bioavailable potent soluble epoxide hydrolase inhibitors. J. Med. Chem. 50, 3825e3840.

Iliff, J.J., Fairbanks, S.L., Balkowiec, A., Alkayed, N.J., 2010a. Epoxyeicosatrienoic acids are endogenous regulators of vasoactive neuropeptide release from trigeminal ganglion neurons. J. Neurochem. 115, 1530e1542.

Iliff, J.J., Jia, J., Nelson, J., Goyagi, T., Klaus, J., Alkayed, N.J., 2010b. Epoxyeicosanoid signaling in CNS function and disease. Prostagl. Other Lipid Mediat 91, 68e84.

Imig, J.D., Simpkins, A.N., Renic, M., Harder, D.R., 2011. Cytochrome P450 eicosanoids and cerebral vascular function. Expert Rev. Mol. Med. 13, e7.

Imig, J.D., Walsh, K.A., Hye Khan, M.A., Nagasawa, T., Cherian-Shaw, M., Shaw, S.M., Hammock, B.D., 2012. Soluble epoxide hydrolase inhibition and peroxisome proliferator activated receptor gamma agonist improve vascular function and decrease renal injury in hypertensive obese rats. Exp. Biol. Med. (Maywood) 237, 1402e1412.

Inceoglu, B., Schmelzer, K.R., Morisseau, C., Jinks, S.L., Hammock, B.D., 2007. Soluble epoxide hydrolase inhibition reveals novel biological functions of epoxyeicosatrienoic acids (EETs). Prostagl. Other Lipid Mediat 82, 42e49.

Inceoglu, B., Zolkowska, D., Yoo, H.J., Wagner, K.M., Yang, J., Hackett, E., Hwang, S.H., Lee, K.S., Rogawski, M.A., Morisseau, C., Hammock, B.D., 2013. Epoxy fatty acids and inhibition of the soluble epoxide hydrolase selectively modulate GABA mediated neurotransmission to delay onset of seizures. PLoS One 8, e80922.

Itoh, Y., Kawamata, Y., Harada, M., Kobayashi, M., Fujii, R., Fukusumi, S., Ogi, K., Hosoya, M., Tanaka, Y., Uejima, H., Tanaka, H., Maruyama, M., Satoh, R., Okubo, S., Kizawa, H., Komatsu, H., Matsumura, F., Noguchi, Y., Shinohara, T., Hinuma, S., Fujisawa, Y., Fujino, M., 2003. Free fatty acids regulate insulin secretion from pancreatic beta cells through GPR40. Nature 422, 173e176.

Koerner, I.P., Jacks, R., DeBarber, A.E., Koop, D., Mao, P., Grant, D.F., Alkayed, N.J., 2007. Polymorphisms in the human soluble epoxide hydrolase gene EPHX2 linked to neuronal survival after ischemic injury. J. Neurosci. 27, 4642e4649.

Korn, S.J., Giacchino, J.L., Chamberlin, N.L., Dingledine, R., 1987. Epileptiform burst activity induced by potassium in the hippocampus and its regulation by GABA-mediated inhibition. J. Neurophysiol. 57, 325e340.

Lein, E.S., Hawrylycz, M.J., Ao, N., Ayres, M., Bensinger, A., Bernard, A., Boe, A.F., Boguski, M.S., Brockway, K.S., Byrnes, E.J., Chen, L., Chen, L., Chen, T.M., Chin, M.C., Chong, J., Crook, B.E., Czaplinska, A., Dang, C.N., Datta, S., Dee, N.R., Desaki, A.L., Desta, T., Diep, E., Dolbeare, T.A., Donelan, M.J., Dong, H.W., Dougherty, J.G., Duncan, B.J., Ebbert, A.J., Eichele, G., Estin, L.K., Faber, C., Facer, B.A., Fields, R., Fischer, S.R., Fliss, T.P., Frensley, C., Gates, S.N., Glattfelder, K.J., Halverson, K.R., Hart, M.R., Hohmann, J.G., Howell, M.P., Jeung, D.P., Johnson, R.A., Karr, P.T., Kawal, R., Kidney, J.M., Knapik, R.H., Kuan, C.L., Lake, J.H., Laramee, A.R., Larsen, K.D., Lau, C., Lemon, T.A., Liang, A.J., Liu, Y., Luong, L.T., Michaels, J., Morgan, J.J., Morgan, R.J., Mortrud, M.T., Mosqueda, N.F., Ng, L.L., Ng, R., Orta, G.J., Overly, C.C., Pak, T.H., Parry, S.E., Pathak, S.D., Pearson, O.C., Puchalski, R.B., Riley, Z.L., Rockett, H.R., Rowland, S.A., Royall, J.J., Ruiz, M.J., Sarno, N.R., Schaffnit, K., Shapovalova, N.V., Sivisay, T., Slaughterbeck, C.R., Smith, S.C., Smith, K.A., Smith, B.I., Sodt, A.J., Stewart, N.N., Stumpf, K.R., Sunkin, S.M., Sutram, M., Tam, A., Teemer, C.D., Thaller, C., Thompson, C.L., Varnam, L.R., Visel, A., Whitlock, R.M., Wohnoutka, P.E., Wolkey, C.K., Wong, V.Y., Wood, M., Yaylaoglu, M.B., Young, R.C., Youngstrom, B.L., Yuan, X.F., Zhang, B., Zwingman, T.A., Jones, A.R., 2007. Genome-wide atlas of gene expression in the adult mouse brain. Nature 445, 168e176.

Li, P.L., Campbell, W.B., 1997. Epoxyeicosatrienoic acids activate K^+ channels in coronary smooth muscle through a guanine nucleotide binding protein. Circ. Res. 80, 877e884.

Li, R., Xu, X., Chen, C., Yu, X., Edin, M.L., Degraff, L.M., Lee, C.R., Zeldin, D.C., Wang, D.W., 2012. Cytochrome P450 2J2 is protective against global cerebral ischemia in transgenic mice. Prostagl. Other Lipid Mediat 99, 68e78.

Liu, X., Qian, Z.Y., Xie, F., Fan, W., Nelson, J.W., Xiao, X., Kaul, S., Barnes, A.P., Alkayed, N.J., 2016a. Functional screening for G protein-coupled receptor targets of 14,15-epoxyeicosatrienoic acid. Prostagl. Other Lipid Mediat. http://dx.doi.org/10.1016/j.prostaglandins.2016.09.002 (In press).

Liu, Y., Wan, Y., Fang, Y., Yao, E., Xu, S., Ning, Q., Zhang, G., Wang, W., Huang, X., Xie, M., 2016b. Epoxyeicosanoid signaling provides multi-target protective effects on neurovascular unit in rats after focal ischemia. J. Mol. Neurosci. 58, 254e265.

Lu, T., VanRollins, M., Lee, H.C., 2002. Stereospecific activation of cardiac ATP-sensitive K(+) channels by epoxyeicosatrienoic acids: a structural determinant study. Mol. Pharmacol. 62, 1076e1083.

Luo, G., Zeldin, D.C., Blaisdell, J.A., Hodgson, E., Goldstein, J.A., 1998. Cloning and expression of murine CYP2Cs and their ability to metabolize arachidonic acid. Arch. Biochem. Biophys. 357, 45e57.

Ma, Y., Zhang, P., Li, J., Lu, J., Ge, J., Zhao, Z., Ma, X., Wan, S., Yao, X., Shen, B., 2015. Epoxyeicosatrienoic acids act through TRPV4-TRPC1-KCa1.1 complex to induce smooth muscle membrane hyperpolarization and relaxation in human internal mammary arteries. Biochim. Biophys. Acta 1852, 552e559.

Marowsky, A., Burgener, J., Falck, J.R., Fritschy, J.M., Arand, M., 2009. Distribution of soluble and microsomal epoxide hydrolase in the mouse brain and its contribution to cerebral epoxyeicosatrienoic acid metabolism. Neuroscience 163, 646e661.

Morisseau, C., Inceoglu, B., Schmelzer, K., Tsai, H.J., Jinks, S.L., Hegedus, C.M., Hammock, B.D., 2010. Naturally occurring monoepoxides of eicosapentaenoic acid and docosahexaenoic acid are bioactive antihyperalgesic lipids. J. Lipid Res. 51, 3481e3490.

Node, K., Ruan, X.L., Dai, J., Yang, S.X., Graham, L., Zeldin, D.C., Liao, J.K., 2001. Activation of Galpha s mediates induction of tissue-type plasminogen activator gene transcription by epoxyeicosatrienoic acids. J. Biol. Chem. 276, 15983e15989.

Qu, W., Bradbury, J.A., Tsao, C.C., Maronpot, R., Harry, G.J., Parker, C.E., Davis, L.S., Breyer, M.D., Waalkes, M.P., Falck, J.R., Chen, J., Rosenberg, R.L., Zeldin, D.C., 2001. Cytochrome P450 CYP2J9, a new mouse arachidonic acid omega-1 hydroxylase predominantly expressed in brain. J. Biol. Chem. 276, 25467e25479.

Riekki, R., Pavlov, I., Tornberg, J., Lauri, S.E., Airaksinen, M.S., Taira, T., 2008. Altered synaptic dynamics and hippocampal excitability but normal long-term plasticity in mice lacking hyperpolarizing GABA A receptor-mediated inhibition in CA1 pyramidal neurons. J. Neurophysiol. 99, 3075e3089.

Runden-Pran, E., Haug, F.M., Storm, J.F., Ottersen, O.P., 2002. BK channel activity determines the extent of cell degeneration after oxygen and glucose deprivation: a study in organotypical hippocampal slice cultures. Neuroscience 112, 277e288.

Sanchez-Mejia, R.O., Newman, J.W., Toh, S., Yu, G.Q., Zhou, Y., Halabisky, B., Cisse, M., Scearce-Levie, K., Cheng, I.H., Gan, L., Palop, J.J., Bonventre, J.V., Mucke, L., 2008. Phospholipase A2 reduction ameliorates cognitive deficits in a mouse model of Alzheimer's disease. Nat. Neurosci. 11, 1311e1318.

Shen, H.C., 2010. Soluble epoxide hydrolase inhibitors: a patent review. Expert Opin. Ther. Pat. 20, 941e956.

Sisignano, M., Park, C.K., Angioni, C., Zhang, D.D., von Hehn, C., Cobos, E.J., Ghasemlou, N., Xu, Z.Z., Kumaran, V., Lu, R., Grant, A., Fischer, M.J., Schmidtko, A., Reeh, P., Ji, R.R., Woolf, C.J., Geisslinger, G., Scholich, K., Brenneis, C., 2012. 5,6-EET is released upon neuronal activity and induces mechanical pain hypersensitivity via TRPA1 on central afferent terminals. J. Neurosci. 32, 6364e6372.

Snyder, G.D., Krishna, U.M., Falck, J.R., Spector, A.A., 2002. Evidence for a membrane site of action for 14,15-EET on expression of aromatase in vascular smooth muscle. Am. J. Physiol. Heart Circ. Physiol. 283, H1936eH1942.

Sodickson, D.L., Bean, B.P., 1996. GABAB receptor-activated inwardly rectifying potassium current in dissociated hippocampal CA3 neurons. J. Neurosci. 16, 6374e6385.

Spector, A.A., Norris, A.W., 2007. Action of epoxyeicosatrienoic acids on cellular function. Am. J. Physiol. Cell Physiol. 292, C996eC1012.

Terashvili, M., Tseng, L.F., Wu, H.E., Narayanan, J., Hart, L.M., Falck, J.R., Pratt, P.F., Harder, D.R., 2008. Antinociception produced by 14,15-epoxyeicosatrienoic acid is mediated by the activation of beta-endorphin and metenkephalin in the rat ventrolateral periaqueductal gray. J. Pharmacol. Exp. Ther. 326, 614e622.

Thompson, C.M., Capdevila, J.H., Strobel, H.W., 2000. Recombinant cytochrome P450 2D18 metabolism of dopamine and arachidonic acid. J. Pharmacol. Exp. Ther. 294, 1120e1130.

Vito, S.T., Austin, A.T., Banks, C.N., Inceoglu, B., Bruun, D.A., Zolkowska, D., Tancredi, D.J., Rogawski, M.A., Hammock, B.D., Lein, P.J., 2014. Post-exposure administration of diazepam combined with soluble epoxide hydrolase inhibition stops seizures and modulates neuroinflammation in a murine model of acute TETS intoxication. Toxicol. Appl. Pharmacol. 281, 185e194.

Vriens, J., Owsianik, G., Fisslthaler, B., Suzuki, M., Janssens, A., Voets, T., Morisseau, C., Hammock, B.D., Fleming, I., Busse, R., Nilius, B., 2005. Modulation of the Ca2 permeable cation channel TRPV4 by cytochrome P450 epoxygenases in vascular endothelium. Circ. Res. 97, 908e915.

Wang, Z., Wei, Y., Falck, J.R., Atcha, K.R., Wang, W.H., 2008. Arachidonic acid inhibits basolateral K channels in the cortical collecting duct via cytochrome P-450 epoxygenase-dependent metabolic pathways. Am. J. Physiol. Ren. Physiol. 294, F1441eF1447.

Watanabe, H., Vriens, J., Prenen, J., Droogmans, G., Voets, T., Nilius, B., 2003. Anandamide and arachidonic acid use epoxyeicosatrienoic acids to activate TRPV4 channels. Nature 424, 434e438.

Wu, H.F., Yen, H.J., Huang, C.C., Lee, Y.C., Wu, S.Z., Lee, T.S., Lin, H.C., 2015. Soluble epoxide hydrolase inhibitor enhances synaptic neurotransmission and plasticity in mouse prefrontal cortex. J. Biomed. Sci. 22, 94.

Xiao, Y.F., Huang, L. Morgan, J.P., 1998. Cytochrome P450: a novel system

modulating Ca^{2}+ channels and contraction in mammalian heart cells. J. Physiol. 508 (Pt 3), 777e792.
Xiao, Y.F., Ke, Q., Seubert, J.M., Bradbury, J.A., Graves, J., Degraff, L.M., Falck, J.R., Krausz, K., Gelboin, H.V., Morgan, J.P., Zeldin, D.C., 2004. Enhancement of cardiac L-type Ca2+ currents in transgenic mice with cardiac-specific over-expression of CYP2J2. Mol. Pharmacol. 66, 1607e1616.
Zhang, W., Koerner, I.P., Noppens, R., Grafe, M., Tsai, H.J., Morisseau, C., Luria, A., Hammock, B.D., Falck, J.R., Alkayed, N.J., 2007. Soluble epoxide hydrolase: a novel therapeutic target in stroke. J. Cereb. Blood Flow. Metab. 27, 1931e1940.
Zou, A.P., Fleming, J.T., Falck, J.R., Jacobs, E.R., Gebremedhin, D., Harder, D.R., Roman, R.J., 1996. Stereospecific effects of epoxyeicosatrienoic acids on renal vascular tone and K(+)-channel activity. Am. J. Physiol. 270, F822eF832.

Abbreviations

AA: arachidonic acid
ACSF: artificial cerebrospinal fluid
AUDA: 12-(3-adamantan-1-yl-ureido) dodecanoic acid
BK_{Ca}: calcium-acitivated big potassium
CA: cornu ammonis
CYP: cytochrome P450-dependent monooxygenase
DHA: docosahexaenoic acid
DHET(s): dihydroxyeicosatrienoic acid(s)
EET(s): epoxyeicosatrienoic acid(s)
EEZE: 14,15 epoxyeicosa-5(Z)-enoic acid
EPSC: excitatory postsynaptic current
EPA: eicosapentaenoic acid
fEPSP: field excitatory postsynaptic potential
GABA: γ-aminobutyric acid
GDPβS: guanosine-5 -O-2-thiodiphosphate
GIRK: G protein coupled/gated inward rectifying potassium
12-HPETE: 12-hydroperoxyeicosatetraenoic acid
I_{hold}: holding current
mEPSC(s): miniature excitatory postsynaptic current(s)
PPR: paired pulse ratio
PC(s): pyramidal cell(s)
RMP: resting membrane potential
SC(s): Schaffer collateral(s)
sEH: soluble epoxide hydrolase
sEHi: soluble epoxide hydrolase inhibitor
tAUCB: trans-4-[4-(3-adamantan-1-y1-ureido)-cyclohexyloxy]-benzoic acid
TTQ: tertiapin Q
TTX: tetrodotoxin

Appendix A

Supplementary Tables

Table 1

Evoked EPSC parameters at Schaffer collateral-CA1 pyramidal cell synapses in absence and presence of tAUCB (1 µM)

	n	Ipeak (pA)	10-90% Risetime (ms)	Decay τ (ms)	I_{hold} (pA)	R_{input} (MΩ)
Baseline	7-10	-274 ± 46	3.2 ± 0.3	10.9 ± 0.8	-80 ± 12	192 ± 24
tAUCB (1 µM)		-290 ± 50	3.3 ± 0.3	11.9 ± 1.0	-85 ± 19	193 ± 29
p-value		0.078	0.116	0.093	0.745	0.903

Mean ± SEM values were determined for EPSCs at 30-32°C. For each cell 30 events were averaged before and after application of tAUCB. The current decay τ was fitted with a mono-exponential function. p-values are the results of paired Student's *t* tests. *n* number of experiments performed.

Table 2

Evoked EPSCs at Schaffer collateral-CA1 pyramidal cell synapses

	n	Amp 1 (pA)	p value	Amp 2 (pA)	p value
Baseline	5	-208 ± 39		-393 ± 61	
11,12 EET (2µM)		-164 ± 37	p<0.05*	-347 ± 69	p<0.05*
Baseline	9	-188 ± 11		-397 ± 36	
EEZE (10 µM)		-267 ± 25	p<0.01**	-472 ± 55	p<0.05*
Baseline	5	-206 ± 11		-428 ± 59	
EEZE (10 µM)		-336 ± 26	p<0.01**	-587 ± 79	p<0.01**
11,12 EET (2µM)		-209 ± 19	p<0.001***	-402 ± 44	p<0.01**

Mean ± SEM values were determined for amplitude 1 and 2 of evoked EPSCs at 30-32°C. For each cell 30 events were averaged under baseline conditions and after application of the respective drug. p values are the result of paired Student's *t* tests applied to the following comparisons: Baseline vs 11,12 EET; baseline vs EEZE and EEZE vs 11,12 EET. *n* number of experiments performed.

Table 3

Summary of mEPSC parameters at Schaffer collateral-CA1 pyramidal cell synapses with K- gluconate internal solution

	n	Frequency (Hz)	Ipeak (pA)	10-90% risetime (ms)	Decay τ (ms)	I_{hold} (pA)	Rinput (MΩ)
Baseline	5	0.66 ± 0.02	-25.8 ± 0.6	1.29 ± 0.12	6.22 ± 0.61	-19.8 ± 3.1	221 ± 21
tAUCB (1µM)		0.83 ± 0.12	-26.0 ± 0.9	1.28 ± 0.08	6.66 ± 0.37	-28.8 ± 1.6	216 ± 30
14,15 EET (2 µM)		0.71 ± 0.10	-28.1 ± 1.2	1.21 ± 0.08	6.28 ± 0.69	-28.5 ± 2.7	209 ± 28
Baseline	5-7	1.22 ± 0.36	-17.8 ± 1.3	1.27 ± 0.07	6.33 ± 0.18	-23.0 ± 6.2	242 ± 34
tAUCB (1µM)		1.17 ± 0.28	-19.1 ± 1.5	1.25 ± 0.06	6.53 ± 0.11	-28.2 ± 5.6	259 ± 38
11,12 EET (2 µM)		1.09 ± 0.31	-17.8 ± 1.8	1.34 ± 0.08	6.90 ± 0.14	-6.3 ± 3.5**	213 ± 12*
Baseline	5	0.80 ± 0.15	-21.2 ± 0.9	1.77 ± 0.16	7.70 ± 0.16	-14.4 ± 10.0	225 ± 32
EEZE (10 µM)		1.21 ± 0.25*	-23.5 ± 1.8	1.45 ± 0.18	7.16 ± 0.60	-17.6 ± 8.5	223 ± 24

Mean ± SEM values were determined for mEPSCs at 30-32°C. For each cell and compound 50-250 events were aligned on 50% rising phase and averaged to obtain kinetic parameters; the current decay τ was fitted with a mono-exponential function. For each compound the mean values determined were compared as follows: Baseline vs tAUCB, tAUCB vs EET, and baseline vs EEZE, respectively. Asterisks indicate the significant differences obtained from these comparisons (p<0.05*, p<0.01**, paired Student's *t* test). *n* number of experiments performed.

Chapter 3

Epoxide hydrolases act as a switch between AA-derived inhibitory EETs and excitatory DHETs, which modulate K_v channels

(Manuscript in preparation)

3.1. Introduction

Epoxide hydrolases (EHs) comprise a family of enzymes that catalyze the addition of a water molecule to potentially genotoxic epoxides, converting them to the corresponding less toxic diols (Arand *et al.*, 2003). Microsomal EH (mEH) and soluble EH (sEH) are the best characterized EHs, which differ in their cellular localization (endoplasmic reticulum vs. cytosol) and activity. mEH is widely known for its detoxification capabilities of xenobiotic derived epoxides, while sEH is best known for its role in the metabolism of endogenous epoxides. Endogenous epoxides are generated from fatty acids (FAs) such as arachidonic acid (AA) in a cytochrome P450 (CYP)-dependent reaction. Several CYP isoenzymes are noted for their particularly high efficiency to epoxygenate AA, namely those from the CYP-2C and CYP-2J family (Spector *et al.*, 2015). These CYP-epoxygenases oxidize either of the four double bonds of AA, generating four epoxide regioisomers: 5,6-, 8,9-, 11,12-, 14,15-epoxyeicosatrienoic acids (EETs), which can further be hydrolyzed by EHs to the corresponding dihydroxyeicosatrienoic acids (DHETs).

sEH shows a substantially higher activity in hydrolyzing EETs relative to mEH and is thus considered as the main enzyme responsible for the metabolism of EETs (Morisseau, 2013). Indeed, under saturating conditions, human sEH is 200 times faster in hydrolyzing 14,15 EET than human mEH (Decker *et al.*, 2012). Nevertheless, mEH exhibits a higher apparent affinity (lower K_m) towards EETs than sEH and is located in physical proximity to CYP epoxygenases. Thus, despite its lower activity, it might contribute to a large extent to the hydrolysis of EETs at sub-saturating concentrations (Marowsky *et al.*, 2017). In terms of substrates preference, sEH and mEH display an almost complimentary preference profile. Based on the catalytic efficiency (k_{cat}/K_m), mouse mEH prefers 11,12-EET >8,9-EET =14,15-EET while mouse sEH prefers (in descending order) 14,15-EET =11,12-EET >8,9-EET (Marowsky *et al*., 2009).

EETs are implicated in a variety of physiological processes. In particular, they are recognized as potent vasodilators in most vascular beds and known to exert angiogenic, anti-inflammatory, and anti-nociceptive effects (Spector *et al.*, 2015). They activate ion channels such as the calcium-activated BK (BK_{Ca}) channels (Campbell *et al.*, 1996; Li *et al.*, 1997); K_{ATP} channels (Lu *et al.*, 2006; Ye *et al.*, 2005) and various transient receptor potential (TRP) channels including TRPV4 (Watanabe *et al.*, 2003), TRPC6 (Fleming *et al.*, 2007) and TRPA1 (Sisignano *et al.*, 2012).

Compared to EETs, DHETs are largely described as less biologically active with only a few studies reporting the opposite (Campbell *et al.*, 2002; Kundu *et al.*, 2013; Larsen *et al.*, 2006).

In brain, earlier studies indicated a role for EETs in opioid-mediated antinociception, stroke, and release of neuropeptides (Iliff *et al.*, 2010; Terashvili *et al.*, 2008). More recently, EETs have been suggested to attenuate epileptic seizures (Inceoglu *et al.*, 2013; Vito *et al.*, 2014; Hung *et al.*, 2015). Their antiepileptic effect might be explained by recent findings from our group that 11,12-EET activates a G-protein coupled inwardly rectifying K^+ (GIRK) channel in CA1 pyramidal cells (PCs), leading to hyperpolarization and reduced excitability. Moreover, 11,12-EET decreases the release of glutamate at the CA3-CA1 synapse (Mule *et al.*, 2017).

Mouse hippocampal CA1-CA3 PCs have been shown to express EET-synthesizing CYP-epoxygenases [*http://mouse.brain-map.org/* (Lein *et al.*, 2007) (Mule *et al.*, 2017)]. Moreover, EET-metabolizing EHs are also expressed in a cell type-specific manner in mouse hippocampus: sEH is located in hippocampal astrocytes, while mEH is observed throughout all CA1-CA3 PCs (Marowsky *et al.*, 2009). Thus, the enzymatic machinery to generate EETs and DHETs is principally present in the mouse hippocampus. However, which effects DHETs exert on synaptic transmission and through which molecular targets has remained an unexplored question.

Here, we investigate how 11,12-DHET modulate synaptic transmission at the CA3-CA1 synapse in mouse hippocampus. Recording from CA3-CA1 synapse using the patch-clamp technique, we further attempted to identify the channels that mediate the 11,12-DHET and 11,12-EET effects. To ascertain the molecular targets, the potential candidate K_v channels were heterologously expressed in chinese hamster ovary (CHO) cells and screened for possible effects of DHET and EETs. Finally, to substantiate the role of EHs in hydrolyzing EETs to DHETs, input-output (I-O) curves were constructed in hippocampal slices obtained from WT control, mEH KO, sEH KO and mEH E404D mice, the latter expressing a gain of function variant of mEH.

3.2.Materials and methods

3.2.1. Mouse brain slice electrophysiology

A. Animals

C57BL/6J, sEH KO (*Ephx2* $^{-/-}$), mEH KO (*Ephx1* $^{-/-}$) and mEH E404D (gain of function variant) mice were used in this study. C57BL/6J mice were obtained from Charles River Laboratories, Germany. sEH KO (Sinal *et al.*, 2000) and mEH KO mice (Miyata *et al.*, 1999) were kindly provided by Dr. F. J. Gonzalez, National Institute of Health, USA. The mouse line carrying the mEH E404D mutation was generated and characterized in our laboratory, as described here (Marowsky *et al.*, 2016). sEH KO, mEH KO and mEH E404D lines were backcrossed for 7-9 generations onto C57BL/6J background prior to this study. Prior experiments from our laboratory confirmed that there were no differences between sEH and mEH WT littermates in CYP-epoxygenases and EH-dependent metabolism and thus were employed as WT control in the current study. Animals were housed in the institutional animal facility with 12:12 dark:light cycle and had *ad libitum* access to standard chow-food and water. Animals between P20 to P42 days were used for the experiments in this study. All experiments were performed in accordance with regulations of the University of Zurich and the veterinary department of the canton of Zurich, Switzerland for animal handling and experimentation.

B. Hippocampal slice preparation

Transverse hippocampal slices (350-400 µm thick) were obtained using a vibrating blade microtome, HM 650 V (Thermo Scientific, UK) as described (Mule *et al.*, 2017; Pannasch *et al.*, 2012) with some modifications. Briefly, a mouse was anesthetized using isoflurane and euthanized by decapitation. The brain was extracted and immediately transferred into ice-cold artificial cerebrospinal fluid (ACSF) equilibrated with 95% O_2 and 5% CO_2 containing (in mM) NaCl (125), $CaCl_2$ (2.5), $MgCl_2$ (1), $NaHCO_3$ (26), KCl (2.5), NaH_2PO_4 (1.25) and glucose (10). The hippocampi were extracted from the brain and mounted on an ice cold metal block supported by agar to obtain transverse hippocampal slices. Slices were collected in an incubating chamber containing ACSF maintained at 35°C, where they were allowed to recover for at least one hour. Thereafter, they were kept at room temperature until further use.

C. Electrophysiology

Slices were mounted on poly-L-lysine (PLL)-coated coverslips and transferred to the recording chamber, continuously perfused with ACSF at a rate of 1.8 ml/min throughout the experiment. All experiments were performed at 30-32°C using an in-line heating system. Hippocampal neurons were visualized by using an upright microscope (BX51Wl, Olympus) equipped with a 20x water-immersion objective, infrared differential interference contrast optics and an infrared video imaging camera (VX55, Till Photonics, Germany).

I. Recordings of field excitatory postsynaptic potentials (fEPSPs)

fEPSPs recordings were carried out in 400 µm thick hippocampal slices with a wide-tip borosilicate glass microelectrode (resistance< 2 MΩ) filled with ACSF. fEPSPs were evoked by stimulating Schaffer collateral (SC) fibers at 0.1 Hz using a wide-tip ACSF-filled glass capillary as shown in *Fig.3.3A*. The stimulation intensity was adapted for every recording (between 20-150 µA) to obtain a sub-maximal fEPSP signal with minimal possible non-synaptic contamination. The fEPSP amplitude: fiber volley (FV) ratio is considered as an indicator of the brain slice health, therefore, only recordings with higher fEPSP: FV ratio (>2-3) were used in this study.

II. Patch-clamp recordings

Patch pipettes (tip resistances ~3-5 MΩ) were pulled and fire-polished from borosilicate glass (GC150F-10, Harvard apparatus, UK) with a horizontal puller (Zeitz instrument, Germany). Patch pipettes were filled with an internal solution containing the following (in mM) K-gluconate (145), Mg-ATP (5), Na-GTP (0.5), EGTA (1) and NaCl (5). The pH was adjusted to 7.3 with 1N KOH, the osmolarity was 305 mOsm. For recording evoked or spontaneous excitatory postsynaptic currents (e/sEPSCs), CA1 PCs were voltage clamped at -70 mV and e/sEPSCs were recorded in the presence of bicuculline (25 µM) to block inhibitory neurotransmission. For miniature EPSCs (mEPSCs), the sodium channel blocker, tetrodotoxin (TTX, 1 µM) was added in addition to bicuculline to block action potential (AP) generation. SC-CA1 recordings, in which depolarization-induced potentiation of excitation (DPE) was studied, were carried out in the presence of bicuculline (25 µM) and the cannabinoid 1 (CB1) receptor antagonist, AM-251 (1 µM).

3.2.2. Heterologous expression system expressing K_v channels

A. Cloning

For the recombinant expression of mouse voltage-gated potassium channels in CHO cells, cDNA clones for mKCNA1 ($mK_v1.1$), mKCNA2 ($mK_v1.2$), mKCNAB1 ($mK_v\beta1$), and mKCND2 ($mK_v4.2$) were purchased from Origene Technologies Inc. USA. The respective open reading frames were amplified from these clones using *Pfu* polymerase and the following primer pairs *(Table 3.1).*

Table 3.1 Primer sequences used for cloning mouse K_v channels.

mKCNA1for	gatcagaattccATGACGGTGATGTCGGGGGAGAA
mKCNA1rev	tatacggccgctaAACATCGGTCAGGAGCTTGCTCTTA
mKCNA2for	gatcagaattccATGACAGTGGCTACCGGAGAC
mKCNA2rev	tatacggccgctaGACATCAGTTAACATTTTGGTAATA
mKCNAB1for	gatcagaattccATGCAAGTCTCCATAGCCTGCACA
mKCNAB1rev	tatacggccgctaTGATCTATAGTCCTTTTTGCTGTAG
mKCND2for	gatcagaattccATGGCAGCCGGTGTTGCAGCATGG
mKCND2rev	tatacggccgctaCAAGGCAGACACCCTGACGATA

The amplified fragments were subsequently digested with *EcoRI* and *EagI* and ligated into the *EcoRI/NotI*-site of the mammalian expression vector pAmCAG_GFP_P2A. This allowed the coexpression of the respective potassium channel subunit and GFP from the same transcript, using a P2A sequence to afford the synthesis of these as two separate polypeptides. The map of pAmCAG_GFP_P2A_mKCNA1 is shown in *(Fig. 3.1)* to visualize this expression strategy. All the final constructs were verified by sequencing to ensure their accordance with the published mouse sequences.

The successful expression of functional K_v channels was verified by recording macroscopic K_v currents from K_v transfected CHO cells using patch-clamp technique (*transfection and patch-clamp recording protocols are described below*). The mKCND2 plasmid cloned with this strategy yielded a suboptimal surface expression of functional $mK_v4.2$ channels, as was evident from the lack of measurable K_v currents in CHO cells transfected with this plasmid. Therefore,

we obtained commercially available (Cat no: SC115436) human KCND2 cDNA cloned in pCMV6-XL5 plasmid from Origene Technologies Inc., USA. Human KCND2 plasmid showed optimal surface expression of functional K_v4.2 channels as was evident from measurable K_v4.2 currents from transiently transfected CHO cells. Therefore, hKCND2 plasmid was used in this study instead of mKCND2. Human K_v4.2 and mouse K_v4.2 share 99% amino acid sequence homology [UniProt database (Consortium, 2017)], however less likely, the potential species-specific difference(s) might exist and can be further investigated using mouse K_v4.2 channels.

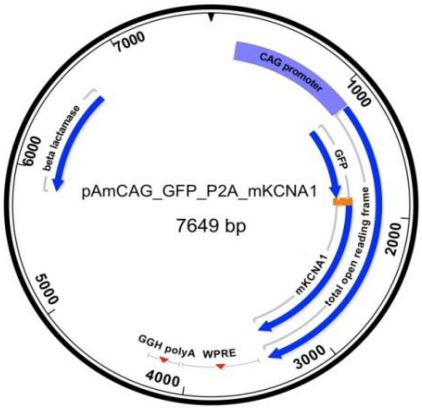

Fig. 3.1 Map of pAmCAG_GFP_P2A_mKCNA1. P2A sequence interspacing between GFP and mKCNA1 transgene. is shown in orange color.

B. Cell maintenance and expression of K_v channels

CHO cells were maintained in T25 cell culture flask in F12-HAM nutrient mixture medium (Invitrogen, USA) supplemented with 5% FCS and 2.5 mM L-glutamine at 37°C under 5% CO_2 in the cell culture incubator. Approximately 50,000 cells were seeded on a PLL-coated glass coverslip and allowed to grow overnight. On the following day, CHO cells were transfected with either of the following K_v channels (cDNA concentration); mouse K_v1.1 (0.5 µg), mouse K_v1.2 (0.5 µg) or human K_v4.2 (1 µg) together with eGFP (0.2 µg) cDNA using Jet pei transfection reagent as per protocol provided by the manufacturer (*link to the online manual* provided by Polyplus transfection, USA). In another set of experiments, K_v1.1 (0.5 µg) or K_v1.2 (0.5 µg) α-subunits were co-transfected with accessory K_vβ1 (1.5 µg) subunits to study the influence of K_vβ1 subunits on the effects of compounds under study. Glass coverslips with transfected cells were used for experimentation 24-48 hours post-transfection. Coverslip was transferred to the recording chamber which was super-fused with an external solution. Green fluorescing (eGFP expressing) cells were identified and used for electrophysiological recording of K_v currents.

C. Electrophysiological recordings

The external solution contained (in mM) NaCl (150), KCl (5.4), $MgCl_2$ (1.0), $CaCl_2$ (2), glucose (10) and HEPES (10). The pH was adjusted to 7.4 with 1N NaOH, the osmolarity was 315 mOsm. Patch pipettes were pulled from borosilicate glass (GC150F-10, Harvard apparatus, UK) and had a tip resistance of 2.5 to 3.5 mΩ. They were filled with an intracellular solution containing (in mM) K-gluconate (145), Mg-ATP (5), Na-GTP (0.5), EGTA (1) and NaCl (5). The pH was adjusted to 7.4 with 1N KOH, the osmolarity was 305 mOsm. All experiments were carried out at room temperature; the calculated reversal potential (E_{rev}) for K^+ with given external-internal combination was -84.4 mV.

After establishing whole-cell configuration, cells were held at -70 mV. Capacitance (C_m) and series resistance (R_s) were compensated and values for C_m and R_s were read from the amplifier dial. The voltage-induced macroscopic K_v currents were recorded with an AM2400 patch-clamp amplifier (AM systems, USA) and digitized at 10 KHz using Digidata 1400 and pClamp 10 software suites (Molecular Devices, USA).Voltage-step protocols used to elicit the K_v currents were adapted from (Decher *et al.*, 2010; Yeung *et al.*, 1999) with some modifications.

Protocol I: The patched cell was held at -70 mV and membrane potential was stepped from test potentials of -90 to +80 mV in incremental step of +10 mV. After each test potential, the membrane potential was stepped back to the original -70 mV holding potential. Outward currents elicited by voltage steps were used to plot current-voltage (I-V) curves and to deduce the E_{rev} value of elicited K_v currents *(Fig 3.2A).*

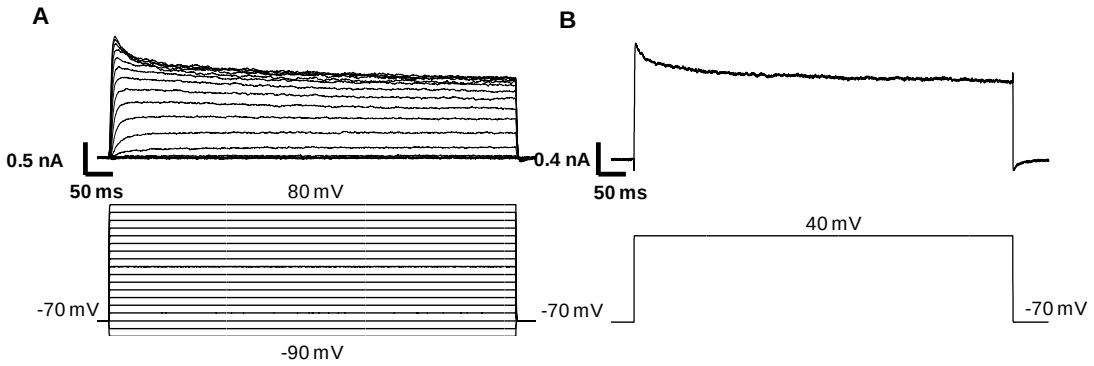

Fig. 3.2 Voltage step protocols used for eliciting K_v currents. **(A)** A representative K_v1.1 I-V curve and corresponding protocol **(B)** Outward K_v1.1 currents and corresponding single step depolarization protocol

Protocol II: The patched cell was held at -70 mV and membrane potential was stepped to the depolarizing test potential of +40 mV every 10 seconds to evoke the outward K_v current for all the tested K_v channels except $K_v1.2$ *(Fig 3.2B)*. The outward $K_v1.2$ currents elicited by depolarizing steps of +20, +30 and +40 mV were extremely large (>10 nA) and rendered recordings unstable, thus we employed depolarizing step of +10 mV every 10 s for recording $K_v1.2$ currents. All compounds were bath-applied via gravity-assisted perfusion and the effect of the test compounds on K_v amplitude at 7-9 min post application was used for analysis

3.2.3. Pharmacology

The GABA antagonist bicuculline and the CB1 receptor antagonist AM-251 were obtained from Tocris Biosciences, UK. The sodium channel blocker TTX was obtained from Bio-trend, Germany. Elaidamide was kindly provided by Dr. Christophe Morisseau, University of California, Davis, USA. The fatty acid amide hydrolase (FAAH) blocker URB-597 was obtained from Hycultec GmbH, Germany. Parent stocks for all the compounds were prepared and stored at -20°C. 11,12-EET and -DHET were obtained from Cayman Chemicals, USA. 11,12-DHET and -EET were dried under nitrogen gas in an inert single-use container and stored at -20°C until use. Dried stocks were re-dissolved in external solution/ACSF just before application. All compounds were prediluted and bath-applied in external solution/ACSF.

3.2.4. Data analysis and statistics

Electrophysiology data were analyzed with IGOR Pro software (Wave Metrics, USA) or pClamp 10 suite (Molecular Devices, USA). Spontaneous and miniature events were analyzed with the Mini Analysis Program (Synaptosoft, USA). The I-V curves recorded with K_v channels in CHO cells were fitted with standard Boltzmann functions using GraphPad Prism 5 (GraphPad, USA). Appropriate statistical tests were employed for testing the significance, such as paired/unpaired Student's *t*-test for comparisons and one-way/two-way-ANOVA followed by a post hoc test for multivariate comparisons. Results are presented as mean±standard error of the mean unless stated otherwise. GraphPad Prism 5 was used for the statistical analysis and preparation of the graphs.

3.3. Results

3.3.1. 11,12-DHET increases excitatory neurotransmission at the mouse CA3-CA1 synapse

To investigate the potential effects of 11,12-DHET on hippocampal synaptic transmission, we stimulated (paired stimulation with an interstimulus interval of 50 ms, at 0.1 Hz) SCs to record fEPSPs at the CA3-CA1 synapse. The fEPSP recordings were made in *stratum radiatum (see recording scheme, Fig. 3.3A)* of WT hippocampal slices. Bath-application of exogenous 11,12-DHET (3 µM) rapidly increased synaptic transmission measured as fEPSP slopes (*Fig. 3.3B-D)*. Slope1 *(Fig. 3.3C)* and slope2 *(Fig. 3.3D)* were significantly increased to 145.3±3% (n=5, p=0.006**) and 139.7±3.4% (n=5, p=0.019*), respectively.

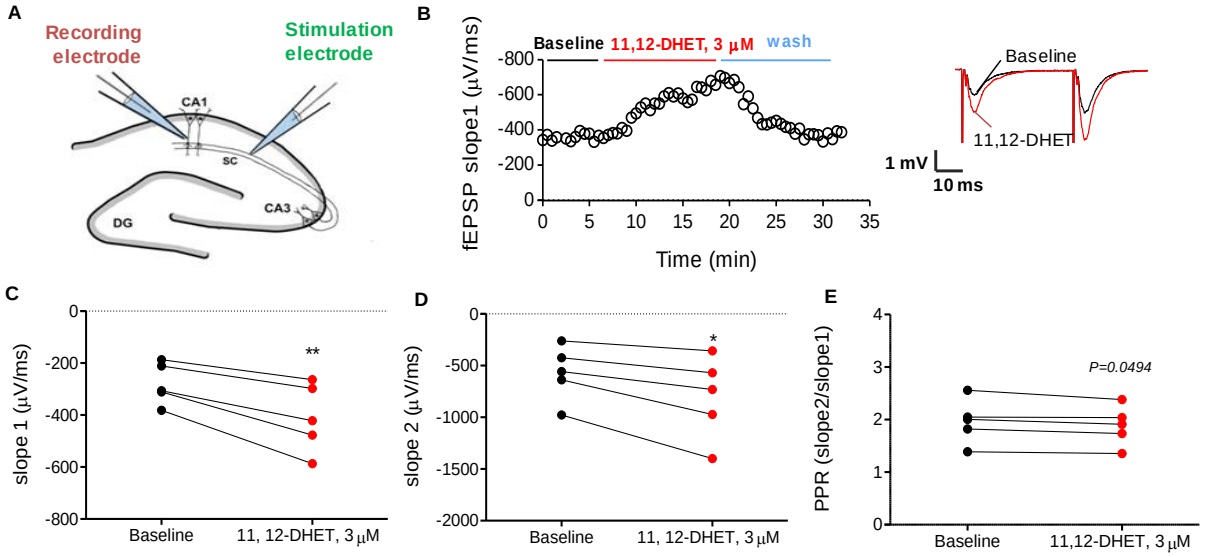

Fig. 3.3 11,12-DHET enhances synaptic transmission at the hippocampal CA3-CA1 synapse.

(A) A schematic illustration showing the site of stimulation (Schaffer collaterals) and recording (*stratum radiatum* of CA1) in the hippocampus. **(B)** A representative time-course and corresponding traces of fEPSPs showing the effect of 11,12-DHET application. Time of DHET application and washing is indicated by red and blue horizontal bars, respectively. A summary graph depicting the effect of 11,12-DHET on average (*of 20 waves*) fEPSP slope 1 **(C)** and slope 2 **(D)**. Application of 11,12-DHET (3 µM) significantly increased slope 1 (n=5, p=0.006**) and slope 2 (n=5, p=0.019*) as compared to the corresponding baselines. Paired Student's *t*-test before vs. after 11,12-DHET treatment was used to test the significance. **(E)** Paired-pulse ratio (PPR: slope2/slope1) before and after application of 11,12-DHET, paired Student's *t*-test before vs. after 11,12-DHET treatment, (n=5, p=0.0494).

Significance was tested using paired Student's *t*-test before vs. after DHET treatment. The observed 11,12-DHET-mediated increase in the fEPSP slopes was washable with ACSF. Moreover, there was a trend towards a decreased paired-pulse ratio (PPR: slope2/slope1, *Fig.*

3.3E) from 1.96±0.37 to 1.88±0.33 in the presence of 11,12-DHET (n=5, p=0.0494, paired Student's *t*-test before vs. after DHET treatment). Such a change in PPR is commonly interpreted as an indication for a presynaptic mechanism.

3.3.2. Depolarization-induced potentiation of excitation can be observed at the CA3-CA1 synapse in presence of the CB1 receptor antagonist AM-251.

Since exogenously applied lipids might not reliably reflect the action of endogenously generated lipids, we next attempted to release CYP-epoxygenase products in the brain slice to investigate their potential effects on CA1 PCs. A recent study demonstrated that AA can be released from CA3 PCs in response to a short depolarizing pulse, which activates the calcium-dependent enzyme phospholipase A_2 ($cPLA_2$) to release AA from lipid membranes. Moreover, the same study showed that *in situ* released AA and/or AA-derived metabolites from CA3 PCs can act as retrograde messengers, which block K_v channels located at presynaptic mossy fiber (Mf) terminals and thus facilitate synaptic transmission at Mf-CA3 synapses. This phenomenon was dubbed depolarization-induced potentiation of excitation (DPE) (Carta *et al.*, 2014). Notably, the Mf-CA3 synapse was investigated in the Carta study, since this particular synapse lacks presynaptic CB1 receptors. These receptors would otherwise mediate retrograde endocannabinoid-mediated signaling and confound the expression of DPE. However, in the presence of CB1 receptor antagonists, a DPE-like phenomenon was also observed and reported at the CB1 receptor expressing CA3-CA1 synapse (Carta *et al.*, 2014).

We, therefore, recorded EPSCs in CA1 PCs in presence of the CB1 receptor antagonist AM-251 (1 µM) and bicuculline (25 µM) and induced DPE, following the protocol from Carta *et al*. CA1 PCs were voltage clamped at -70 mV and depolarized to -10 mV for 9 s. In line with (Carta *et al.*, 2014), we observed a potentiation of EPSC amplitude 1 (5 min post-depolarization, 120±2.6%; n=7; p=0.023*, paired Student's *t*-test before vs. after depolarization). Unlike in the earlier report by Carta, DPE in our experiments continued to increase up to 15 min *(Fig. 3.4A-D)*. Additionally, we observed a significant decrease in PPR *(Fig. 3.4E)* from 2.34±0.18 to 2.21±0.18% (n=7; p=0.032*), which confirms the earlier report that DPE is presynaptically expressed.

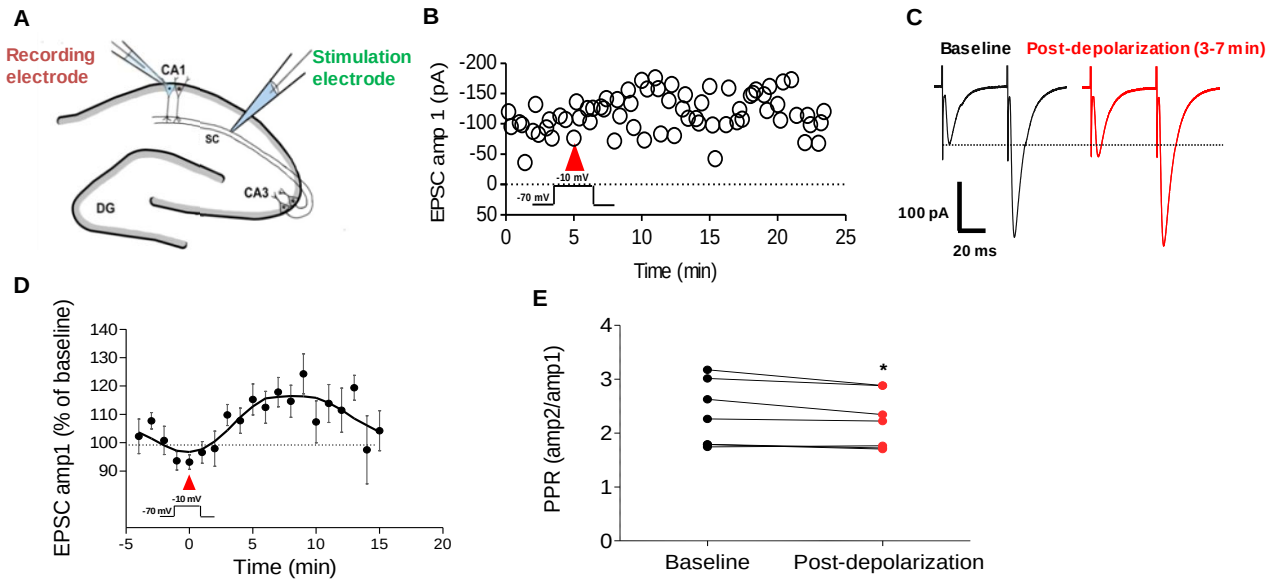

Fig. 3.4. DPE is expressed at CA3-CA1 synapse in the presence of CB1 receptor antagonist

(A) A schematic illustration showing the site of stimulation (Schaffer collaterals) and recording (CA1 PCs). **(B)** A representative time-course of EPSC amplitude 1 recorded in a CA1 PCs before and after depolarization to -10 mV for 9 s. The red arrow depicts the time of depolarization. **(C)** Representative traces of EPSC amplitude 1 before (average of 30 waves) and 3-7 (average of 24 waves) minutes post-depolarization. **(D)** The summary time-course (n=7) of normalized EPSC amplitude 1 plotted against time. The red arrow depicts the time of depolarization. **(E)** DPE at the CA3-CA1 synapse is expressed presynaptically, as evident from the significantly decreased PPR (amp2/amp1), paired Student's *t*-test before vs. after depolarization (n=7, p=0.032*).

To examine the potential role of CYP-epoxygenase products in the expression of DPE, further experiments were conducted, using specific blocker of the respective enzymatic pathways. All the following DPE experiments were carried out in the presence of bicuculline (25 µM) and AM-251 (1 µM).

3.3.3. DHETs might be potential mediators of DPE at the CA3-CA1 synapse

In accord with the previously published results the $cPLA_2$ blocker $AACOCF_3$ (10 µM) abolished the expression of DPE (Two-way ANOVA, $AACOCF_3$ treatment significantly affected the outcome; $F=38$, $p<0.0001$), confirming $cPLA_2$-mediated release of AA as requisite for the expression of DPE *(Fig. 3.5A and B)*. To exclude the contribution of putative AA metabolites as DPE mediators, Carta *et al.* employed selective blockers of lipoxygenase (LOX) and cyclooxygenase (COX), which are involved in the generation of prostaglandins and leukotrienes, respectively. However, the possible involvement of CYP-epoxygenase metabolites such as EETs and DHETs remained unexplored.

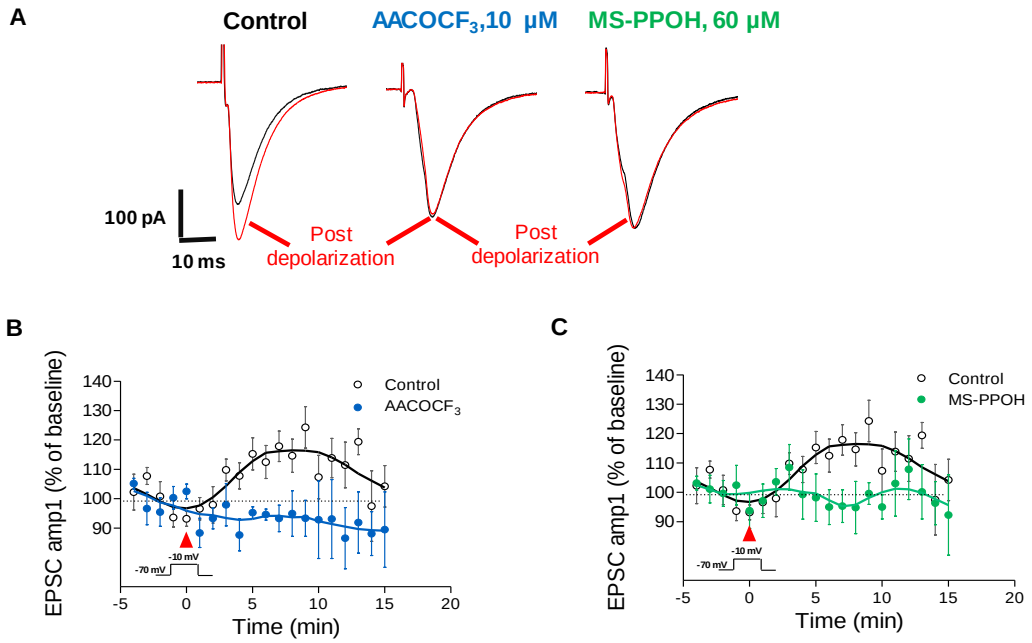

Fig. 3.5. Pre-treatment with inhibitors of $cPLA_2$ and CYP-epoxygenases abolishes DPE in CA1 PCs.

(A) Representative EPSC traces recorded under control conditions and after pre-incubation with the $cPLA_2$ blocker $AACOCF_3$ (10 µM) and the CYP-epoxygenase blocker MS-PPOH (60 µM). The summary time-course plots of SC-EPSC amplitude 1 normalized to the baseline shows that pre-treatment with $AACOCF_3$ (n=3) **(B)** and MS-PPOH (n=4) **(C)** significantly abolished DPE compared to the control experiments (n=7). Two-way ANOVA, treatment and time post-depolarization as two variables were employed. Overall, treatment with inhibitors significantly affected the results. For $AACOCF_3$ treatment ($F=38$, $p<0.0001$) and for MS-PPOH treatment ($F=15.58$, $p=0.0001$), however, the effects of treatments were not statistically significant at every time point. The red arrows depict the time of depolarization.

DHETs are generated in a two-step reaction (*see schematic in Fig. 3.7*), catalyzed by two sets of enzymes: CYP-epoxygenases, which catalyze the epoxygenation of AA to EETs and subsequently the epoxide hydrolases mEH/sEH, which metabolize EETs to DHETs. We addressed both enzymatic systems. First, we recorded EPSCs in the presence of the CYP-epoxygenase blocker MS-PPOH (60 µM). Pre-treatment of MS-PPOH significantly abrogated the expression of DPE compared to control experiments (Two-way ANOVA, MS-PPOH treatment significantly affected the outcome; $F=15.58$, $p=0.0001$). These experiments suggest the potential involvement of CYP-epoxygenase-generated metabolites such as EETs and/or DHETs in the expression of DPE at the CA3-CA1 synapse *(Fig. 3.5C).* Our observation of pro-excitatory effects of 11,12-DHET at the CA3-CA1 synapse *(Fig. 3.3)* implied that DHETs rather than inhibitory EETs could be the potential mediators of DPE at the CA3-CA1 synapse. Of the two prominent EHs responsible for DHET generation, mEH is expressed in CA1 and CA3 PCs

(Marowsky *et al.*, 2009). Therefore, we studied the potential influence of elaidamide, a selective mEH inhibitor (Morisseau *et al.*, 2001), on DPE (*Fig. 3.6A-B).* Elaidamide is degraded by FAAH, thus DPE experiments with elaidamide were carried out in the presence of the selective FAAH inhibitor URB-597 (1 µM). Expression of DPE at the CA3-CA1 synapse was significantly abolished in the presence of elaidamide (Two-way ANOVA, elaidamide treatment significantly affected the outcome; $F=42.48$, $p<0.0001$). In addition, we studied the expression of DPE in brain slices obtained from mEH KO mice *(Fig. 3.6C-D).*

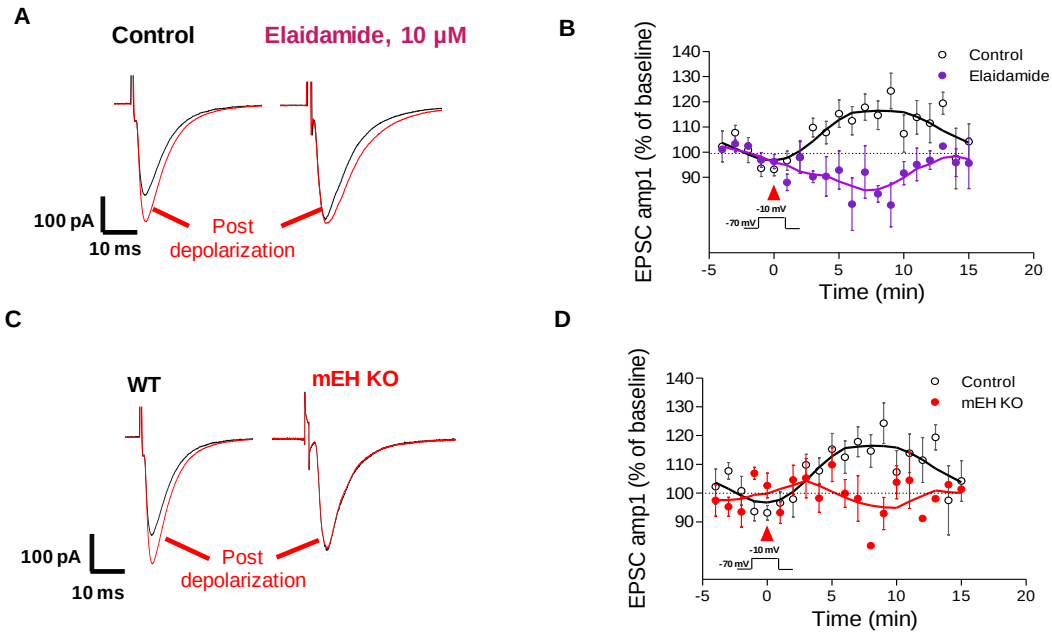

Fig. 3.6. Pharmacological inhibition or genetic ablation of mEH abolishes DPE at the CA3-CA1 synapse

(A) Representative EPSC traces recorded in CA1 PCs under control condition and in the presence of the mEH blocker-elaidamide (10 µM). **(B)** The summary time-course plot of EPSC amplitude 1 normalized to the baseline shows a reduced expression of DPE in the presence of elaidamide (n=3) compared to control experiments (n=7). Two-way ANOVA, treatment and time as two variables were employed. Overall, treatment with elaidamide significantly affected the results ($F=42.48$, $p<0.0001$). However, the treatment effects were not statistically significant at every tested time point. **(C)** Representative EPSC traces recorded in the CA1 PCs from WT and mEH KO mice. **(D)** The summary time-course plot of EPSC amplitude 1 normalized to the baseline show reduced expression of DPE in CA1 PCs from mEH KO (n=3) compared to those from the WT mice (n=7). Two-way ANOVA, genotype and time as two variables were employed. Overall, genotypes significantly affected the result ($F=12.2$, $p=0.0006$), however the effect of genotype is not significant at every tested time point. The red arrows depict the time of depolarization.

DPE at the CA3-CA1 synapse was significantly reduced in mEH KO slices compared to those from WT slices (Two-way ANOVA, effect of genotype significantly affected the outcome; $F=12.2$, $p=0.0006$).

These findings taken together with the MS-PPOH results strongly suggest that a CYP-epoxygenase-derived and mEH-generated metabolite such as a DHET might contribute to the expression of DPE at the CA3-CA1 synapse. However, additional experiments are needed to strengthen these preliminary data.

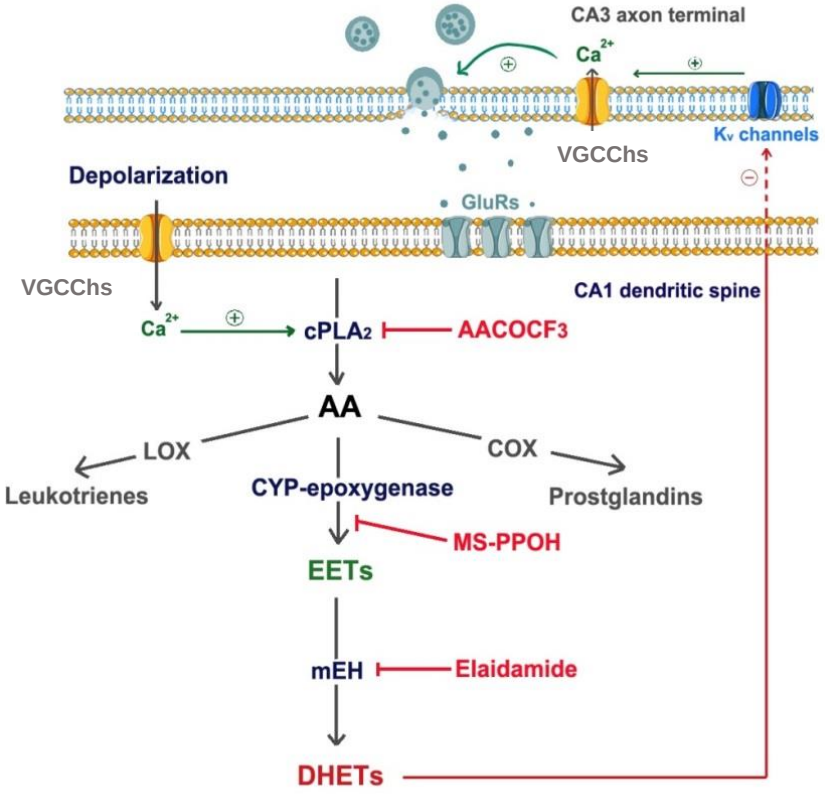

Fig. 3.7 mEH-derived DHETs as potential DPE mediators

Depolarization of the postsynaptic CA1 neuron triggers Ca^{+2} influx via voltage-gated calcium channels (VGCChs) which further activates $cPLA_2$ to release AA from the neuronal membrane. AA can be metabolized to EETs and DHETs via CYP-epoxygenase and mEH, respectively. We employed pharmacological blockers (marked in red) to elucidate the potential DPE mediators. Our results suggest that DHETs generated in the postsynaptic CA1 neuron by mEH activity might block presynaptic K_v channels in a retrograde manner to facilitate the release of glutamate from CA3 axon terminal.

3.3.4. 11,12-DHET blocks heterologously expressed $K_v1.2$ and $K_v4.2$ channels

Further, we explored the potential molecular target(s) underlying the excitatory effects of 11,12-DHET and 11,12-EET. It has been shown that AA and its metabolites are capable of modulating

several K_v channels (Boland *et al.*, 2008; Oliver *et al.*, 2004). Moreover, presynaptic K_v channels have been implicated in DPE at the Mf-CA3 synapse (Carta *et al.*, 2014).

We investigated the potential effect of 11,12-DHET and -EET-mediated modulation of K_v channels in a heterologous expression system. 11,12-DHET did not have any effect on steady-state currents mediated by $K_v1.1$ or $K_v1.1$ in combination with the beta subunit 1 *(Fig. 3.8A-B)*. However, 11,12-DHET (1 µM) exhibited a significant voltage-dependent block of $K_v1.2$ channel, particularly at higher depolarizing steps between +50 to +70 mV (Two-way ANOVA, voltage: $F=65.4$, $p<0.0001$ and DHET treatment: $F=11.9$, $p<0.0001$ significantly affected the outcome). The voltage dependence of block is evident in the I-V curve (*Fig. 3.8C)*. However, due to the instability of recordings at higher depolarizing steps, we had to use suboptimal 10 mV depolarizing step to test the effect of 11,12-DHET on steady-state $K_v1.2$ currents (*Fig. 3.8D)*. Nevertheless, 11,12-DHET (1-3 µM) produced a small, but significant block of $K_v1.2$ by 11.92±3% (n=5; p=0.002**, paired Student's *t*-test before vs. after 11,12-DHET treatment). Furthermore, 11,12-DHET (1 µM) exerted a significant voltage-dependent block of inactivating $K_v4.2$ channels *(Fig. 3.8E)* (Two-way ANOVA, voltage; $F=30.53$, $p=0.0007$ and DHET treatment; $F=36.56$, $p<0.0001$ significantly affected the outcome). Specifically, 11,12-DHET significantly blocked $K_v4.2$ peak currents by 24.5±5.6% (n=5; p=0.016*, paired Student's *t*-test before vs. after 11,12-DHET treatment) elicited in response to a depolarizing step of +40 mV *(Fig. 3.8F)*. We further tested the potential effect of 11,12-EET on steady-state $K_v1.2$ currents elicited at a +10 mV depolarizing step (*Fig. 3.8G)*. Application of 11,12-EET led to opposite effect compared to those exerted by 11,12-DHET. We observed a small increase of $K_v1.2$ current after 11,12-EET (1µM) treatment (4.9±1.5%; n=4; p=0.051, paired Student's *t*-test before vs. after 11,12-EET treatment).

Our results from the heterologous expression system suggest that $K_v1.2$ and $K_v4.2$ might be molecular targets for 11,12-DHET and -EET.

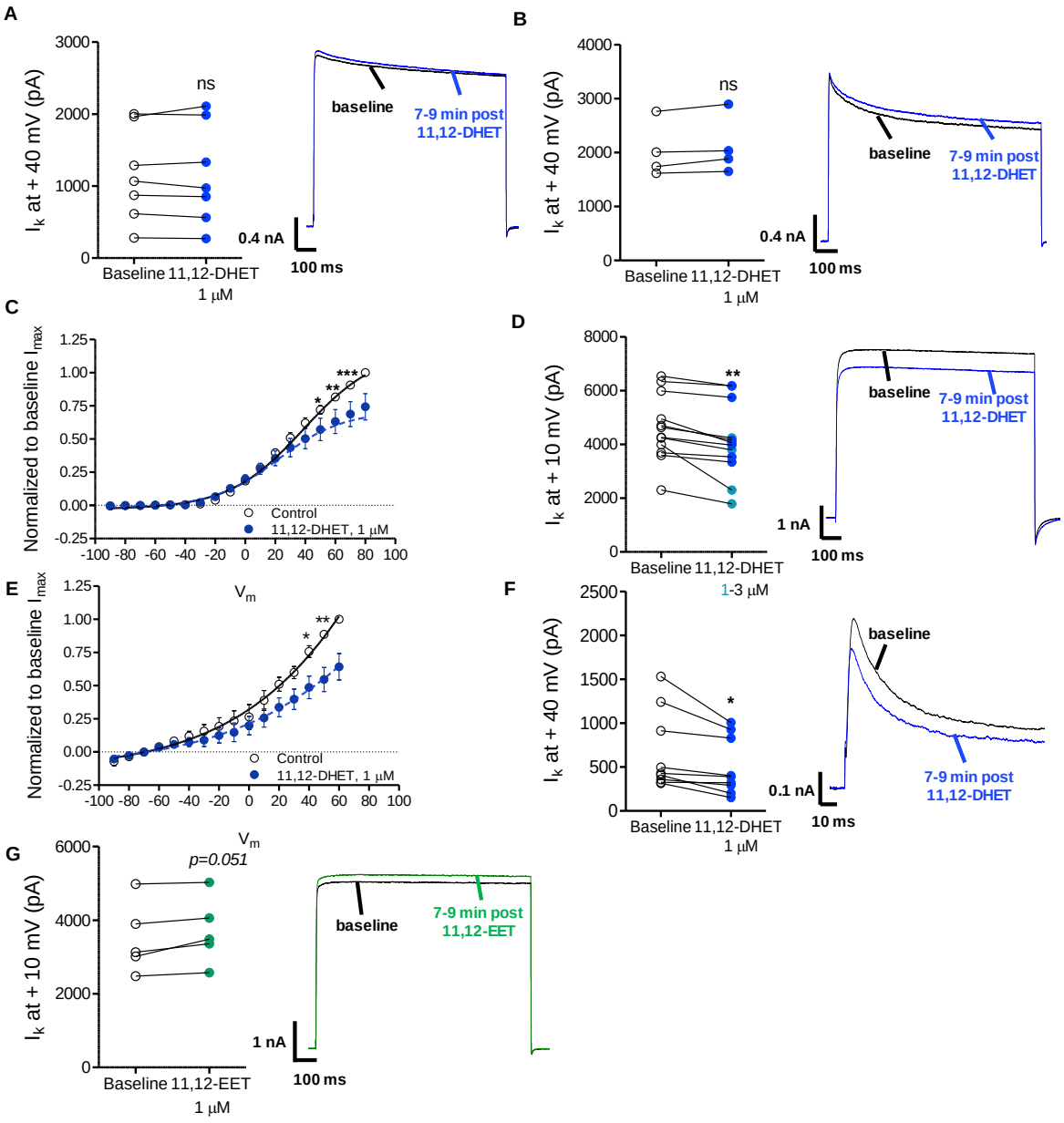

Fig. 3.8 Effect of 11,12-DHET and 11,12-EET on K_v channels expressed in the heterologous expression system

Summary plots and corresponding representative traces showing the effect of 11,12-DHET (1 µM) on **(A)** K_v1.1 currents (n=7, p=0.97, paired Student's *t*-test) and **(B)** K_v1.1+ K_vβ1 currents (n=4, p=0.97, paired Student's *t*-test) elicited at a depolarizing step of +40 mV. **(C)** 11,12-DHET (1 µM) significantly blocked K_v1.2 currents measured as I-V curves (n=7, two-way ANOVA followed by Bonferroni's post hoc test, p<0.05*, p<0.01**, p<0.001***; I_{max} values were used for normalization and thus were excluded while running ANOVA). **(D)** 11,12-DHET (1-3 µM) significantly blocked K_v1.2 elicited at a depolarizing step of +10 mV (n=12, p=0.002**, paired Student's *t*-test), data points in this plot are color coded as follows: ● represents 1 µM and ● represents 3 µM. **(E)** 11,12-DHET (1 µM) significantly blocked K_v4.2 measured as I-V curves (n=4, two-way ANOVA followed by Bonferroni's post hoc test, p<0.05*, p<0.01**; I_{max} values were used for normalization and thus were excluded while running ANOVA) and **(F)** K_v4.2 elicited at depolarizing step of 40 mV (n=9, p=0.002**, paired Student's *t*-test). **(G)** 11,12-EET (1 µM) increased the opening of K_v1.2 elicited at depolarizing step of 10 mV (n=5, p=0.051, paired Student's *t*-test).

3.3.5. Genetic ablation/enhancement of EHs result in altered basal synaptic transmission

Previous studies have indicated that lack of either EHs (mEH KO or sEH KO) reduces the synthesis of DHETs, while the presence of hyperactive EH (mEH E404D) results in an increased synthesis of DHETs relative to the respective WT controls (Marowsky *et al.*, 2016; Marowsky *et al.*, 2017). As EHs control the balance between inhibitory EETs and excitatory DHETs, we sought to evaluate if the altered ratio between inhibitory EETs and excitatory DHETs in these transgenic animals results in the alteration of basal excitatory neurotransmission. To this aim, we generated I-O curves by stimulating SCs with the incremental stimulation intensity from 5 to 45 µA (input) and recorded CA1 fEPSPs in *stratum radiatum* (output) *(see material methods)*. We recorded I-O curves from WT, sEH KO, mEH KO and mEH E404D mice and compared them with corresponding age-matched WT controls.

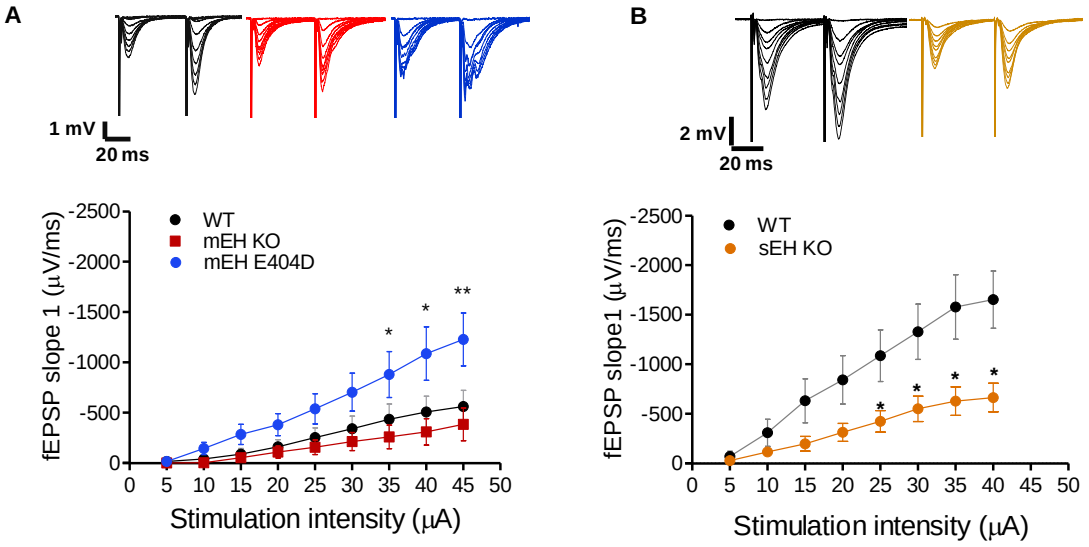

Fig. 3.9. Genetic ablation of EH activity reduces basal synaptic transmission while genetic enhancement of EH activity increases it at the CA3-CA1 synapse

(A) Representative traces and fEPSP I-O curves obtained from age-matched WT (n=5), mEH KO (n=4) and mEH E404D (n=6) mice. Two-way ANOVA, genotype, and time as two variables were employed; overall, genotypes significantly affected the fEPSP slopes (WT vs. mEH KO: $F=4.28$, $p< 0.04$ and WT vs. mEH E404D: $F=19.27$, $p<0.0001$). Moreover, mEH E404D showed significantly higher slope compared to the mEH KO, Bonferroni's multiple comparison post hoc test, $p<0.05$*, $p<0.001$** **(B)** Representative traces and I-O curves obtained from age-matched WT (n=6) and sEH KO (n=6) mice. The fEPSP slopes were significantly reduced in sEH KO mice compared to the ones from WT mice, unpaired Student's *t*-test, WT vs. sEH KO (n=6 each, $p<0.05$*).

Our I-O experiments with mEH KO, mEH E404D and age-matched (P20 to P30) WT revealed that the genotype significantly affects fEPSP slopes (Two-way ANOVA, WT vs. mEH KO:

F=4.28, p=0.04 and WT vs. mEH E404D: F=19.27, p<0.0001). Moreover, Bonferroni's post hoc test revealed that I-O curves recorded in mEH E404D slices showed significantly increased basal synaptic transmission (measured as fEPSP slopes) compared to the ones obtained in mEH KO slices *(Fig. 3.9A).* Further, we measured potential genotype-specific differences in sEH KO mice compared to the age-matched (P35 to P42) WT mice *(Fig. 3.9B).* The I-O curves obtained from sEH KO mice showed a significant decrease in basal synaptic transmission compared to the ones obtained from WT mice (n=6 each, p<0.05*, unpaired Student's *t*-test).

Our findings from I-O experiments implicated a role for EHs in the modulation of basal synaptic neurotransmission. To substantiate these findings, we recorded s/mEPSCs in CA1 PCs from WT, mEH KO, and mEH E404D mice. In addition, we investigated if passive membrane properties [resting membrane potential (RMP) and input resistance (R_{input})] of CA1 PCs are altered in these mice. Passive membrane properties and sEPSCs/mEPSCs kinetic properties were not influenced by genotypes. However, mEH E404D exhibited significantly higher mEPSC frequency (one-way ANOVA followed by Bonferroni's post hoc tests, p<0.05*, compared to WT and mEH KO) *(Table 3.2).* Such an increase in mEPSC frequency is generally regarded of the presynaptic origin.

Table 3.2. Passive membrane properties and kinetic properties of mEPSCs and sEPSCs recorded in CA1 PCs of WT, mEH KO and mEH E404D mice.

Membrane properties	**WT** *(n)*	**mEH KO** *(n)*	**mEH E404D** *(n)*
RMP (mV)	-69.73 ± 0.48 *(25)*	-69.84 ± 0.45 *(24)*	-70.20 ± 0.31 *(9)*
R_{input} (MΩ)	166.99 ± 8.56 *(25)*	183.44 ± 8.97 *(26)*	163.89 ± 16.14 *(9)*

sEPSC	**WT** *(n)*	**mEH KO** *(n)*	**mEH E404D** *(n)*
Amplitude (pA)	27.43 ± 2.30 *(10)*	24 ± 2.10 *(8)*	29.53 ± 4.05 *(4)*
Frequency (Hz)	0.73 ± 0.06 *(9)*	0.93 ± 0.10 *(8)*	1.05 ± 0.29 *(4)*
Rise time (ms)	1.18 ± 0.06 *(9)*	1.15 ± 0.15 *(7)*	1.03 ± 0.17 *(4)*
Decay time (ms)	6.96 ± 0.27 *(9)*	6.66 ± 0.28 *(8)*	5.54 ± 0.23 *(3)*

mEPSC	**WT** *(n)*	**mEH KO** *(n)*	**mEH E404D** *(n)*
Amplitude (pA)	19.86 ± 1.25 *(10)*	16.23 ± 0.68 *(12)*	20.55 ± 2.59 *(7)*
Frequency (Hz)	0.75 ± 0.08 *(9)*	0.79 ± 0.10 *(12)*	**1.25 ± 0.16* *(7)***
Rise time (ms)	1.31 ± 0.09 *(10)*	1.33 ± 0.11 *(12)*	1.16 ± 0.16 *(7)*
Decay time (ms)	6.84 ± 0.45 *(9)*	6.63 ± 0.33 *(12)*	6.12± 0.32 *(6)*

Taken together, both mEH and sEH are likely to play a modulating role in synaptic transmission probably via regulating the ratio between inhibitory EETs and excitatory DHETs.

3.4. Discussion

Membrane-derived lipids such as AA (or its metabolites) have been shown to alter synaptic transmission in the hippocampus via modulation of presynaptic K_v channels (Carta *et al.*, 2014). Recently, we have shown that the AA-derived metabolite, 11,12-EET, suppresses excitatory transmission at the CA3-CA1 synapse in mouse hippocampus (Mule *et al.*, 2017). EHs responsible for metabolizing neuroactive 11,12-EET to 11,12-DHET are expressed in the mouse hippocampus and in principle can generate 11,12-DHET. However, the potential influence of AA-derived 11,12-DHET on synaptic transmission and its underlying mechanism(s) has not yet been reported.

Here, we demonstrate that exogenous 11,12-DHET enhances excitatory transmission at the CA3-CA1 synapse in mouse hippocampus. In addition, we showed that *in situ* released DHETs could be one of the mediators of DPE at the CA3-CA1 synapse. Further using heterologous expression system, we identified $K_v1.2$ as a common effector for 11,12-DHET and -EET. In addition, 11,12-DHET also modulated the $K_v4.2$ channels. These K_v channels might underlie the excitatory effects of 11,12-DHET and inhibitory effects of 11,12-EET. Finally, we observed reduced basal synaptic transmission in mice with genetically ablated EHs while it was enhanced in mice expressing mEH E404D, a hyperactive variant of mEH. These observations lead to the intriguing hypothesis that EHs might act as an endogenous switch between inhibition and excitation in mouse hippocampus.

3.4.1. Exogenous 11,12-DHET is a pro-excitatory lipid mediator

We investigated the potential influence of exogenous 11,12-DHET on basal synaptic transmission using extracellular fEPSP recordings at the CA3-CA1 synapse. Extracellular fEPSP recordings are well suited to study the potential net effect of 11,12-DHET application for two reasons: First, the fEPSP signals are sampled from an intact network of neurons including inhibitory interneurons. Secondly, unlike intracellular patch-clamp recording, extracellular nature of fEPSP recording preserves the intracellular milieu of neurons (Andersen, 2007). We observed pro-excitatory effects of 11,12-DHET on synaptic transmission at CA3-CA1 synapse, probably via

presynaptic effector(s) as indicated by a trend towards decreased PPR. Generally, a decrease in PPR is regarded as an indication of the underlying presynaptic target(s) but it does not categorically rule out the possibility of a combination of pre- and postsynaptic targets. Moreover, observed 11,12-DHET-mediated decrease of PPR is small and suggests a combination of pre-and postsynaptic effector(s) for DHETs.

3.4.2. *In situ*-generated DHETs might be the mediators of DPE

We adapted DPE protocol for the CA3-CA1 synapse to explore the contribution of CYP-epoxygenase-generated metabolites to the expression of DPE, which was left unexplored in the original report (Carta *et al.*, 2014). Abolition of DPE in the presence of MS-PPOH, a CYP-epoxygenase blocker, suggested the requisite of CYP-epoxygenase-derived metabolites such as EETs or DHETs for the expression of DPE *(Fig. 3.5).* Reported inhibitory effects of exogenous 11,12-EET (Mule *et al.*, 2017) and the pro-excitatory effect of exogenous 11,12-DHET in the CA3-CA1 synapse (*Fig. 3.3*) pointed towards the likelihood that DHETs, rather than EETs, could be the potential mediators of DPE. Therefore, we employed a combination of pharmacological blockers and genetic ablation of EHs to test if EETs or DHETs are the potential mediators of DPE *(Fig. 3.7).*

sEH and mEH are the two major EHs responsible for the biosynthesis of DHETs and are expressed in mouse hippocampus. Owing to its higher activity, sEH is generally considered the main EH responsible for the conversion of EETs to DHETs, while the contribution of 'slower' mEH is considered marginal (Morisseau, 2013). Given the purportedly major role of sEH in DHETs biosynthesis, targeting sEH for studying the potential contribution of DHETs to DPE is a natural choice. However, mEH in the mouse hippocampal PCs might be equally, if not more, an important determinant of DHET synthesis and potentially DPE expression for the following two reasons: First, mEH is expressed in the mouse CA1 PCs-a relevant domain for DHET synthesis if it were to act as DPE mediator, while sEH is expressed in the astrocytes (Marowsky *et al.*, 2009). Secondly, mEH, like the majority of EET-synthesizing CYP-epoxygenase, is an endoplasmic reticulum-resident enzyme and it has been proposed that CYP can form a physical complex with mEH which might favor efficient DHETs synthesis. Indeed, a recent study from our group provided evidence for such a complex formation between EETs-generating CYPs and DHETs-generating mEH in non-neuronal cells (Leon *et al.*, 2017). Such an arrangement, in theory, might

result in substrate channeling (EETs) and efficient mEH-mediated-DHET synthesis in mouse CA1 PCs which co-express mEH and CYP. Thus, despite its lower catalytic efficiency, mEH might be a major determinant of DHET synthesis in CA1 PCs and thus was targeted in our experiments.

Our data show that pharmacological inhibition or genetic ablation of mEH abolishes DPE, suggesting an important contribution of mEH-derived DHETs in the expression of DPE at the CA3-CA1 synapse. However, these observations need to be ascertained further by increasing the number of experiments (n). Moreover, we have not empirically ruled out the potential contribution of sEH-derived DHETs to DPE in our experiments at CA3-CA1 synapse which can be investigated by employing sEH inhibitors and/or sEH KO mice.

3.4.3. Complementary effects of 11,12-DHET and-EET are potentially mediated by pre- and postsynaptic K_v channels

We screened K_v channels as potential molecular target(s) underlying the pro-excitatory effects of 11,12-DHET and inhibitory effects of 11,12-EET observed in CA3-CA1 synapse by transiently expressing candidate K_v channels in CHO cells. Voltage-gated potassium channels from the K_v1 subfamily are predominantly expressed in the axonal initial segment and presynaptic terminals. $K_v1.1$ and 1.2 are the most common isoforms expressed in the CA1 PCs and conduct non-inactivating D-type currents (Ovsepian *et al.*, 2016). $K_v1.x$ channels are known to regulate neurotransmitter release via altering the presynaptic AP duration and resultant calcium influx in the axon terminals (Trimmer, 2015; Geiger *et al.*, 2000). Moreover, inhibition of presynaptic K_v channels in MfBs by AA has been shown to increase the glutamate release and contribute to DPE (Carta *et al.*, 2014). These observations suggest that modulation of $K_v1.1$ and $K_v1.2$ might underlie the pro-excitatory effects of 11,12-DHET (as a mediator of DPE) and inhibitory effects of 11,12-EET in CA3-CA1 synapse. Indeed, we identified $K_v1.2$ as a common effector for 11,12-DHET and -EET, the former blocked, whereas latter showed a trend towards increased conductance of heterologously expressed $K_v1.2$ channels. The opposite effects of 11,12-DHET and -EET observed on $K_v1.2$ channels in CHO cells might explain complementary effects of these molecules observed in the CA3-CA1 synapse.

Although the use of non-neuronal heterologous expression system in our experiments enabled us to identify individual K_v channels as 11,12-DHET/EET molecular targets, the extent and

relevance of observed effect in the intact neuronal system is a matter of extrapolation. Especially, due to the fact that most abundant K_v1.1 and 1.2 α-subunits in CA3 and CA1 PCs almost always exist as heterotetramers (Ovsepian *et al.*, 2016). These heterotetrameric K_v1.1/1.2 channels are implicated in the regulation of neurotransmitter release and somatic excitability in PCs (Kole *et al.*, 2012; Rama *et al.*, 2017; Trimmer, 2015). To address this, we attempted to express heterotetrameric K_v1.1/1.2-channels in CHO cells as they exist in native neurons by co-transfecting K_v1.1 and K_v1.2 cDNA in varying ratios (1:1 to 1:5). However, due to the differential transfection efficiency and/or unitary conductances of constituting K_v channels, we could not reliably express heterotetrameric channels in CHO cells and had to study individual homotetrameric K_v1.2 channels. Thus, 11,12-DHET/-EET-mediated modulation of K_v1.2 channels observed in our experiments might be quantitatively different (lower or higher) on native neuronal heterotetrameric K_v1.1/1.2 channels. This possibility, ideally, needs to be tested with direct patch-clamp recording from the CA3 axon terminals in mouse brain slices, however, the small size of the CA3 axonal terminals (unlike MfB) is restrictive.

In our experiments, the effect of 11,12-DHET was restricted to K_v1.2 while K_v1.1 was unaltered. Depending upon the stoichiometry and positioning, presence of blocker sensitive K_v subunit(s) in heterotetrameric complex might result in a block of whole heterotetrameric K_v1.1/1.2 channel (Al-Sabi *et al.*, 2013). Therefore, it is plausible that 11,12-DHET-mediated block of K_v1.2 subunits in native heterotetrameric K_v1.1/1.2 channel might be sufficient to block conductance of native channels to produce pro-excitatory effects. However, this possibility needs to be ascertained in a native neuronal system employing selective K_v1.1/1.2 blockers such as α-dendrotoxin and tetraethylammonium (TEA) chloride (moderately selective for K_v1.1). K_v blockers, in particular, TEA chloride, often exhibits only moderate level of selectivity and might block other structurally related K_v1.x channels to a varying degree. This unintended alteration of other K_v channels might be a confounding factor.

K_v4.2 channels, on the other hand, are expressed in the somatodendritic compartment and conducts A-type currents which are responsible for regulation of backpropagating AP via modulating integration of synaptic inputs (Hoffman *et al.*, 1997; Johnston *et al.*, 2000; Ramakers *et al.*, 2002). Moreover, A-type currents have been shown to negatively influence NMDAR-mediated EPSC amplitude in CA1 PCs: Lack of A-type current (infected with dominant negative pore mutant of K_v4.2) showed increased NMDA-EPSC amplitude whereas expression of

functionally conducting $K_v4.2$ channels showed decreased NMDA-EPSC amplitude compared to the uninfected controls in CA1 PCs (Jung *et al.*, 2008). These observations point towards the role of A-type currents in maintenance of CA1 dendritic excitability. Increased dendritic excitability by means of $K_v4.2$ inhibition might reflect in enhanced EPSC or EPSP amplitude/slope.

In our slice experiments, application of 11,12-DHET increased fEPSP slopes, potentially via a combination of pre- and postsynaptic effectors. Having identified $K_v1.2$ as a potential presynaptic effector for 11,12-DHET, we further screened $K_v4.2$ channels in CHO cells as a potential postsynaptic effector. We observed 11,12-DHET-mediated block of $K_v4.2$ channels *(Fig. 3.8E-F).* in CHO cells which might, at least in part, explain the DHET-mediated increase in fEPSP slope observed at CA3-CA1 synapse. Interestingly, our fEPSP recording exclusively measured synaptic currents at *stratum radiatum* of CA1 region without eliciting somatic AP. Being a voltage-gated channel, activation of $K_v4.2$ is coupled to the change in membrane potential and intuitively might not contribute to the alteration of synaptic currents in our recording paradigm. However, possibility of synaptic currents-mediated change in local dendritic potential leading to activation of voltage-gated $K_v4.2$ channels in our recording paradigm cannot be ruled out.

Despite the limitation of experimental paradigm used (non-neuronal heterologous system), our findings strongly support the likelihood that $K_v1.2$ and $K_v4.2$ are molecular targets for DHET-mediated excitatory effects in hippocampal neurons. Moreover, 11,12-EET-mediated activation of $K_v1.2$ channels might be more pertinent on presynaptic neuronal heterotetrameric channels and underlie the inhibitory effects of 11,12-EET observed at the CA3-CA1 synapse.

3.4.4. The role of EHs beyond detoxification: an endogenous switch between inhibition and excitation in the hippocampus?

We investigated potential consequences of the altered ratio between inhibitory EETs and excitatory DHETs by recording I-O curves in transgenic mice (mEH and sEH KO and mEH E404D). As expected, we observed significantly enhanced basal synaptic transmission in slices from mice expressing mEH E404D while it was reduced in the slices obtained from mEH KO mice compared to the WT. Surprisingly, genetic ablation of non-neuronal sEH also resulted in significant reduction of basal synaptic transmission compared to the corresponding age-matched WT controls. The observed contribution of sEH could be due to several factors: Namely, hippocampal astrocytes express the enzymatic machinery to generate EETs and DHETs

(Amruthesh *et al.*, 1993; Marowsky *et al.*, 2009). It has been shown that glutamate released at the synapse can extrasynaptically activate astrocytic glutamate receptors to increase the cytosolic calcium levels. The enhanced cytosolic calcium triggers activation of $cPLA_2$ to release AA from astrocytic membrane and subsequently leads to the synthesis of EETs (Stella *et al.*, 1994; Alkayed *et al.*, 1997; Haydon *et al.*, 2006). Stimulation of SCs, as in our I-O recording paradigm, might result in the activation of such glutamate-induced synthesis of EETs and potentially DHETs through astrocytic sEH.

Another reason could be the fEPSP I-O paradigm used in our experiments to record synaptic currents. fEPSP are recorded from populations of neurons (unlike single CA1 PCs in DPE experiment) and involves activation of a number of synapses which proportionally enhances the likelihood of glutamate-activated EET- and DHET synthesis from astrocytes. Moreover, higher catalytic efficiency of sEH might counterbalance its lack of neuronal expression and emerge as predominant contributor determining the DHET biosynthesis. These observations taken together with our results are compatible with the possibility that sEH-derived DHETs from the astrocytes could exhibit pro-excitatory effects at the CA3-CA1 synapse in WT mice. The reduced basal synaptic transmission observed in our I-O experiments with sEH KO mice can be attributed to the lack of sEH derived DHETs. Given the differential expression, subcellular localization and catalytic efficiency of mEH and sEH, it is difficult to predict the relative contribution of mEH and sEH to the DHETs biosynthesis relevant for its pro-excitatory effects in mouse hippocampus

Our recent report of inhibitory effects of EETs in the CA3-CA1 synapse (Mule *et al.*, 2017) taken together with the observed excitatory effects of DHETs in the present study at the same synapse pose interesting questions: What underlies the reduced basal synaptic transmission observed in mice lacking EHs? Whether it is stabilization of inhibitory EETs or absence of pro-excitatory DHETs? The lack of a reasonably sensitive analytical method for detecting EETs/DHETs concentration at the relevant microenvironment makes it difficult to address these questions experimentally. However, these findings lead to the intriguing hypothesis that EHs (sEH and mEH) might serve as an endogenous switch between inhibition and excitation by regulating the ratio of inhibitory EETs and excitatory DHETs. In addition to our findings presented here, a few studies support the notion of an important role of EH in the maintenance of hippocampal inhibition-excitation balance. For instance, expression of sEH has been shown to be upregulated

in pilocarpine-induced epileptic mice (Vito *et al.*, 2014), this upregulation of sEH potentially lead to an imbalance of inhibitory EETs and excitatory DHETs and underlie the pathological hyperexcitability associated with epilepsy.

Based on general consensus that sEH is main determinant of EET:DHET ratio, role of sEH in experimentally induced epilepsy has already been investigated in a few studies. Genetic ablation/ pharmacological inhibition of sEH attenuated the epileptic seizures in various animal models of epilepsy (Inceoglu *et al.*, 2013; Hung *et al.*, 2015; Vito *et al.*, 2014). Our results offer mechanistic explanation(s) for antiepileptic effects observed in these studies. Moreover, in addition to sEH, our findings strongly suggest an important role for mEH in regulation of excitation and inhibition in mouse hippocampus. To best of our knowledge, unlike sEH, mEH inhibition has not been explored for potential antiepileptic properties. In light of our results, it is highly desirable to explore small molecule mEH blockers for their antiepileptic potential in experimentally induced epilepsy.

3.5. Bibliography

Al-Sabi A, Kaza SK, Dolly JO, Wang J (2013). Pharmacological characteristics of $K_v1.1$-and $K_v1.2$-containing channels are influenced by the stoichiometry and positioning of their α subunits. *Biochemical Journal* **454**(1)**:** 101-108.

Alkayed NJ, Birks EK, Narayanan J, Petrie KA, Kohler-Cabot AE, Harder DR (1997). Role of P-450 arachidonic acid epoxygenase in the response of cerebral blood flow to glutamate in rats. *Stroke* **28**(5)**:** 1066-1072.

Amruthesh SC, Boerschel MF, McKinney JS, Willoughby KA, Ellis EF (1993). Metabolism of arachidonic acid to epoxyeicosatrienoic acids. Hydroxyeicosatetraenoic acids, and prostaglandins in cultured rat hippocampal astrocytes. *Journal of neurochemistry* **61**(1)**:** 150-159.

Andersen P (2007). *The hippocampus book*. edn. Oxford university press.

Arand M, Cronin A, Oesch F, Mowbray SL, Alwyn Jones T (2003). The telltale structures of epoxide hydrolases. *Drug metabolism reviews* **35**(4)**:** 365-383.

Boland LM, Drzewiecki MM (2008). Polyunsaturated fatty acid modulation of voltage-gated ion channels. *Cell biochemistry and biophysics* **52**(2)**:** 59-84.

Campbell WB, Deeter C, Gauthier KM, Ingraham RH, Falck JR, Li P-L (2002). 14, 15-Dihydroxyeicosatrienoic acid relaxes bovine coronary arteries by activation of K_{Ca} channels. *American Journal of Physiology-Heart and Circulatory Physiology* **282**(5)**:** H1656-H1664.

Campbell WB, Gebremedhin D, Pratt PF, Harder DR (1996). Identification of epoxyeicosatrienoic acids as endothelium-derived hyperpolarizing factors. *Circulation research* **78**(3)**:** 415-423.

Carta M, Lanore F, Rebola N, Szabo Z, Da Silva SV, Lourenço J, *et al.* (2014). Membrane lipids tune synaptic transmission by direct modulation of presynaptic potassium channels. *Neuron* **81**(4)**:** 787-799.

Consortium U (2017). UniProt: the universal protein knowledgebase. *Nucleic acids research* **45**(D1)**:** D158-D169.

Decher N, Streit AK, Rapedius M, Netter MF, Marzian S, Ehling P, *et al.* (2010). RNA editing modulates the binding of drugs and highly unsaturated fatty acids to the open pore of K_v potassium channels. *The EMBO journal* **29**(13)**:** 2101-2113.

Decker M, Adamska M, Cronin A, Di Giallonardo F, Burgener J, Marowsky A, *et al.* (2012). EH3 (ABHD9): the first member of a new epoxide hydrolase family with high activity for fatty acid epoxides. *Journal of lipid research* **53**(10)**:** 2038-2045.

Fleming I, Rueben A, Popp R, Fisslthaler B, Schrodt S, Sander A, *et al.* (2007). Epoxyeicosatrienoic acids regulate Trp channel-dependent Ca^{2+} signaling and hyperpolarization in endothelial cells. *Arteriosclerosis, thrombosis, and vascular biology* **27**(12)**:** 2612-2618.

Haydon PG, Carmignoto G (2006). Astrocyte control of synaptic transmission and neurovascular coupling. *Physiological reviews* **86**(3)**:** 1009-1031.

Hoffman DA, Magee JC, Colbert CM, Johnston D (1997). K^+ channel regulation of signal propagation in dendrites of hippocampal pyramidal neurons. *Nature* **387**(6636)**:** 869-875.

Hung Y-W, Hung S-W, Wu Y-C, Wong L-K, Lai M-T, Shih Y-H, *et al.* (2015). Soluble epoxide hydrolase activity regulates inflammatory responses and seizure generation in two mouse models of temporal lobe epilepsy. *Brain, behavior, and immunity* **43:** 118-129.

Iliff JJ, Jia J, Nelson J, Goyagi T, Klaus J, Alkayed NJ (2010). Epoxyeicosanoid signaling in CNS function and disease. *Prostaglandins & other lipid mediators* **91**(3)**:** 68-84.

Inceoglu B, Zolkowska D, Yoo HJ, Wagner KM, Yang J, Hackett E, *et al.* (2013). Epoxy fatty acids and inhibition of the soluble epoxide hydrolase selectively modulate GABA mediated neurotransmission to delay onset of seizures. *PloS one* **8**(12)**:** e80922.

Johnston D, Hoffman DA, Magee JC, Poolos NP, Watanabe S, Colbert CM, *et al.* (2000). Dendritic potassium channels in hippocampal pyramidal neurons. *The Journal of physiology* **525**(1)**:** 75-81.

Kim J, Jung S-C, Clemens AM, Petralia RS, Hoffman DA (2007). Regulation of dendritic excitability by activity-dependent trafficking of the A-type K^+ channel subunit K_v4. 2 in hippocampal neurons. *Neuron* **54**(6)**:** 933-947.

Kole MH, Stuart GJ (2012). Signal processing in the axon initial segment. *Neuron* **73**(2)**:** 235-247.

Kundu S, Roome T, Bhattacharjee A, Carnevale KA, Yakubenko VP, Zhang R, *et al.* (2013). Metabolic products of soluble epoxide hydrolase are essential for monocyte chemotaxis to MCP-1 *in vitro* and *in vivo*. *Journal of lipid research* **54**(2)**:** 436-447.

Larsen BT, Miura H, Hatoum OA, Campbell WB, Hammock BD, Zeldin DC, *et al.* (2006). Epoxyeicosatrienoic and dihydroxyeicosatrienoic acids dilate human coronary arterioles via BK_{Ca} channels: implications for soluble epoxide hydrolase inhibition. *American Journal of Physiology-Heart and Circulatory Physiology* **290**(2)**:** H491-H499.

Lein ES, Hawrylycz MJ, Ao N, Ayres M, Bensinger A, Bernard A, *et al.* (2007). Genome-wide atlas of gene expression in the adult mouse brain. *Nature* **445**(7124)**:** 168-176.

Leon ACO, Marwosky A, Arand M (2017). Evidence for a complex formation between CYP2J5 and mEH in living cells by FRET analysis of membrane protein interaction in the endoplasmic reticulum (FAMPIR). *Archives of Toxicology***:** 1-10.

Li P-L, Campbell WB (1997). Epoxyeicosatrienoic acids activate K^+ channels in coronary smooth muscle through a guanine nucleotide binding protein. *Circulation research* **80**(6)**:** 877-884.

Lu T, Ye D, Wang X, Seubert JM, Graves JP, Bradbury JA, *et al.* (2006). Cardiac and vascular K_{ATP} channels in rats are activated by endogenous epoxyeicosatrienoic acids through different mechanisms. *The Journal of physiology* **575**(2)**:** 627-644.

Marowsky A, Burgener J, Falck J, Fritschy JM, Arand M (2009). Distribution of soluble and microsomal epoxide hydrolase in the mouse brain and its contribution to cerebral epoxyeicosatrienoic acid metabolism. *Neuroscience* **163**(2)**:** 646-661.

Marowsky A, Haenel K, Bockamp E, Heck R, Rutishauser S, Mule N, *et al.* (2016). Genetic enhancement of microsomal epoxide hydrolase improves metabolic detoxification but impairs cerebral blood flow regulation. *Archives of Toxicology* **90**(12)**:** 3017-3027.

Marowsky A, Meyer I, Erismann-Ebner K, Pellegrini G, Mule N, Arand M (2017). Beyond detoxification: a role for mouse mEH in the hepatic metabolism of endogenous lipids. *Archives of Toxicology***:** 1-15.

Miyata M, Kudo G, Lee Y-H, Yang TJ, Gelboin HV, Fernandez-Salguero P, *et al.* (1999). Targeted disruption of the microsomal epoxide hydrolase gene microsomal epoxide hydrolase is required for the carcinogenic activity of 7, 12-dimethylbenz [a] anthracene. *Journal of Biological Chemistry* **274**(34)**:** 23963-23968.

Morisseau C (2013). Role of epoxide hydrolases in lipid metabolism. *Biochimie* **95**(1)**:** 91-95.

Morisseau C, Newman JW, Dowdy DL, Goodrow MH, Hammock BD (2001). Inhibition of microsomal epoxide hydrolases by ureas, amides, and amines. *Chemical research in toxicology* **14**(4)**:** 409-415.

Mule NK, Leon ACO, Falck JR, Arand M, Marowsky A (2017). 11,12-Epoxyeicosatrienoic acid (11,12-EET) reduces excitability and excitatory transmission in the hippocampus. *Neuropharmacology*.

Oesch F, Daly J (1972). Conversion of naphthalene to trans-naphthalene dihydrodiol: Evidence for the presence of a coupled aryl monooxygenase-epoxide hydrase system in hepatic microsomes. *Biochemical and biophysical research communications* **46**(4)**:** 1713-1720.

Oliver D, Lien C-C, Soom M, Baukrowitz T, Jonas P, Fakler B (2004). Functional conversion between A-type and delayed rectifier K^+ channels by membrane lipids. *Science* **304**(5668)**:** 265-270.

Ovsepian SV, LeBerre M, Steuber V, O'leary VB, Leibold C, Dolly JO (2016). Distinctive role of K V 1.1 subunit in the biology and functions of low threshold K^+ channels with implications for neurological disease. *Pharmacology & Therapeutics* **159:** 93-101.

Pannasch U, Sibille J, Rouach N (2012). Dual electrophysiological recordings of synaptically-evoked astroglial and neuronal responses in acute hippocampal slices. *JoVE (Journal of Visualized Experiments)*(69)**:** e4418-e4418.

Rama S, Zbili M, Fékété A, Tapia M, Benitez MJ, Boumedine N, *et al.* (2017). The role of axonal K_v1 channels in CA3 pyramidal cell excitability. *Scientific Reports* **7**.

Ramakers GM, Storm JF (2002). A postsynaptic transient K^+ current modulated by arachidonic acid regulates synaptic integration and threshold for LTP induction in hippocampal pyramidal cells. *Proceedings of the National Academy of Sciences* **99**(15)**:** 10144-10149
Sinal CJ, Miyata M, Tohkin M, Nagata K, Bend JR, Gonzalez FJ (2000). Targeted disruption of soluble epoxide hydrolase reveals a role in blood pressure regulation. *Journal of Biological Chemistry* **275**(51)**:** 40504-40510.

Sisignano M, Park C-K, Angioni C, Zhang DD, von Hehn C, Cobos EJ, *et al.* (2012). 5, 6-EET is released upon neuronal activity and induces mechanical pain hypersensitivity via TRPA1 on central afferent terminals. *Journal of Neuroscience* **32**(18)**:** 6364-6372.

Spector AA, Kim H-Y (2015). Cytochrome P 450 epoxygenase pathway of polyunsaturated fatty acid metabolism. *Biochimica et Biophysica Acta (BBA)-Molecular and Cell Biology of Lipids* **1851**(4)**:** 356-365.

Terashvili M, Tseng LF, Wu H, Narayanan J, Hart LM, Falck JR, *et al.* (2008). Antinociception produced by 14, 15-epoxyeicosatrienoic acid is mediated by the activation of β -endorphin and Met-enkephalin in the rat ventrolateral periaqueductal gray. *Journal of Pharmacology and Experimental Therapeutics* **326**(2)**:** 614-622.

Trimmer JS (2015). Subcellular localization of K^+ channels in mammalian brain neurons: remarkable precision in the midst of extraordinary complexity. *Neuron* **85**(2)**:** 238-256.

Vito ST, Austin AT, Banks CN, Inceoglu B, Bruun DA, Zolkowska D, *et al.* (2014). Post-exposure administration of diazepam combined with soluble epoxide hydrolase inhibition stops seizures and modulates neuroinflammation in a murine model of acute TETS intoxication. *Toxicology and applied pharmacology* **281**(2)**:** 185-194.

Watanabe H, Vriens J, Prenen J, Droogmans G, Voets T, Nilius B (2003). Anandamide and arachidonic acid use epoxyeicosatrienoic acids to activate TRPV4 channels. *Nature* **424**(6947)**:** 434-438.

Ye D, Zhou W, Lee H-C (2005). Activation of rat mesenteric arterial K_{ATP} channels by 11, 12-epoxyeicosatrienoic acid. *American Journal of Physiology-Heart and Circulatory Physiology* **288**(1)**:** H358-H364.

Yeung SY, Millar JA, Mathie A (1999). Inhibition of neuronal K_V potassium currents by the antidepressant drug, fluoxetine. *British journal of pharmacology* **128**(7)**:** 1609-1615.

Chapter 4

Altered susceptibility to morphine-mediated antinociception in sEH KO mice

4.1. Introduction

Cytochrome P450 (CYP) epoxygenases catalyze the epoxygenation of fatty acid (FAs) to bioactive epoxides. Amongst more than 100 murine CYP isoenzymes, CYP-2C and -2J are most commonly noted for their epoxygenase activity (Iliff *et al.*, 2010; Spector *et al.*, 2015). However, several other CYP isoenzymes such as CYP-4x1 are capable of FA epoxygenation in mouse brain (Al-Anizy *et al.*, 2006). Arachidonic acid (AA) is amongst the most studied FAs and is metabolized by CYP-epoxygenases to four regioisomers: 5,6-, 8,9-, 11,12- and 14,15-epoxyeicosatrienoic acid (EET), which further can be hydrolyzed to the corresponding less active diols by soluble epoxide hydrolase (sEH) and microsomal epoxide hydrolase (mEH) (Miksys *et al.*, 2002; Marowsky *et al.*, 2009; Spector *et al.*, 2015).

In addition to EETs, other CYP-epoxygenase-derived bioactive FA epoxides include docosahexaenoic acid-derived epoxydocosapentaenoic acids (EpDPEs), eicosapentaenoic acid-derived epoxyeicosatetraenoic acid (EpETEs) and linoleic acid-derived epoxyoctadecenoic acid (EpOMEs) (Wagner *et al.*, 2014). Amongst these bioactive FA epoxides, EETs are the most studied ones and are best known for their potent vasodilatory effects, by virtue of which they play an important role in neurovascular coupling (Farr *et al.*, 2011). In addition to their vasodilatory effects, EETs exhibit pro-angiogenic and anti-inflammatory properties which collectively might underlie the neuroprotective potential of EETs (Iliff *et al.*, 2010; Spector *et al.*, 2015).

Of the four regioisomers, 14,15- and 11,12-EET are the most synthesized in the mouse brain (Sanchez-Mejia *et al.*, 2008) and have been suggested to underlie the antinociceptive effects in rat neuropathic and inflammatory pain models (Wagner *et al.*, 2013). Interestingly, a study demonstrated strong antinociception in rats after microinjection of 14,15-EET into the periaqueductal gray (PAG), a brain region involved in opioid antinociception, presumably by activating endogenous endorphin release (Terashvili *et al.*, 2008). The potential involvement of 14,15-EET in opioid-mediated antinociception was further supported by studies demonstrating the attenuation of morphine-mediated and stress-induced antinociception in transgenic mice with neuron-specific ablation of CYP-reductase. CYP-reductase is indispensable for CYP activity and its ablation would render all neuronal CYPs (including CYP-epoxygenases) inactive (Conroy *et al.*, 2010; Hough *et al.*, 2014). In addition, microinjection of a CYP-epoxygenase inhibitor, CC12 in the rostral ventromedial medulla of WT mice also attenuated morphine-mediated

antinociception suggesting the requisite of functional CYP-epoxygenase for opioid-mediated antinociception (Conroy *et al.*, 2013). Furthermore, a recent study employed a cluster knock out strategy, wherein the genetic ablation of CYP-2C cluster (noted for its epoxygenase activity) reduced subcutaneously administered morphine-mediated antinociception by 41%. However, genetic ablation of the non-epoxygenase cluster, CYP-2D and CYP-3A did not alter morphine-mediated antinociception (Hough *et al.*, 2015).

These studies collectively point towards the potential involvement of CYP-epoxygenases-derived FA epoxides(s) in opioid-mediated antinociception. Moreover, these findings taken together with an earlier report of 14,15-EET-mediated antinociception in rats (Terashvili *et al.*, 2008) suggest that 14,15-EET might potentiate opioid signaling. The potential effect of 14,15-EET on opioid signaling might be mediated via one of the following mechanism(s):

1. 14,15-EET might enhance the endogenous opioid release as suggested by (Terashvili *et al.*, 2008).
2. They might facilitate agonist binding or allosteric modulation of mu-opioid receptors (MOR).
3. The might alter downstream signaling component(s) to enhance MOR signaling.

sEH-catalyzed hydrolysis is a major determinant of the bioavailability of FA epoxides including 14,15-EET and genetic ablation or inhibition of sEH have been shown to prolong the bioactivity of these epoxides *in vivo* (Anandan *et al.*, 2011; Zhang *et al.*, 2007). Therefore, we used sEH KO mice to test the potential influence of metabolic stabilization of sEH substrates in opioid-mediated antinociception using the tail flick paradigm. Furthermore, to investigate the potential influence of 14,15-EET on MOR signaling, we heterologously expressed MORs and its effector G-protein coupled inwardly rectifying K^+ (GIRK) channels in host cells.

4.2. Materials and methods

4.2.1. Nociceptive testing

4.2.1.1. Animals

Adult, 8 weeks old, C57BL/6J and *Ephx2* null (sEH KO) mice were used for nociceptive testing. The sEH KO mice (Sinal *et al.*, 2000) were provided by Dr. Frank Gonzalez (National Institute of Health, Bethesda, USA) and C57BL/6J mice were obtained from Charles River Laboratories

(Germany). sEH KO mice were backcrossed with C57BL/6J for at least 7-9 generations. The genotype was confirmed by using standard polymerase chain reaction as described here (Marowsky *et al.*, 2017). Sexually dimorphic expression of sEH has been shown in the experimental mice (Qin *et al.*, 2015). Therefore, we exclusively used male mice. Mice were group-housed in a room with 12 hours light/dark cycle and had *ad libitum* access to standard chow-food and water. Animal experiments were carried out according to the Swiss Federal Law under the license 196/2012 granted by the Kantonale Veterinärsamt Zürich, Switzerland.

4.2.1.2. Tail flick experiments

The tail flick paradigm is widely employed for assaying efficacy of pharmacological agents on supraspinal heat-induced thermal pain in rodents. In the present study, mice were allowed to acclimatize to the experimentation room before experiments. All animal experiments were carried out at the same time of the day (9 am to 2 pm) to avoid diurnal variations. Each mouse was placed in a Plexiglas tube and the ventral surface of the tail (between 3 and 5 cm from the tip) and was exposed to the radiant heat to induce thermal pain. The tail flick analgesiometer (IITC, Chicago, USA) was used to record tail withdrawal latency (in seconds) as a readout for radiant heat-induced thermal pain. Heat intensity was calibrated to keep the basal tail withdrawal latency between 3-4 seconds. Three baseline latency readings were recorded before subcutaneous (sc) application of either saline or morphine. Tail flick latencies were recorded at 20, 40, 60 and 90 minutes post-injection. In the absence of tail withdrawal, a 10 s cut-off was exercised to avoid permanent tissue damage. The experimenters were blinded to the drug(s) injected and genotype of the animals to avoid bias. Data are presented as the percent maximum possible effect (% MPE).

$$\%\,\boldsymbol{MPE} = \frac{(\boldsymbol{post\ injection\ latency} - \boldsymbol{baseline\ latency})}{(\mathbf{10} - \boldsymbol{baseline\ latency})}$$

4.2.2. *In vitro* electrophysiology in the heterologous expression system

4.2.2.1. HEK-293T cell maintenance and transfection

Heterologous expression system carrying functionally coupled MOR-GIRK in HEK-293T cells was established for electrophysiological assays. HEK-293T cells were maintained at 37°C in 95% O_2, 5% CO_2, in DMEM medium (Invitrogen, USA), supplemented with 5% fetal bovine

serum. For transient transfections, 50,000 to 70,000 cells were seeded out on 12 mm glass coverslips placed in 3.5 cm plate and allowed to grow overnight before transfection. HEK-293T cells were transiently transfected with rat MOR (0.5-0.75 µg), together with the human [GIRK1 (Kir 3.1)/GIRK2 (Kir 3.2A)] (1-1.5 µg) and eGFP (0.1-0.15 µg) cDNA using JetPei transfection reagent (Polyplus transfection, USA). MOR and GIRK plasmids were kindly provided by Dr. Volker Hoellt (Bailey *et al.*, 2003) and Dr. Graeme Henderson (Johnson *et al.*, 2006), respectively. HEK-293T cells were used for experimentation 24-48 hours post-transfection. A coverslip with HEK-293T cells was transferred to the recording chamber and superfused with an external solution throughout the experiment. Axiovert 200 fluorescence inverted microscope (Carl-Zeiss, Germany) was used to visualize the green fluorescing (eGFP expressing) HEK-293T cells. The eGFP expression was considered as a marker for MOR-GIRK expression and green cells were used for patch-clamp recording. Mock-transfected cells and non-GFP expressing cells did not respond to application of MOR agonist, DAMGO.

4.2.2.2. Electrophysiological recordings

A high potassium external solution containing (in mM) NaCl (125), KCl (30), $MgCl_2$ (1.0), $CaCl_2$ (2), glucose (10) and HEPES (10) The pH was adjusted to 7.4 with 1N NaOH, and osmolarity was 315 mOsm) was used for electrophysiological recordings. Patch pipettes were pulled from borosilicate glass capillaries, (GC150F-10, Harvard apparatus, UK) and had a tip resistance of 2.5 to 3.5 mΩ when filled with an internal solution containing the following (in mM) K-gluconate (145), Mg-ATP (5), Na-GTP (0.5), EGTA (1) and NaCl (5). The pH was adjusted to 7.3 with 1N KOH, the osmolarity was 305 mOsm.

Whole-cell macroscopic currents were recorded using AM2400 patch-clamp amplifier (AM systems, USA) and digitized at 10 KHz using Digidata 1400 and pClamp 10 software suites (Molecular Devices, USA). After establishing the whole-cell configuration, whole-cell capacitance and series resistance were compensated using amplifier circuitry. The cell was clamped (V_h) at -80 mV; the calculated reversal potential was E_{rev}=-40 mV for K^+ for the given external-internal combination. DAMGO-induced inward GIRK currents were measured as a readout for MOR activation.

4.2.2.3. Drug application system

To avoid DAMGO-induced desensitization of MOR, DAMGO exposure to a patched cell was limited to five seconds. We employed two channeled, gravity-assisted application system comprising two fused silica capillaries. Two channels were operated close (~ 50-100 μm) to a patched cell so that the drugs could be delivered to the cell directly. The first channel was used exclusively for delivering drugs such as DAMGO or DAMGO+EETs, while the second channel was used for the external solution to wash the drug(s) off the cell. Fast solution exchange was achieved by switching quickly from first channel (drug) to the second (wash) using micromanipulator as shown in *Fig.4.2A*. The MOR antagonist-naloxone and the GIRK blocker barium chloride were used to validate the specificity of DAMGO-induced currents.

4.2.3. Drugs and solutions

14,15-EET was kindly provided by Dr. John Falck, University of Texas, Southwestern Medical Center, Texas, USA. All other drugs were obtained from Sigma-Aldrich except DAMGO ([D-Ala^2, *N*-MePhe^4, Gly-ol]-enkephalin), which was obtained from Tocris Bioscience, UK. All the drugs were dissolved in water except 14,15-EET which was dissolved in dimethyl sulfoxide (DMSO). DMSO tends to be unstable during storage and therefore to avoid contribution of the nonspecific contaminants generated during storage, all the experiments investigating the influence of DMSO were carried out with the ultra-pure anhydrous DMSO supplied in individually packed light-protected containers from Life Technologies, Thermo Fischer Scientific, USA. All the drugs were prediluted in the external solution to yield desired concentration before application.

4.2.4. Data analysis and statistics

All data are expressed as mean±standard error of mean unless stated otherwise. All concentration-response curves were fitted with $\log_{10}$ (concentration of DAMGO in nM) vs. response using GraphPad Prism 5 (GraphPad Software, USA). Appropriate statistical tests were used for testing the significance, such as Student's *t*-test for comparisons and two-way-ANOVA followed by a post hoc test for multivariate comparisons.

4.3. Results

4.3.1. Sub-maximal dose of morphine exhibits higher antinociception in sEH KO compared to WT mice

We tested the influence of metabolic stabilization of CYP-epoxygenase-derived FA epoxides such as EETs in sEH KO mice. We measured supraspinal antinociception by using tail flick latency in response to the thermal heat as shown in *(Fig. 4.1A)*. First, we tested for genotype-specific differences in the thermal pain sensitivity between WT and sEH KO mice. No significant difference in baseline latencies between sEH KO vs. WT mice was observed, indicating the lack of influence of sEH substrates on basal opioid signaling *(Fig. 4.1B)*. Stressful situations such as forced swimming and restraining are known to activate the endogenous opioid system and lead to 'stress-induced antinociception' (Maier, 1986; Mogil *et al.*, 1996). In our experiments, mice were briefly restrained in the Plexiglas tube for tail flick latency measurements. Interestingly, we observed a significantly higher restrain-induced antinociception in saline-treated sEH KO mice 60 min post-saline injection compared to the saline-treated WT counterparts *(Fig. 4.1C)*. This finding suggests a potential involvement of FA epoxides in stress-induced antinociception in line with a recent report, which implicated neuronal CYP-epoxygenase activity in stress-induced analgesia (Hough *et al.*, 2014).

Further, we studied the effect of metabolic stabilization of epoxygenated FAs on morphine-mediated antinociception. We observed significantly higher antinociception (measured as % MPE) at (1 mg/kg) of morphine administered SC in sEH KO as compared to WT mice *(Fig. 4.1D)*. This finding suggests the potential involvement of bioactive FA epoxides such as EETs in the potentiation of MOR signaling in sEH KO mice.

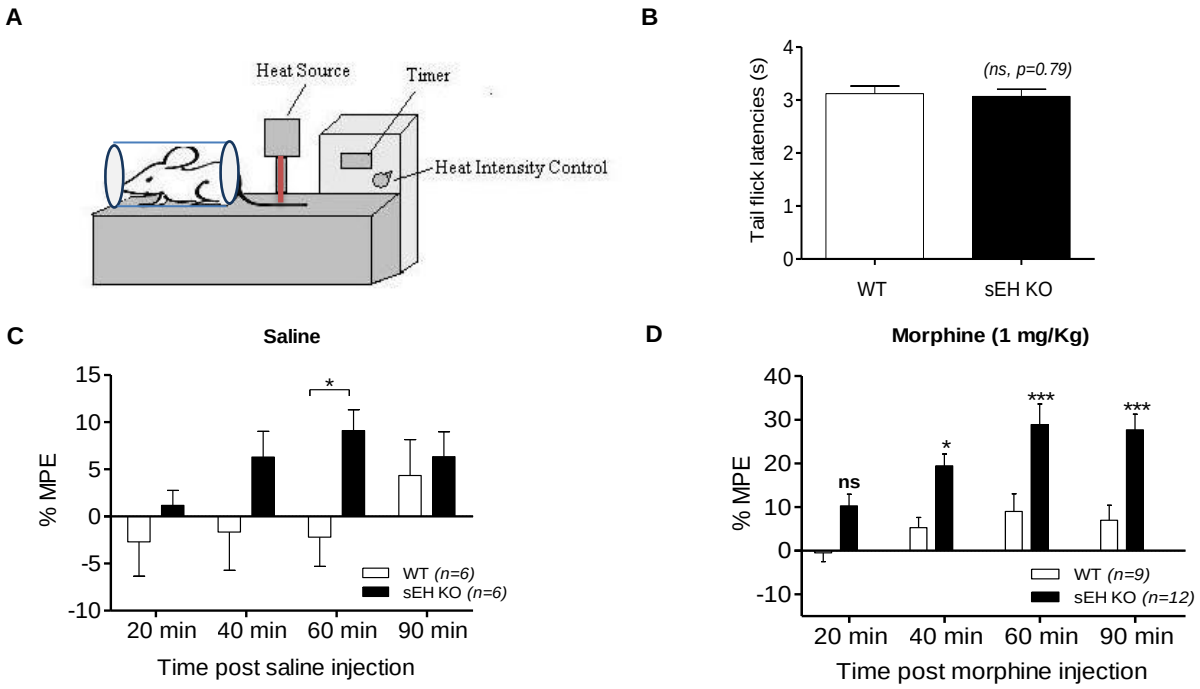

Fig. 4.1 sEH KO mice exhibit significantly higher morphine-mediated antinociception compared to age-matched WT mice.
(A) Schematic illustration of the tail flick analgesiometer used in this study. **(B)** Baseline tail flick latencies for WT (n=10) vs. sEH KO (n=14) mice, unpaired Student's *t*-test. The percent maximum possible effect (MPE) measured in saline **(C)** or morphine (1 mg/kg) treated **(D)** WT and sEH KO mice, unpaired Student's *t*-test for saline treated WT vs. sEH KO at every time point was used. Two-way ANOVA followed by Bonferroni posttest for morphine treated WT vs. sEH KO mice was used to test the significance, *p<0.05, ***p<0.001.

4.3.2. The MOR-GIRK heterologous expression system to study the MOR signaling *in vitro*

We built a two-channel gravity-assisted drug application system to minimize agonist exposure to MORs *(Fig. 4.2A).* Further, we validated the functional coupling of MOR-GIRK system by recording DAMGO-induced inward GIRK currents *(Fig. 4.2B).* We also verified the inward rectification - a unique biophysical signature of DAMGO-induced GIRK currents by recording current-voltage curve *(Fig. 4.2C and D).* Additionally, we used the MOR antagonist naloxone and the GIRK blocker barium chloride to validate the specificity of DAMGO-induced inward GIRK currents.

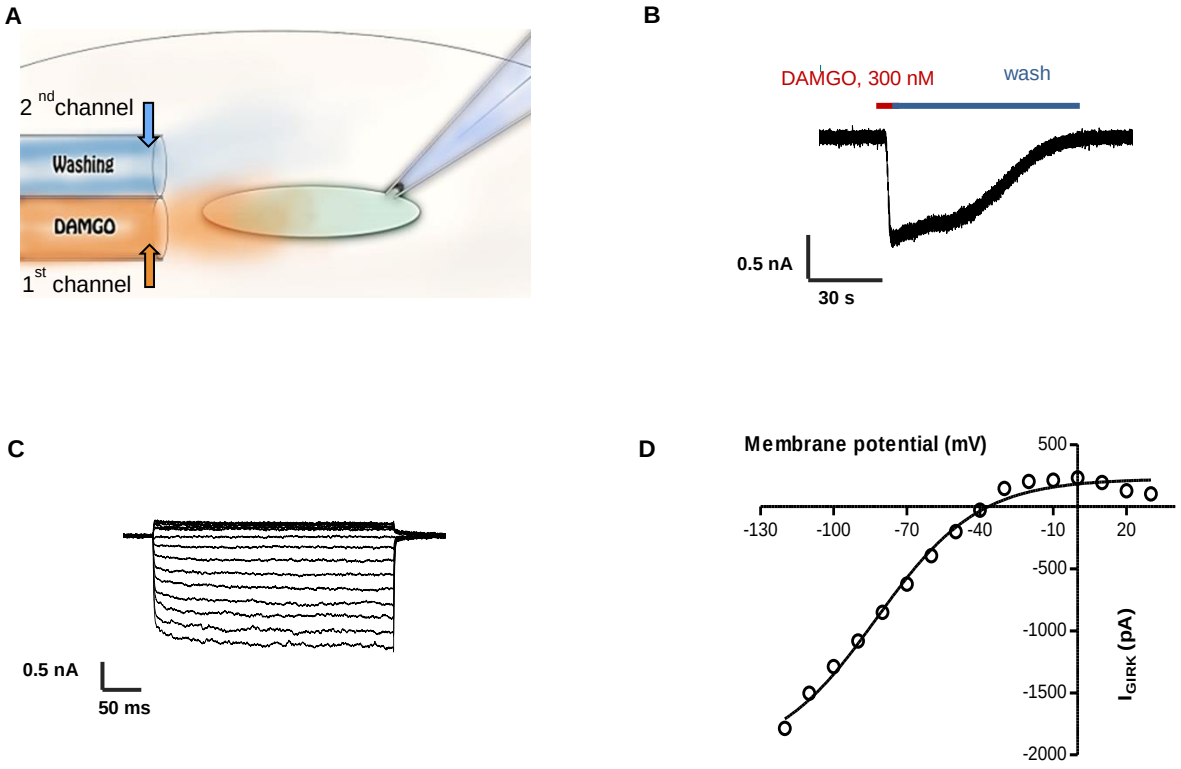

Fig. 4.2 Drug application system and characterization of DAMGO-induced GIRK currents in the heterologous expression system.
(A) Schematic representation of the two-channel application system used for on cell application of drug(s) or washing. **(B)** A representative patch-clamp recording showing DAMGO-induced GIRK currents measured at V_h=-80 mV in HEK-293T cells transiently expressing MOR and GIRK channels. DAMGO-induced GIRK currents are typically inwardly rectifying with a reversal potential of -40 mV, as shown s representative traces **(C)** and in a current-voltage plot **(D)**.

4.3.3. 14,15-EET does not directly activate MOR or GIRK channels in HEK-293T cells

First, we verified the expression of functional GIRK channels in HEK-293T cells using a positive control, n-propanol, 100 mM *(Fig. 4.3A)*. Application of n-propanol activated GIRK channels directly, confirming the functional expression of GIRK channels in these cells. Further, we tested the possibility of a direct effect of 14,15-EET (1 µM) on GIRK channels in HEK-293T cells. We did not observe any EET-mediated activation of GIRK *(Fig. 4.3B)*. Moreover, we tested the possibility of a direct effect of 14,15-EET (0.3 and 3 µM) on MOR signaling in HEK-293T cells expressing both MOR and GIRK and we did not observe any MOR-GIRK activation by 14,15-EET *(Fig. 4.3C and D)*. Additionally, we confirmed the functional coupling between MOR and GIRK in these cells by application of the MOR agonist-DAMGO. These findings demonstrate

that 14,15-EET does not activate MOR or GIRK directly and might potentiate the MOR signaling via other indirect mechanisms such as facilitation of agonist binding to MOR.

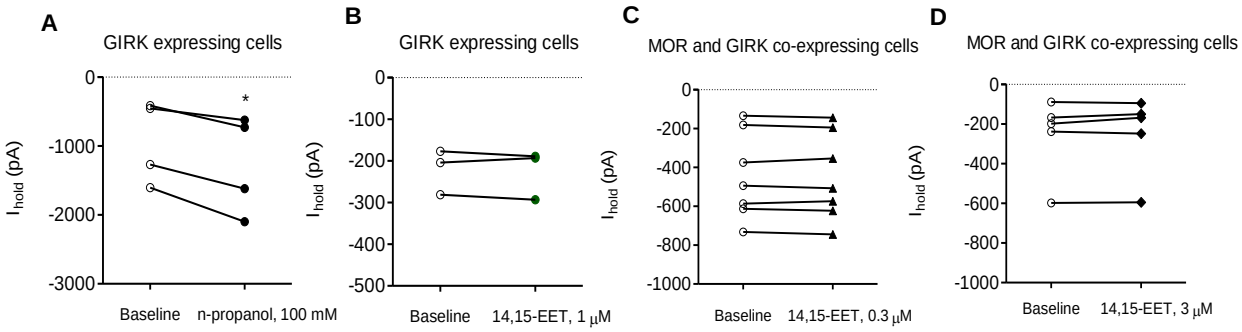

Fig. 4.3 14,15-EET does not activate MOR or GIRK channels directly in GIRK- or MOR/GIRK-expressing HEK-293T cells.
(A) n-propanol (100 mM), a positive control for GIRK activation significantly increased GIRK conduction (n=4). Application of 14,15-EET (1 μM) did not alter the GIRK conductance directly in GIRK expressing cells (n=3) **(B)** Similarly, application of 0.3 μM and 3 μM 14,15-EET did not activate GIRK channels via MOR in MOR/GIRK co-expressing cells (**C** and **D**; n=7 and 5, respectively), paired Student's *t*-test.

4.3.4. 14,15-EET does not alter DAMGO concentration-response curve in HEK-293T cells

We applied DAMGO using two-channeled application system which ensured faster solution exchange and minimized DAMGO-induced desensitization of MOR signaling *(see material-methods).* We evaluated the effectiveness of our drug application system by carrying out two consecutive concentration-response curves (CRCs) of DAMGO (3, 10, 30, 100 and 300 nM) in the same cell expressing functionally-coupled MORs and GIRK channels *(Fig. 4.4A)*. We did not observe significant desensitization of MOR responses when the CRC was repeated in the same cell, allowing to conclude that our experimental paradigm is amenable to study the potential influence of EET on DAMGO CRCs. CRCs were fitted with $\log_{10}$ (DAMGO concentration in nM) vs. normalized I_{GIRK}, using three parameters fit using GraphPad Prism 5 suite to calculate EC50 values for DAMGO. The calculated EC50 for the first and second CRCs were 14.4 and 17 nM, respectively *(Fig. 4.4B)*.

To evaluate the potential influence of 14,15-EET on DAMGO CRCs, we carried out two CRCs in a cell; the first CRC was carried out with DAMGO plus vehicle control (0.003%/0.03% DMSO) while the second one was with DAMGO plus 14,15-EET (0.3/3 μM dissolved in DMSO, 0.03 and 0.003% final concentration of DMSO). Co-application of 14,15-EET (0.3 and 3 μM) did not

alter the DAMGO CRCs significantly. The calculated EC50 value for DAMGO in the presence and absence of 14,15-EET (0.3 µM) were 5.6 and 5.4 nM, respectively *(Fig. 4.4C)*. Co-application of 14,15-EET (3 µM) marginally shifted DAMGO EC50 from 7.5 to 5 nM *(Fig. 4.4D)*.

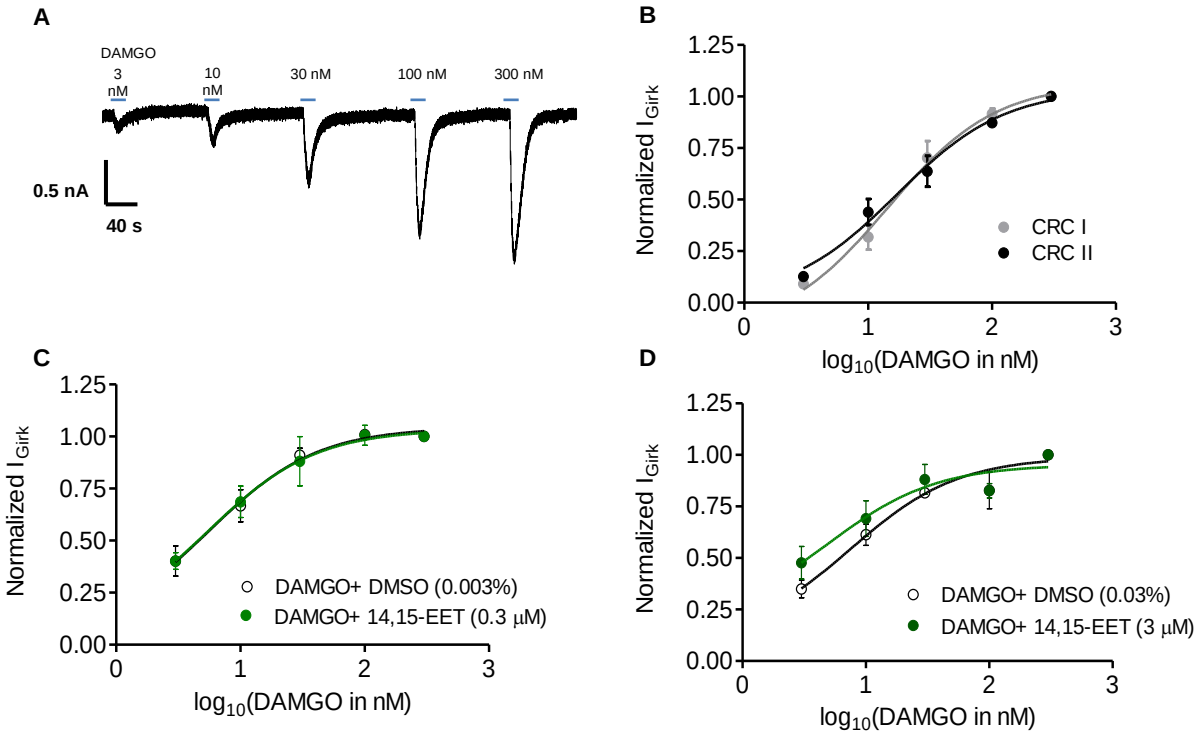

Fig. 4.4 14,15-EET does not alter the concentration-response curve for DAMGO in MOR/GIRK-expressing HEK-293T cells.
(A) A representative trace of a CRC obtained by applying 3, 10, 30, 100 and 300 nM of DAMGO. **(B)** Average CRC plot showing no desensitization in a control experiment where two consecutive CRCs (I and II) were recorded in the same cell. Effect of 0.3 µM (n=6) and 3 µM (n=5) 14,15-EET on DAMGO CRC compared to the corresponding DMSO controls is shown in **(C)** and **(D)**, respectively.

4.3.5. DMSO (used as a vehicle) potentiated MOR signaling in the heterologous expression system.

Unexpectedly, we observed that the calculated EC50 values in the presence of DMSO used as vehicle control *(Fig. 4.4C and D, 5.6 and 5.4 nM, respectively)* were lower than the one observed with the control CRC *(Fig. 4.4B,14.4 nM)* carried out in the absence of DMSO, suggesting the influence of DMSO on MOR signaling. To investigate the potential influence of DMSO on MOR activity, we tested the possibility of direct activation of MOR signaling by DMSO in the

heterologous system expressing functional MOR and GIRK. DMSO (0.001, 0.003, and 0.03%) did not activate MOR signaling in the absence of DAMGO. We ensured the functional MOR-GIRK coupling by applying DAMGO at the end of every recording *(Fig. 4.5A and B)*.

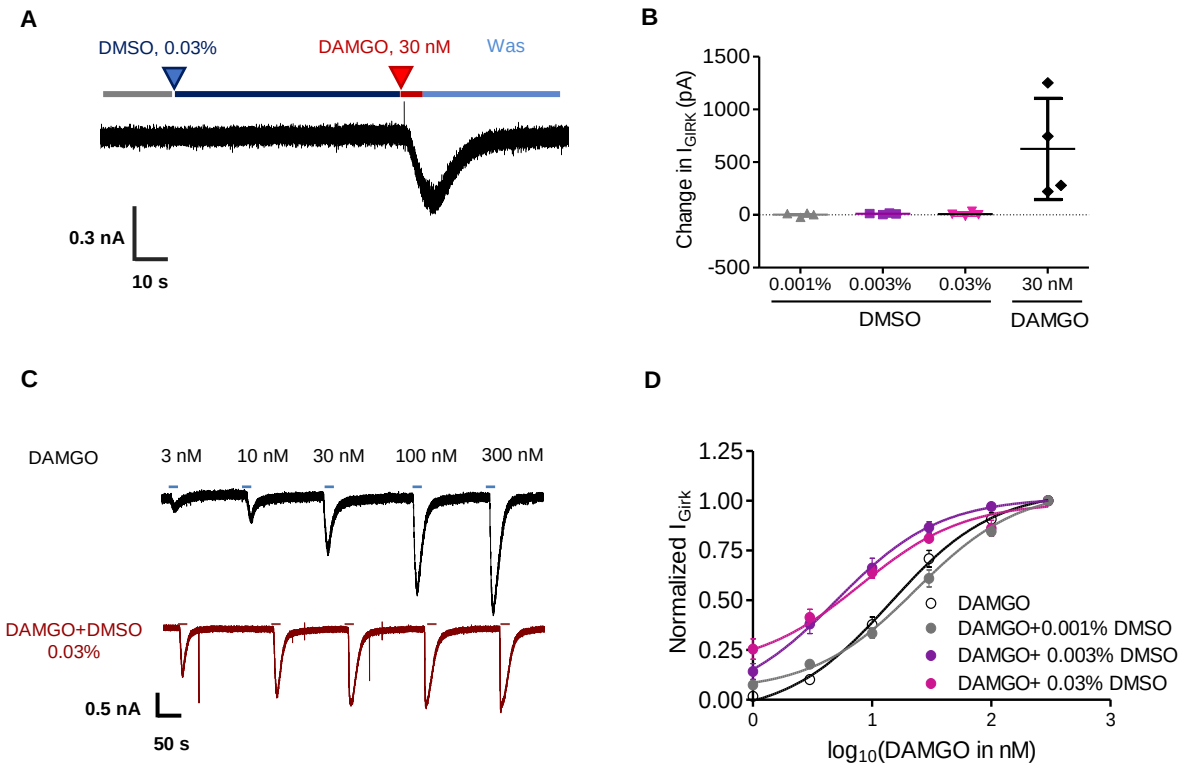

Fig. 4.5 DMSO potentiates DAMGO-induced activation of MOR signaling in MOR/GIRK-expressing HEK-293T cells.
(A) A representative trace showing the effect of DMSO (0.03%) and DAMGO, 30 nM on I_{GIRK}. **(B)** A scatter plot showing average change in DMSO/DAMGO-induced I_{GIRK} (n=4 each). **(C)** A representative trace showing the effect of DMSO (0.03%) on DAMGO CRC**. (D**) Average CRC plot showing the effect of DMSO (0.001%, n=9; 0.003%, n= 10; and 0.03%, n=12) on DAMGO CRC.

Further, we investigated the potential effect of (0.001, 0.003% and 0.03%) DMSO on DAMGO CRCs. DAMGO CRCs were shifted significantly towards the left in the presence of 0.003% and 0.03% of DMSO. The DMSO-induced leftward shift of CRCs was evident from the lower calculated EC50 values. The calculated EC50 values for control DAMGO CRC was 14.3 nM which was shifted to 5 nM and 7.9 nM by 0.003 and 0.03% DMSO, respectively *(Fig. 4.5C and D)*. Effect of the lowest concentration of DMSO (0.001%) was not significantly different from the control CRC recorded in the absence of DMSO *(Fig. 4.5D)*.

4.4. Discussion

In the present study, we demonstrated that metabolic stabilization of epoxygenated FAs by genetic ablation of sEH leads to the potentiation of morphine-mediated antinociception in mice. Earlier reports implicated CYP-epoxygenase derived metabolite(s) in the regulation of opioid signaling and morphine-mediated analgesia. Our findings from sEH KO mice taken together with an earlier report of 14,15-EET-mediated antinociception in rats (Terashvili *et al.*, 2008) suggest that 14,15-EET might enhance the MOR signaling and underlie the effects observed in CPR/CYP-epoxygenase and sEH transgenic mice. Therefore, we further investigated the potential effect of 14,15-EET on MOR signaling in the heterologous expression system expressing functional MOR and GIRK channels. Counterintuitively, 14,15-EET did not show any effects on MOR signaling in this heterologous expression system. Surprisingly, DMSO (used as a vehicle) potentiated MOR signaling in this system.

4.4.1. Metabolic stabilization of FA epoxides potentiates morphine-mediated antinociception *in vivo*

Morphine activates the opioid signaling to produce antinociception which can be measured in experimental animals using animal models of pain such as tail flick latency measurement. Using tail flick paradigm, we demonstrated that the potential metabolic stabilization of bioactive FA epoxides in sEH KO mice as suggested by (Wagner *et al.*, 2017) resulted in a significantly higher antinociception with a sub-maximal dose of morphine compared to the WT mice. Moreover, we also observed significantly higher stress-induced antinociception in sEH KO mice compared to the WT mice. Both findings are compatible with prior reports which implicated CYP-epoxygenase-derived metabolites in morphine-mediated and stress-induced antinociception (Conroy *et al.*, 2010; Hough *et al.*, 2014).

Based on these findings, the present study implicates the role of CYP-epoxygenase generated FA epoxides which are also the substrate for sEH such as EETs in the modulation of opioid signaling. However, in addition to EETs, other CYP-epoxygenase derived bioactive FA epoxides such as EpDPEs, EpETEs, and EpOMEs are also good substrates for sEH (Morisseau *et al.*, 2010; Spector *et al.*, 2015; Wagner *et al.*, 2014). Amongst all the bioactive FA epoxides, EETs have been suggested to underlie antinociceptive effects in rat neuropathic and inflammatory pain models (Wagner *et al.*, 2013). Of the four EET regioisomers, 14,15-EET is the most preferred

substrate for sEH (Imig, 2012; Morisseau *et al.*, 2010) and has been shown to exhibit strong antinociception in rats (Terashvili *et al.*, 2008). Our findings and an earlier report implicated that 14,15-EET might be a relevant mediator and potentiate MOR signaling to underlie the potentiating effect observed in sEH KO animals.

4.4.2. 14,15-EET does not potentiate MOR signaling in the heterologous expression system

Further, we investigated the potential mechanisms for 14,15-EET-mediated potentiation of MOR signaling using the heterologous expression system. Contrary to expectations, 14,15-EET did not potentiate DAMGO-induced MOR activation in this heterologous system. This striking lack of 14,15-EET effect in the heterologous system can be attributed to several possibilities as discussed below.

1. The heterologous expression system may lack certain neuron-specific downstream effector(s) which might be critical for 14,15-EET to exert activity. For instance, regulators of G-protein signaling (RGS) belong to a family of GTPase-accelerating proteins, which accelerate GTP hydrolysis by the G_{α} subunit of heterotrimeric G proteins and thus shorten the duration of GPCR signaling (De Vries *et al.*, 2000). RGS proteins such as RGS2, RGS4, RGS6, RGS7, RGS8, RGS9-2, RGS11, RGS19, and RGS20 have been reported as negative modulators of MOR signaling, of which RGS4 and 9-2 are the most commonly reported (Traynor, 2012). In addition, RGS9-2 enhances MOR signaling at the spinal site (Papachatzaki *et al.*, 2011). The activity of these RGS proteins is further regulated through a multitude of mechanisms including altered expression, intracellular localization and posttranslational modifications (Kach *et al.*, 2012). 14,15-EET might regulate the activity of RGS4 and/or 9-2 to potentiate the MOR signaling and consequently opioid-mediated antinociception. This, however, needs to be evaluated in a suitable *in vitro* system expressing MOR and RGS4/9-2.

2. The surface availability of MOR is an important determinant of magnitude and duration of MOR signaling. Trafficking of MOR to the membrane is a finely-tuned process which involves plethora of downstream proteins and mechanisms such as endosomal sorting (Zhang *et al.*, 2015). Interestingly, EETs induce the translocation of transient receptor potential-C (TRPC) channels to the endothelial cell membranes via cAMP/PKA-dependent mechanism (Fleming *et al.*, 2007). Similarly, EETs might enhance surface expression of MORs by altering their trafficking to the neuronal plasma membrane.

3. Alternatively, the observed effect of ablated CYP-epoxygenase and sEH on morphine-mediated antinociception in mice could be attributed to other bioactive epoxy FA metabolites, such as EpDPEs, EpETEs, and EpOMEs. Interestingly, a recent study implicated that DHA-derived EpDPEs are capable of suppressing diabetic neuropathic pain with the antinociceptive effect being antagonized by application of the MOR antagonist naloxone (Wagner *et al.*, 2017).

4.4.3. DMSO potentiates DAMGO-mediated MOR activation

We found that DMSO lacks any direct effect on MOR activity in absence of the MOR agonist DAMGO: However, we observed a significant potentiation of MOR signaling by DMSO (0.003% and 0.03%), concentrations which are routinely used for *in vitro* and *in vivo* pharmacological assays. These findings suggest a potential role of DMSO as a positive modulator of DAMGO-induced activation of MOR signaling.

Interestingly, some older studies suggested that DMSO itself could exhibit antinociception in animal models of nociception (Haigler *et al.*, 1983; Haigler *et al.*, 1981). However, these findings could not be confirmed in a recent study (Takeda *et al.*, 2016). This observed lack of DMSO-mediated antinociception is compatible with our *in vitro* observation that DMSO does not activate MOR signaling directly. Although DMSO lacks direct effect on MOR, it might potentiate DAMGO-induced MOR activation. This notion is further supported by a study that reported the lack of antinociceptive effect of DMSO when microinjected directly into the ventrolateral PAG. Interestingly, DMSO (2%) enhanced the potency of morphine when co-administered in rats (Fossum *et al.*, 2008) which is compatible with our observation of DMSO-mediated potentiation of DAMGO-induced MOR signaling. Furthermore, DMSO-mediated potentiation of MOR signaling has been reported in the clinical settings as well; cancer patients concurrently receiving morphine and DMSO-cryoprotected hematopoietic stem cells transplant infusion unexpectedly showed severe respiratory depression, a classical side effect of morphine-mediated MOR activation (Caselli *et al.*, 2009).

These reports, taken together with our findings strongly suggest the role of DMSO as a positive modulator of agonist-induced MOR signaling. Our findings recommend a caution for the concurrent use of DMSO and opioid agonists such as morphine or DAMGO for both, as a vehicle for pharmacological assays and as a cryoprotectant in the clinical settings.

4.5. Bibliography

Al-Anizy M, Horley NJ, Kuo CW, Gillett LC, Laughton CA, Kendall D, et al. (2006). Cytochrome P450 Cyp4x1 is a major P450 protein in mouse brain. The FEBS journal 273(5): 936-947.

Anandan SK, Webb HK, Chen D, Wang YXJ, Aavula BR, Cases S, *et al.* (2011). 1-(1-Acetyl-piperidin-4-yl)-3-adamantan-1-yl-urea (AR9281) as a potent, selective, and orally available soluble epoxide hydrolase inhibitor with efficacy in rodent models of hypertension and dysglycemia. *Bioorganic & medicinal chemistry letters* 21(3): 983-988.

Bailey CP, Couch D, Johnson E, Griffiths K, Kelly E, Henderson G (2003). μ-Opioid receptor desensitization in mature rat neurons: lack of interaction between DAMGO and morphine. *Journal of Neuroscience* 23(33): 10515-10520.

Caselli D, Tintori V, Messeri A, Frenos S, Bambi F, Aricò M (2009). Respiratory depression and somnolence in children receiving dimethylsulfoxide and morphine during hematopoietic stem cells transplantation. *haematologica* 94(1): 152-153.

Conroy JL, Fang C, Gu J, Zeitlin SO, Yang W, Yang J, *et al.* (2010). Opioids activate brain analgesic circuits through cytochrome P450/epoxygenase signaling. *Nature neuroscience* 13(3): 284-286.

Conroy JL, Nalwalk JW, Phillips JG, Hough LB (2013). CC12, a P450/epoxygenase inhibitor, acts in the rat rostral, ventromedial medulla to attenuate morphine antinociception. *Brain research* 1499: 1-11.

De Vries L, Zheng B, Fischer T, Elenko E, Farquhar MG (2000). The regulator of G protein signaling family. *Annual review of pharmacology and toxicology* 40(1): 235-271.

Farr H, David T (2011). Models of neurovascular coupling via potassium and EET signalling. *Journal of theoretical biology* 286: 13-23.

Fleming I, Rueben A, Popp R, Fisslthaler B, Schrodt S, Sander A, *et al.* (2007). Epoxyeicosatrienoic acids regulate Trp channel–dependent Ca^{2+} signaling and hyperpolarization in endothelial cells. *Arteriosclerosis, thrombosis, and vascular biology* 27(12): 2612-2618.

Fossum EN, Lisowski MJ, Macey TA, Ingram SL, Morgan MM (2008). Microinjection of the vehicle dimethyl sulfoxide (DMSO) into the periaqueductal gray modulates morphine antinociception. *Brain research* 1204: 53-58.

Haigler HJ, Spring DD (1983). Comparison of the analgesic effects of dimethyl sulfoxide and morphine. *Annals of the New York Academy of Sciences* 411(1): 19-27.

Haigler HJ, Spring DD (1981). DMSO (dimetyl sulfoxide), morphine and analgesia. *Life sciences* 29(15): 1545-1553.

Hough LB, Nalwalk JW, Ding X, Scheer N (2015). Opioid analgesia in P450 gene cluster knockout mice: a search for analgesia-relevant isoforms. *Drug Metabolism and Disposition* 43(9): 1326-1330.

Hough LB, Nalwalk JW, Yang W, Ding X (2014). Significance of neuronal cytochrome P450 activity in opioid-mediated stress-induced analgesia. *Brain research* 1578: 30-37.

Iliff JJ, Jia J, Nelson J, Goyagi T, Klaus J, Alkayed NJ (2010). Epoxyeicosanoid signaling in CNS function and disease. *Prostaglandins & other lipid mediators* 91(3): 68-84.

Imig JD (2012). Epoxides and soluble epoxide hydrolase in cardiovascular physiology. *Physiological reviews* 92(1): 101-130.

Johnson EA, Oldfield S, Braksator E, Gonzalez-Cuello A, Couch D, Hall KJ, *et al.* (2006). Agonist-selective mechanisms of μ-opioid receptor desensitization in human embryonic kidney 293 cells. *Molecular Pharmacology* 70(2): 676-685.

Kach J, Sethakorn N, Dulin NO (2012). A finer tuning of G protein signaling through regulated control of RGS proteins. *American Journal of Physiology-Heart and Circulatory Physiology*.

Maier SF (1986). Stressor Controllability and Stress-Induced Analgesia. *Annals of the New York Academy of Sciences* 467(1): 55-72.

Marowsky A, Burgener J, Falck J, Fritschy J-M, Arand M (2009). Distribution of soluble and microsomal epoxide hydrolase in the mouse brain and its contribution to cerebral epoxyeicosatrienoic acid metabolism. Neuroscience 163(2): 646-661.

Marowsky A, Meyer I, Erismann-Ebner K, Pellegrini G, Mule N, Arand M (2017). Beyond detoxification: a role for mouse mEH in the hepatic metabolism of endogenous lipids. *Archives of Toxicology*: 1-15.

Miksys SL, Tyndale RF (2002). Drug-metabloizing cytochrome P450s in the brain. *Journal of psychiatry & neuroscience: JPN* 27(6): 406.

Mogil JS, Sternberg WF, Balian H, Liebeskind JC, Sadowski B (1996). Opioid and nonopioid swim stress-induced analgesia: a parametric analysis in mice. *Physiology & behavior* 59(1): 123-132.

Morisseau C, Inceoglu B, Schmelzer K, Tsai H-J, Jinks SL, Hegedus CM, *et al.* (2010). Naturally occurring monoepoxides of eicosapentaenoic acid and docosahexaenoic acid are bioactive antihyperalgesic lipids. *Journal of lipid research* 51(12): 3481-3490.

Papachatzaki MM, Antal Z, Terzi D, Szücs P, Zachariou V, Antal M (2011). RGS9-2 modulates nociceptive behaviour and opioid-mediated synaptic transmission in the spinal dorsal horn. *Neuroscience letters* 501(1): 31-34.

Qin J, Kandhi S, Froogh G, Jiang H, Luo M, Sun D, *et al.* (2015). Sexually dimorphic phenotype of arteriolar responsiveness to shear stress in soluble epoxide hydrolase-knockout mice. *American Journal of Physiology-Heart and Circulatory Physiology* 309(11): H1860-H1866.

Sanchez-Mejia RO, Newman JW, Toh S, Yu G-Q, Zhou Y, Halabisky B, *et al.* (2008). Phospholipase A_2 reduction ameliorates cognitive deficits in a mouse model of Alzheimer's disease. *Nature neuroscience* 11(11): 1311-1318.

Sinal CJ, Miyata M, Tohkin M, Nagata K, Bend JR, Gonzalez FJ (2000). Targeted disruption of soluble epoxide hydrolase reveals a role in blood pressure regulation. *Journal of Biological Chemistry* 275(51): 40504-40510.

Spector AA, Kim H-Y (2015). Cytochrome P 450 epoxygenase pathway of polyunsaturated fatty acid metabolism. *Biochimica et Biophysica Acta (BBA)-Molecular and Cell Biology of Lipids* 1851(4): 356-365.

Takeda K, Pokorski M, Okada Y (2016). Thermal Sensitivity and Dimethyl Sulfoxide (DMSO). *Allergy and Respiration*: 45-50.

Terashvili M, Tseng LF, Wu H, Narayanan J, Hart LM, Falck JR, *et al.* (2008). Antinociception produced by 14, 15-epoxyeicosatrienoic acid is mediated by the activation of β-endorphin and Met-enkephalin in the rat ventrolateral periaqueductal gray. *Journal of Pharmacology and Experimental Therapeutics* 326(2): 614-622.

Traynor J (2012). μ-Opioid receptors and regulators of G protein signaling (RGS) proteins: from a symposium on new concepts in mu-opioid pharmacology. *Drug and alcohol dependence* 121(3): 173-180.

Wagner K, Inceoglu B, Dong H, Yang J, Hwang SH, Jones P, *et al.* (2013). Comparative efficacy of 3 soluble epoxide hydrolase inhibitors in rat neuropathic and inflammatory pain models. *European journal of pharmacology* 700(1): 93-101.

Wagner K, Vito S, Inceoglu B, Hammock BD (2014). The role of long chain fatty acids and their epoxide metabolites in nociceptive signaling. *Prostaglandins & other lipid mediators* 113: 2-12.

Wagner KM, McReynolds CB, Schmidt WK, Hammock BD (2017). Soluble epoxide hydrolase as a therapeutic target for pain, inflammatory and neurodegenerative diseases. *Pharmacology & Therapeutics*.

Zhang W, Koerner IP, Noppens R, Grafe M, Tsai HJ, Morisseau C, *et al.* (2007). Soluble epoxide hydrolase: a novel therapeutic target in stroke. *Journal of Cerebral Blood Flow & Metabolism* 27(12): 1931-1940.

Zhang X, Bao L, Li S (2015). Opioid receptor trafficking and interaction in nociceptors. *British journal of pharmacology* 172(2): 364-374.

Chapter 5

General Discussion

Arachidonic acid (AA) serves as a source for several bioactive eicosanoids including epoxyeicosatrienoic acids (EETs) and dihydroxyeicosatrienoic acids (DHETs). EETs have been shown to exert a plethora of bioactivities such as vasodilation, anti-inflammation, and angiogenesis. DHETs, on the other hand, are generally regarded less active or devoid of any bioactivity at all (Spector *et al.*, 2015). The potential role of these lipid mediators on neuronal excitability, synaptic transmission, and their underlying molecular targets remained largely unexplored to date. In this dissertation, we investigated the potential role of 11,12-EET, 14,15-EET and 11,12-DHET on neuronal excitability and synaptic transmission in the mouse hippocampal neurons Furthermore, we studied the effect of 14,15-EET on heterologously expressed MORs. Main findings of this dissertation are discussed extensively in respective chapters. This section addresses the unexplored aspects in the light of current literature.

5.1. 11,12-EET and -DHET exhibit complementary effects in the hippocampal PCs via combination of pre- and postsynaptic effectors

In hippocampal PCs, 11,12-EET (and to marginal extent 14,15-EET) suppressed excitatory synaptic transmission, whereas 11,12-DHET enhanced it. We identified 11,12-EET-mediated activation of hyperpolarizing G-protein coupled inwardly rectifying K^+ (GIRK) channels via putative EET receptors (EETRs) as a postsynaptic effector underlying inhibitory effects of 11,12-EET. Moreover, using heterologous expression system, we identified $K_v1.2$ and $K_v4.2$ as potential effectors for 11,12-EET/-DHET. 11,12-DHET exhibited significant block of $K_v1.2$ and $K_v4.2$ channels. The observed DHET-mediated block of $K_v1.2$ in heterologous cells indicates a potential modulation of neuronal $K_v1.1/1.2$ heterotetramers which are present in presynaptic terminals and regulate glutamate release (Geiger *et al.*, 2000; Ovsepian *et al.*, 2016; Trimmer, 2015). By contrast, 11,12-EET exhibited a trend towards enhanced activation of these channels in the heterologous system which is consistent with opposite effects of 11,12-DHET and -EET observed on synaptic transmission at CA3-CA1 synapse.

Moreover, postsynaptically expressed $K_v4.2$ hippocampal PCs have been implicated in the regulation of synaptic integration and dendritic excitability (Ramaker *et.al.*, 2006, Trimmer 2015; Jung *et al.*, 2008). 11,12-DHET-mediated block of $K_v4.2$ in heterologous cells points towards potential block of $K_v4.2$ channels in neurons and thus serve as postsynaptic effectors for 11,12-DHET effect *(Fig. 5.1)*.

Our data also point towards the yet unidentified presynaptic effectors for 11,12-EET and allows us to hypothesize the presence of presynaptically expressed EETR(s), which might regulate the neurotransmitter release from presynaptic terminals. Indeed, several studies proposed and assessed the existence of putative EETR(s) underlying EET-mediated bioactivities. A few studies indicated that putative EETR(s) is $G_{\alpha s}$-coupled and modulate calcium-activated BK (BK_{Ca}) channels (Fukao *et al*., 2001; Li *et al*., 1997; Li *et al*., 1999). This possibility is compatible with the existence of putative EETR(s) that modulate K_v channels. However, to date, definite identification of such high-affinity EETR(s) remains unknown (Liu *et al.*, 2016; Spector *et al.*, 2015; Wong *et al.*, 1997).

Notably, presynaptic K_v channels such as K_v1.1/1.2 are reportedly regulated via known G-protein coupled receptors (GPCRs) such as Mu-opioid receptors (MOR) in some neuronal circuits. MOR expression is primarily restricted to the GABAergic interneurons and it has been shown that activation of presynaptic MOR attenuates GABAergic synaptic inputs to central nucleus of amygdala projecting neurons in the basolateral amygdala, presumably via modulation of K_v1.1/1.2 channels (Finnegan *et al*., 2006). Similar attenuation of GABAergic inputs has been reported in rat subthalamic nucleus (Shen *et al*., 2002). These observations are compatible with the possibility that EETs might alter neurotransmitter release by activating presynaptically expressed known GPCR(s) or yet unidentified EETR(s) *(Fig 5.1).*

5.2. Epoxide hydrolases as endogenous 'switch' between inhibition and excitation

Our findings suggest that microsomal and soluble epoxide hydrolase (mEH and sEH) play a key role in the regulation of the ratio between inhibitory 11,12-EET and excitatory 11,12-DHET and thus, may serve as a 'physiological switch' between inhibition and excitation in the hippocampus. This hypothesis was supported by our findings showing higher basal synaptic transmission in slices from mice expressing a mEH variant with higher activity (mEH E404D), while it was reduced in mice lacking one of the main EHs (mEH and sEH KO). Moreover, we observed significantly higher miniature excitatory postsynaptic current frequency in CA1 PCs from mEH E404D slices. This potentiation in excitatory synaptic transmission in mEH E404D CA1 PCs might be caused by DHETs, which block presynaptic K_v channels and thus increase glutamate release at the respective synapse. Indeed, 11,12-DHET was able to block

heterologously expressed $K_v1.2$ channels significantly by 11.92±3%; at a test potential of +10 mV.

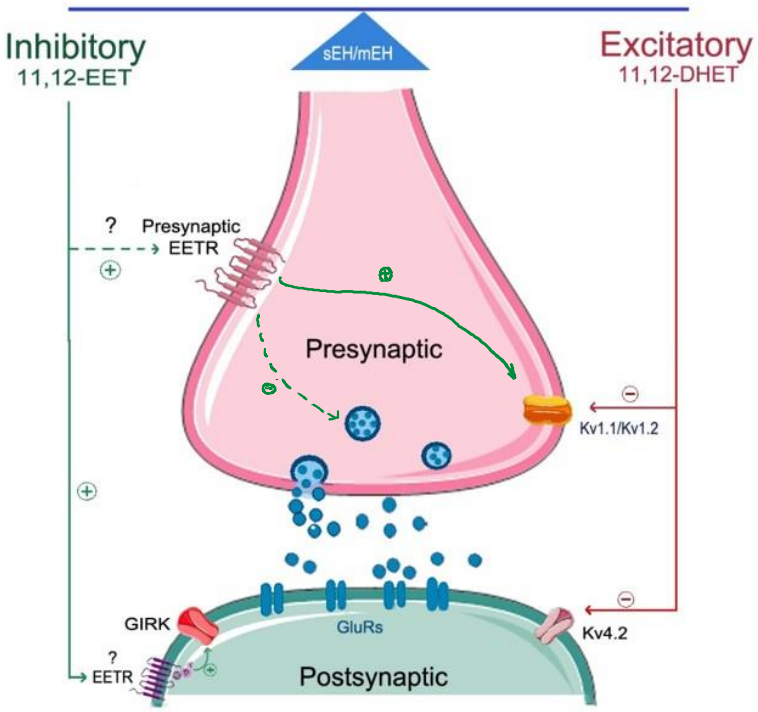

Fig. 5.1. Working model of potential switch functions of EHs via EETs- and DHETs-mediated modulation of pre- and postsynaptic effectors.

5.3. Mice lacking sEH exhibit higher morphine-mediated antinociception

Several studies implicated CYP-epoxygenases-derived fatty acids (FAs)-epoxides such as EETs in opioid-mediated antinociception (Conroy *et al.*, 2010; Hough *et al.*, 2015; Hough *et al.*, 2014; Terashvili *et al.*, 2008). In our experiments with sEH KO, we observed significantly higher morphine-mediated antinociception which points towards the involvement of sEH substrates in the morphine-mediated antinociception. Our observation taken together with an earlier report of 14,15-EET-mediated antinociception in rats (Terashvili *et al.*, 2008) suggested that 14,15-EET might potentiate opioid signaling. However, 14,15-EET did not affect MOR activity, neither when applied alone nor in combination with the MOR agonist DAMGO in a heterologous expression system. Our results are compatible with an earlier report of no direct activity of 14,15-EET on MOR (Terashvili *et al.*, 2008). Furthermore, high throughput screening for 14,15-EET GPCRs did not find high-affinity binding to MOR (Liu *et al.*, 2016). These studies suggest

indirect mechanism(s) for 14,15-EET-mediated potentiation of MOR. Alternatively, host cells used in our experiments may lack a crucial molecular component for enhancing MOR signaling by 14,15-EETs.

Our finding of 11,12-EET-mediated activation of GIRK channels in CA1 PCs, through putative EETR(s), put forth an interesting hypothesis: 11,12-EET-mediated activation of GIRK via EETR(s) or EETR-MOR crosstalk could be an underlying mechanism for higher antinociception observed in sEH KO mice. This possibility, however, needs to be investigated in the relevant neuronal system such as peripheral nociceptors or neurons from the supraspinal regions involved in the endogenous opioid pathways such as periaqueductal grey (PAG) and central nucleus of the amygdala.

5.4. Pathophysiological implications

The potential 'switch' function of mEH and sEH could become even more pertinent under pathological conditions such as stroke, epilepsy, and hypoxia, when basal free AA levels are dramatically increased which might result in an increased levels of neuroactive EETs and/or DHETs in brain (Bazan *et al.*, 1986; Bazán, 1970; Gardiner *et al.*, 1981; Siesjö *et al.*, 1989). In addition, EH activity is also altered under pathological conditions; expression of sEH has been shown to be increased in pilocarpine-induced epilepsy in mice (Hung *et al.*, 2015). Moreover, mEH expression has been detected in tumor-associated glioma and in astrogliosis associated with epileptic seizures in human brain (Kessler *et al*., 2000). Furthermore, mEH expression is elevated in hippocampus of Alzheimer's disease patients (Liu *et al*., 2006). Higher EETs generation coupled with higher epoxide hydrolase activity might tilt the physiological balance between inhibitory EETs towards the excitatory DHETs. Indeed, epileptic seizures induced by pentylenetetrazol resulted in altered EET:DHET ratio in favor of DHETs (Inceoglu *et al*., 2013).

Moreover, our findings of inhibitory effects of EETs and excitatory effects of DHETs offer mechanistic insights to the prior studies reporting beneficial effects of sEH inhibition/ablation in several animal models of epilepsy such as GABA antagonist-induced delayed onset seizures (Inceoglu *et al.*, 2013), tetramethylenedisulfotetramine (TETS)-induced tonic seizures (Vito *et al.*, 2014), pilocarpine-induced and amygdala kindling-induced epilepsy (Hung *et al.*, 2015). Similarly, genetic ablation/pharmacological inhibition of sEH is linked to the beneficial effects

in animal models of stroke, this effect is majorly attributed to the EETs-mediated antiinflammation and neuroprotection (Iliff *et al.*, 2010; Zhang *et al.*, 2007). In addition to the inflammation, stroke-associated excitotoxicity is one of the primary causes of neuronal death in stroke (Chamorro *et al.*, 2016). Based on our findings, one can speculate that the reported beneficial effects of EETs in stroke models, at least in part, could be attributed to the EET-mediated dampening of neuronal excitability. In the absence of characterized putative EETR(s), inhibition of sEH by small molecule inhibitors is actively being explored as a therapeutic target for pain, inflammatory and neurodegenerative diseases (Wagner *et al.*, 2017). A better understanding of the functions and identification of molecular targets for these neuroactive lipid mediators might offer better avenues for therapeutic intervention.

5.5. Outlook

The potential role of mEH and sEH as a 'switch' between hippocampal excitation and inhibition can be further corroborated in alternate *in vitro* and *in vivo* experimental paradigms. Moreover, the underlying molecular mechanism(s) for higher morphine-mediated antinociception observed in sEH KO mice needs to be ascertained. This can be achieved by investigating the influence of FA epoxides on MOR signaling in suitable extracellular system expressing potential effectors. Amongst other possibilities, downstream regulation of RGS protein and in turn MOR signaling by FA epoxides such as EETs/EpOMEs is desirable.

The possibility of putative G-protein coupled EETR has been evaluated by means of binding assays and high throughput screening with 14,15-EET against GPCR libraries, however, it did not result in the identification of high-affinity EETR to date (Li *et al.*, 1997; Li *et al.*, 1999; Liu *et al.*, 2016). Our findings strongly suggest the possible existence of 11,12-EET-specific EETR(s) and this possibility can be explored by means of high throughput screening against a library of known and orphan GPCRs. Identification and characterization of these receptors could advance the basic research in this field and extend its impact to the possible clinical usefulness.

5.6. Bibliography

Bazan N, Birkle D, Tang W, Reddy TS (1986). The accumulation of free arachidonic acid, diacylglycerols, prostaglandins, and lipoxygenase reaction products in the brain during experimental epilepsy. *Advances in neurology* **44:** 879-902.

Bazán NG (1970). Effects of ischemia and electroconvulsive shock on free fatty acid pool in the brain. *Biochimica et Biophysica Acta (BBA)-Lipids and Lipid Metabolism* **218**(1)**:** 1-10.

Chamorro Á, Dirnagl U, Urra X, Planas AM (2016). Neuroprotection in acute stroke: targeting excitotoxicity, oxidative and nitrosative stress, and inflammation. *The Lancet Neurology* **15**(8)**:** 869-881.

Conroy JL, Fang C, Gu J, Zeitlin SO, Yang W, Yang J, *et al.* (2010). Opioids activate brain analgesic circuits through cytochrome P450/epoxygenase signaling. *Nature neuroscience* **13**(3)**:** 284-286.

Finnegan TF, Chen S-R, Pan H-L (2006). μ Opioid receptor activation inhibits GABAergic inputs to basolateral amygdala neurons through K_v1.1/1.2 channels. *Journal of Neurophysiology* **95**(4)**:** 2032-2041.

Fukao M, Mason HS, Kenyon JL, Horowitz B, Keef KD (2001). Regulation of BK_{Ca} channels expressed in human embryonic kidney 293 cells by epoxyeicosatrienoic acid. Molecular Pharmacology 59(1): 16-23.

Gardiner M, Nilsson B, Rehncrona S, Siesjö BK (1981). Free fatty acids in the rat brain in moderate and severe hypoxia. *Journal of neurochemistry* **36**(4)**:** 1500-1505.

Geiger JR, Jonas P (2000). Dynamic control of presynaptic Ca^{2+} inflow by fast-inactivating K^+ channels in hippocampal mossy fiber boutons. *Neuron* **28**(3)**:** 927-939.

Hough LB, Nalwalk JW, Ding X, Scheer N (2015). Opioid analgesia in P450 gene cluster knockout mice: a search for analgesia-relevant isoforms. *Drug Metabolism and Disposition* **43**(9)**:** 1326-1330.

Hough LB, Nalwalk JW, Yang W, Ding X (2014). Significance of neuronal cytochrome P450 activity in opioid-mediated stress-induced analgesia. *Brain research* **1578:** 30-37.

Hung Y-W, Hung S-W, Wu Y-C, Wong L-K, Lai M-T, Shih Y-H, *et al.* (2015). Soluble epoxide hydrolase activity regulates inflammatory responses and seizure generation in two mouse models of temporal lobe epilepsy. *Brain, behavior, and immunity* **43:** 118-129.

Iliff JJ, Jia J, Nelson J, Goyagi T, Klaus J, Alkayed NJ (2010). Epoxyeicosanoid signaling in CNS function and disease. *Prostaglandins & other lipid mediators* **91**(3)**:** 68-84.

Inceoglu B, Zolkowska D, Yoo HJ, Wagner KM, Yang J, Hackett E, *et al.* (2013). Epoxy fatty acids and inhibition of the soluble epoxide hydrolase selectively modulate GABA mediated neurotransmission to delay onset of seizures. *PloS one* **8**(12)**:** e80922.

Kessler R, Hamou M-F, Albertoni M, de Tribolet N, Arand M, Van Meir EG (2000). Identification of the putative brain tumor antigen BF7/GE2 as the (de) toxifying enzyme microsomal epoxide hydrolase. Cancer research 60(5): 1403-1409.

Kim J, Jung S-C, Clemens AM, Petralia RS, Hoffman DA (2007). Regulation of dendritic excitability by activity-dependent trafficking of the A-type K^+ channel subunit K_v4. 2 in hippocampal neurons. Neuron 54(6): 933-947.

Li P-L, Campbell WB (1997). Epoxyeicosatrienoic acids activate K^+ channels in coronary smooth muscle through a guanine nucleotide binding protein. Circulation research 80(6): 877-884.

Li P-L, Chen C-L, Bortell R, Campbell WB (1999). 11, 12-Epoxyeicosatrienoic acid stimulates endogenous mono-ADP-ribosylation in bovine coronary arterial smooth muscle. Circulation research 85(4): 349-356.

Liu X, Qian Z-y, Xie F, Fan W, Nelson JW, Xiao X, *et al.* (2016). Functional screening for G protein-coupled receptor targets of 14, 15-epoxyeicosatrienoic acid. *Prostaglandins & other lipid mediators*.

Liu M, Sun A, Shin EJ, Liu X, Kim SG, Runyons CR, et al. (2006). Expression of microsomal epoxide hydrolase is elevated in Alzheimer's hippocampus and induced by exogenous β-amyloid and trimethyl-tin. European Journal of Neuroscience 23(8): 2027-2034.

Ovsepian SV, LeBerre M, Steuber V, O'leary VB, Leibold C, Dolly JO (2016). Distinctive role of $K_V1.1$ subunit in the biology and functions of low threshold K^+ channels with implications for neurological disease. *Pharmacology & Therapeutics* **159:** 93-101.

Ramakers GM, Storm JF (2002). A postsynaptic transient K^+ current modulated by arachidonic acid regulates synaptic integration and threshold for LTP induction in hippocampal pyramidal cells. *Proceedings of the National Academy of Sciences* **99**(15)**:** 10144-10149.

Shen KZ, Johnson SW (2002). Presynaptic modulation of synaptic transmission by opioid receptor in rat subthalamic nucleus in vitro. *The Journal of physiology* **541**(1)**:** 219-230.

Siesjö BK, AGARDH CD, Bengtsson F, SMITH ML (1989). Arachidonic acid metabolism in seizures. *Annals of the New York Academy of Sciences* **559**(1)**:** 323-339.

Spector AA, Kim H-Y (2015). Cytochrome P 450 epoxygenase pathway of polyunsaturated fatty acid metabolism. *Biochimica et Biophysica Acta (BBA)-Molecular and Cell Biology of Lipids* **1851**(4)**:** 356-365.

Terashvili M, Tseng LF, Wu H, Narayanan J, Hart LM, Falck JR, *et al.* (2008). Antinociception produced by 14, 15-epoxyeicosatrienoic acid is mediated by the activation of β-endorphin and Met-enkephalin in the rat ventrolateral periaqueductal gray. *Journal of Pharmacology and Experimental Therapeutics* **326**(2)**:** 614-622.

Trimmer JS (2015). Subcellular localization of K^+ channels in mammalian brain neurons: remarkable precision in the midst of extraordinary complexity. *Neuron* **85**(2)**:** 238-256.

Vito ST, Austin AT, Banks CN, Inceoglu B, Bruun DA, Zolkowska D, *et al.* (2014). Post-exposure administration of diazepam combined with soluble epoxide hydrolase inhibition stops seizures and modulates neuroinflammation in a murine model of acute TETS intoxication. *Toxicology and applied pharmacology* **281**(2)**:** 185-194.

Wagner KM, McReynolds CB, Schmidt WK, Hammock BD (2017). Soluble epoxide hydrolase as a therapeutic target for pain, inflammatory and neurodegenerative diseases. *Pharmacology & Therapeutics*.

Wong PY, Lai P-S, Shen S-Y, Belosludtsev YY, Falck J (1997). Post-receptor signal transduction and regulation of 14 (R), 15 (S)-epoxyeicosatrienoic acid (14, 15-EET) binding in U-937 cells. *Journal of lipid mediators and cell signalling* **16**(3)**:** 155-169.

Zhang W, Koerner IP, Noppens R, Grafe M, Tsai H-J, Morisseau C, *et al.* (2007). Soluble epoxide hydrolase: a novel therapeutic target in stroke. *Journal of Cerebral Blood Flow & Metabolism* **27**(12)**:** 1931-1940.

Abbreviations

AA: arachidonic acid

ACSF: artificial cerebrospinal fluid

AHR: aromatic hydrocarbon receptor

ALA: α-linolenic acid

AMPAR: α-amino-3-hydroxy-5-methylisoxazole-4-propionic acid receptor

APs: action potentials

AUDA: 12-(3-adamantan-1-yl-ureido) dodecanoic acid

BBB: blood-brain barrier

BK_{Ca}: calcium-activated BK

CA: cornu ammonis

CB1: cannabinoid 1 receptor

CHO: chinese hamster ovary

CNS: central nervous system

COX: cyclooxygenases

$cPLA_2$: cytoplasmic phospholipase A_2

CPR: CYP-reductase

CRCs: concentration-response curves

CYPs: cytochrome P450

DGGCs: dentate gyrus granule cells

DHA: docosahexaenoic acid

DHET: dihydroxyeicosatrienoic acid

DIC: differential interference contrast

DiHOMEs: dihydroxy-12Z-octadecenoic acid

DOR: delta-opioid receptor

DSE: depolarization-induced suppression of excitation

DSI: depolarization-induced suppression of inhibition

DTx: dendrotoxin

EC: entorhinal cortex

EDH/RF: endothelium-derived hyperpolarizing/relaxing factors

EETs: epoxyeicosatrienoic acids

EEZE: 14,15-epoxyeicosa-5(Z)-enoic acid

EHs: epoxide hydrolases

EPA: eicosapentaenoic acid

EpDPEs: derived epoxydocosapentaenoic acids

EpETEs: eicosapentaenoic acid-derived epoxyeicosatetraenoic acid

EpOMEs: epoxy-octadecenoic acids

EPSCs: excitatory postsynaptic currents

ER: endoplasmic reticulum

ETYA: 5,8,11,14-eicosatetraynoic acid

FAAH: fatty acid amide hydrolase

FABPs: fatty acid binding proteins

fEPSPs: field excitatory postsynaptic potential recordings

FV: fiber volley

GABA: γ-aminobutyric acid

GDPβS: guanosine-5'-O(2-thiodiphosphate)

GIRK: G-protein coupled inwardly rectifying K^+

GPCRs: G-protein-coupled receptors

HETEs: hydroxyeicosatetraenoic acids

HF: hippocampal formation

HpETEs: hydroperoxyeicosatetraenoic acids

I_A: A-type currents

I_D: D-type currents

I_{hold}: holding current

I_{KCa}: Ca^{2+} activated potassium channels

INs: interneurons

I-O: input-output

IPSCs/Ps: inhibitory postsynaptic currents/potentials

IR: immunoreactivity

KAR: kainate receptors

KChIPs: K_v channel interacting proteins

k_{cat}/K_m: catalytic efficiency

K_2P: two-pore domain K^+

LA: linoleic acid

LOX: lipoxygenases

LTP: long-term potentiation

MAGL: monoacylglycerol lipase

mEH: microsomal epoxide hydrolases

mEPSC: miniature excitatory postsynaptic currents

Mfs: mossy fiber

MfBs: mossy fiber boutons

MOR: Mu-opioid receptor

NADH: nicotinamide adenine dinucleotide-hydrogen (reduced)

NADPH: nicotinamide adenine dinucleotide phosphate hydrogen (reduced)

NMDAR: N-methyl-D-aspartate receptor

PAG: periaqueductal gray

PCs: pyramidal cells

PGH_2: prostaglandins H_2

PLL: poly-L-lysine

PPAR: peroxisome proliferator-activated receptor

PPF: paired-pulse facilitation

PPR: paired pulse ratio

PTGER: prostaglandin E receptor

PUFAs: polyunsaturated fatty acids

RMP: resting membrane potential

SCs: Schaffer collaterals

sEH: soluble epoxide hydrolases

sEHis: sEH inhibitors

SEM: standard error of mean

SNP: single nucleotide polymorphism

SOCE: store-operated calcium entry

tAUCB: trans-4-[4-(3-adamantan-1-y1-ureido)-cyclohexyloxy]-benzoic acid

TCDD: 2,3,7,8-tetrachlorodibenzo-p-dioxin

TEA: tetraethylammonium

TETS: tetramethylenedisulfotetramine

TP: thromboxane prostaglandin

TRP: transient receptor potential

TRPC: transient receptor potential-C

TTQ: tertiapin Q

TTX: tetrodotoxin

TxA_2: thromboxane A_2

VGCChs: voltage-gated calcium channels

VGPChs: voltage-gated potassium channels

VGSChs: voltage-gated sodium channels

V_{max}: maximum velocity

2-AG: 2-arachidonoyl glycerol

12-HPETE: 12-hydroperoxyeicosatetraenoic acid

Acknowledgements

This is truly an overwhelming feeling while I write acknowledgments, my life as a PhD student flashes in front of my eyes! As humans, we need the help of fellow humans, lest intellectual and material progress ceases. I am indebted to the help and support of many people, without them this dissertation would not have been completed. My gratitude for all those who helped me directly or indirectly through this arduous but exciting journey is taking the form of humble words! Please accept my apologies beforehand; if you are not in my mind now, you will be in my heart for good.

First and foremost, I would like to thank **Prof. Dr. Michael Arand** *(Erni)* for offering me the opportunity to pursue PhD in his group. I could not thank him enough for his guidance, recommendations and above all patience throughout the progress of this work. I must thank him for his constant support in testing times. I am amazed at his endearing curiosity towards science coupled with the ability to come up with rational experimental design to address it. It gave me a 'career goal' and will inspire me for years to come! I would like to thank members of my thesis committee **Prof. Dr. Hanns Ulrich Zeilhofer** and **Prof. Dr. Wolf-Hagen Schunck** for their time, inputs and efforts. I would like to acknowledge **Dr. Anne Marowsky** for her diligent supervision and all the help with experimentation planning, designing and analyzing over the years, I really appreciate it! I am thankful to her for offering her scientific expertise which helped me a lot to learn, improve, and apply my skills in the fascinating field of slice electrophysiology. Her timely guidance, at a times helpful criticisms, shaped me develop a realistic person I am today. I am especially thankful for her helpful inputs for improving this dissertation and constant encouragement for improving scientific writing skills.

I would like to thank all current and former lab members for making my PhD life lively. In particular, *Monika, Kira, Bettina, Beau, Philip, Olga* and all *Toxies et.al*. Special thanks go to *Imke Myer* for her help with CHO cell culture and cloning of K_v channels used in this work. I would like to thank all the current and former IPT members and Friends on Irchel campus, especially *Karthik* for all those geeky discussions! I would like to thank Institute of

Pharmacology and Toxicology (IPT), University of Zurich for providing a state of art research facilities and congenial environment to carry out this work successfully.

I would like to acknowledge residents of Vinzenz house for creating a place I can call ‘home’ in Switzerland. Special thanks go to Indian gang *et.al* you guys made me feel at home. I could not thank enough to *Jyoti* for instilling me with positivity and inculcating self-belief. Above all, offering simple solutions to most complex problems is an art and she is an adept practitioner of it! I would like to thank *Alok* for his brotherly advices and tasty food, *Kumar, Joy, and Meysam* thank you for all those nice memories!

I owe a deep gratitude to people back home in India, who unconditionally supported me and at a times with my eccentric choices (pursuing a PhD is not one of them!). I acknowledge *Ruhi* for her help, unconditional support and being instrumental in keeping my spirit high. My deepest gratitude goes to my family: Aai, baba, my sisters Neelam, Nirmala, and little Samu for their unconditional love, inspiration, selfless sacrifices and constant encouragement throughout my life. This is the greatest learning experience of my life, so far. I hope to apply it to attain goals in my life. It transformed me into a person *who wishes to be known, if at all, as a man who fights really hard for what he believes in’* I am thankful to everyone who contributed directly or indirectly towards offering me this learning experience.

Finally, I bow before the Almighty in the name of the science and humbly submit in front of him a minuscule piece of work on the grand scale of this universe.

Curriculum Vitae

Nandkishor K. Mule

Nationality: Indian
D.O.B.: November 28, 1985
n.mule@pharma.uzh.ch

Loorenstrasse 74,
CH-8053, Zürich, Switzerland.
Mobile: +41 78 856 31 95

Research experience

Aug 2011-present	**Doctoral researcher**, Institute of Pharmacology and Toxicology, University of Zurich, Switzerland.
Jul 2010-Aug 2011	**Research Associate**, Biocon-Bristol Myers Squibb (BMS) Research Centre, India

Education

Aug 2011-present	**PhD in Neuroscience**, Institute of Pharmacology and Toxicology**,** University of Zurich, Switzerland. Dissertation title *" The Role of Epoxygenated Arachidonic Acid-Derived Metabolites in Neuronal Transmission"*
Jul 2008-Jun 2010	**Master of Science (Pharmacology)**, [CGPA 9.14/10], National Institute of Pharmaceutical Education and Research (NIPER), Mohali, India.
Jul 2005-Jun 2008	**Bachelor of Pharmacy**, [First class: 68.33%], Bombay College of Pharmacy, University of Mumbai, India.
Aug 2003-Jun 2005	**Diploma in Pharmacy**, Kamala Nehru Polytechnic (Pharmacy), India.

Poster presentations

- Drug discovery network Zurich (DDNZ) symposium, ETH Zurich, Switzerland (2017)
- Swiss Society of Pharmacology & Toxicology (SSPT), spring meeting, Bern, Switzerland (2015 & 2012)
- Institute poster day, Institute of Pharmacology and Toxicology, University of Zurich, Switzerland (2014, 2013)
- Eurotox, Interlaken, Switzerland (2013)
- Society for neuroscience (sfn) annual meeting, San Diego, USA (2013)
- Neuroscience Center Zurich (ZNZ) retreat (2013)

Publications

1. **Nandkishor Mule**, Anette Orjuela León, John R Falck, Michael Arand, Anne Marowsky ***(2017)***. *11,12-Epoxyeicosatrienoic acid (11,12 EET) reduces excitability and excitatory transmission in the hippocampus.* Neuropharmacology, 123.

2. **Nandkishor Mule**, *et.al. Epoxide hydrolases act as a switch between AA-derived excitatory EETs and inhibitory DHETs, which modulate K_v channels* ***(manuscript in preparation)***.

3. **Nandkishor Mule**, *et.al. Altered susceptibility to morphine-mediated antinociception in sEH KO mice* ***(manuscript in preparation)***.

4. Anne Marowsky, Imke Meyer, Kira Erismann-Ebner, Giovanni Pellegrini, **Nandkishor Mule**, Michael Arand ***(2017)***. *Beyond detoxification: a role for mouse mEH in the hepatic metabolism of endogenous lipids.* Archive für Toxikologie (*Article in press, DOI: 10.1007/s00204-017-2060-4)*.

5. Anne Marowsky, Karen Haenel, Ernesto Bockamp, Rosario Heck, Sibylle Rutishauser, **Nandkishor Mule**, Diana Kindler, Markus Rudin, Michael Arand ***(2016)***. *Genetic enhancement of microsomal epoxide hydrolase improves metabolic detoxification but impairs cerebral blood flow regulation*. Archive für Toxikologie, 90(12).

I hereby declare that the above information is true and correct to the best of my knowledge and belief.

Place: Zurich Nandkishor K. Mule
